

PROJECT ADMINISTRATION DATA SHEET

ORIGINAL REVISION NO. _____

Project No. G-41-612 (R6104-OA0) GTRC/~~ST~~ DATE 3 / 5 / 86

Project Director: Drs. A. Zangwill & D. Liberman School TKM Physics

Sponsor: U. S. Department of Energy, Oak Ridge, TN

Type Agreement: Grant No. DE-FG05-86ER45243

Award Period: From 3/1/86 To 2/29/88 (Performance) 5/29/88 (Reports)

Sponsor Amount:	<u>This Change</u>	<u>Total to Date</u>
Estimated: \$	<u>53,782</u>	\$ <u>109,369</u>
Funded: \$	<u>53,782</u>	\$ <u>53,782 (Through 2/28/87)</u>

Cost Sharing Amount: \$ None Cost Sharing No: N/A

Title: Local Many-Body Effects in the Optical Response of Narrow Band Solids

ADMINISTRATIVE DATA

OCA Contact Brian J. Lindberg X4820

1) Sponsor Technical Contact:

Dr. Thomas A. Kitchens
Office of Basic Energy Sciences, ER-132
U. S. Dept. of Energy
19901 Germantown Rd.
Germantown, Md. 20874
(301) 353-3426

2) Sponsor Admin/Contractual Matters:

Marlena Clark, Contract Specialist
U. S. DOE/Oak Ridge Operations
Procurement and Contracts Div.
Contract Management Branch
P. O. Box E, Oak Ridge, TN 37831
(615) 576-7599

Defense Priority Rating: N/A Military Security Classification: N/A
 (or) Company/Industrial Proprietary: N/A

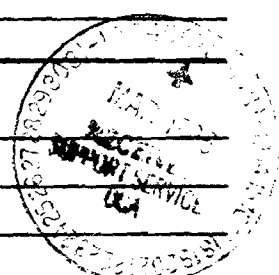
RESTRICTIONS

See Attached N/A Supplemental Information Sheet for Additional Requirements.

Travel: Foreign travel must have prior approval - Contact OCA in each case. Domestic travel requires sponsor approval where total will exceed greater of \$500 or 125% of approved proposal budget category.

Equipment: Title vests with grantee. However, DOE has the right to transfer ownership of any item of equipment having a unit acquisition cost of \$1,000 or more.

COMMENTS:



COPIES TO: SPONSOR'S I. D. NO. 02.141.002.86.009

- | | | |
|---------------------------------|----------------------------------|-----------------------------|
| Project Director | Procurement/EES Supply Services | GTRC |
| Research Administrative Network | Research Security Services | Library |
| Research Property Management | <u>Reports Coordinator (OCA)</u> | Project File |
| Accounting | Research Communications (2) | Other <u>A. Jones/Legal</u> |

GEORGIA INSTITUTE OF TECHNOLOGY
OFFICE OF CONTRACT ADMINISTRATION

NOTICE OF PROJECT CLOSEOUT

Date 12/14/88

Project No. G-41-612

Center No. R6104-OA0

Project Director A. Zangwill

School/Lab Physics

Sponsor US Department of Energy

Contract/Grant No. DE-FG05-86ER45243

GTRC XX GIT

Prime Contract No. N/A

Title Local Many-Body Effects in the Optical Response of Narrow Band Solids

Effective Completion Date 8/31/88 (Performance) 11/30/88 (Reports)

Closeout Actions Required:

- None
- Final Invoice or Copy of Last Invoice
- Final Report of Inventions and/or Subcontracts - Patent Questionnaire to PI.
- Government Property Inventory & Related Certificate
- Classified Material Certificate
- Release and Assignment
- Other _____

Includes Subproject No(s). _____

Subproject Under Main Project No. _____

Continues Project No. _____ Continued by Project No. _____

Distribution:

- | | |
|--|--|
| <input checked="" type="checkbox"/> Project Director | <input checked="" type="checkbox"/> <u>Reports Coordinator</u> (OCA) |
| <input checked="" type="checkbox"/> Administrative Network | <input checked="" type="checkbox"/> GTRC |
| <input checked="" type="checkbox"/> Accounting | <input checked="" type="checkbox"/> Project File |
| <input checked="" type="checkbox"/> Procurement/GTRI Supply Services | <input checked="" type="checkbox"/> Contract Support Division (OCA) |
| <input checked="" type="checkbox"/> Research Property Management | <input type="checkbox"/> Other _____ |
| <input type="checkbox"/> Research Security Services | _____ |

G-41-612

FORM DOE 538
(Rev. 10-80)

U.S. DEPARTMENT OF ENERGY
NOTICE OF ENERGY RD&D PROJECT

OMB Approval
No. 1901-0021

APPROVED FOR USE BY
SMITHSONIAN SCIENCE INFORMATION EXCHANGE

1. Descriptive title of work
Local Many-Body Effects in the Optical Response of Narrow Band Solids

2. Performing organization control number _____ 3. Contract or grant number
Work status New Continuing Terminated DOE-FG05-86ER45243

4. Contractor's principal investigator/project manager and address where work is performed
A. Name (Last, First, MI) Zangwill, Andrew B. Phone: FTS- (404) 894-7333
C. Research organization
business address: Street School of Physics/Georgia Inst. of Tech. Com.- _____
City Atlanta State GA Zip _____

5. A. Name of performing organization Georgia Institute of Technology School of Physics
(Organization) (Department)
B. Mailing address (If different from 4C) _____ C. Circle only one code for TYPE OF ORGANIZATION PERFORMING R&D
(See instructions):
 CU FF IN NP ST TA US XX EG
D. Location where the work is being performed _____
E. Country sponsoring research _____

6. Supporting organization
A. Program division or office (Full name) Division of Materials Science
B. Technical monitor (Last, First, MI) Kitchens, Thomas C. Phone: FTS- (301) 353-3426
D. Address (If different from DOE Hqs.) _____ Com.- _____
E. Administrative monitor (Last, First, MI) Clark, Marlana (Oak Ridge)

7. Project schedule
A. Start date 3/1/86 B. Expected completion date 2/29/88
(Month) (Year) (Month) (Year)

8. Funding in thousands of dollars (Funds represent budget obligations for operating and capital equipment)

Funding organization(s)	Current FY	Next FY
A. DOE	53.782	55.587
B.		
C.		

D. For DOE projects, enter budgeting and reporting classification code _____
E. Interagency agreement (Specify funding agency) _____
F. Agency in-house effort (Check if applicable) _____
G. EPA "pass-thru" funding (Check if applicable) _____

Note: Funding Section utilization is optional on Federal Financial Assistance Programs: grants, direct payments, cooperative agreements, loan guarantees, and other related programs.

9. Descriptive summary of work (Limit to 200 words. Include objective, approach, results to date and their significance, and expected product. Quantify where possible).

Calculations are performed to study the optical response of intermetallic compounds in the energy range relevant to synchrotron radiation resonant photoemission experiments. The method is a generalization of the time-dependent local density approximation (TDLDA) which includes many-body effects at the level of the random phase approximation. The first system to be studied is an atom-in-jellium to assess to effect of a solid state environment on an essentially atomic absorption phenomena. Later studies will move to cluster models.

10. List the five most descriptive publications in the last year that are available to the public which have resulted from the project (Please give a complete bibliographic citation. Use additional sheets if necessary).

11. General technology categories (Enter applicable code of codes from instructions).

F1 F2

12. Type of research activity (Check applicable activities)

- | | |
|---|--|
| A. <input checked="" type="checkbox"/> Basic research | H. <input type="checkbox"/> Mathematical model development |
| B. <input type="checkbox"/> Applied research | I. <input type="checkbox"/> Data analysis/assessments |
| C. <input type="checkbox"/> Laboratory scale R&D | J. <input type="checkbox"/> Information systems management |
| D. <input type="checkbox"/> Technology development | K. <input type="checkbox"/> Policy analysis |
| E. <input type="checkbox"/> Field study | L. <input type="checkbox"/> Socioeconomic |
| F. <input type="checkbox"/> Pilot plant scale R&D | M. <input type="checkbox"/> Other (Specify) _____ |
| G. <input type="checkbox"/> Full scale demonstration | N. <input type="checkbox"/> Not applicable |

13. keywords (Please list 5 keywords).

14. Is this research project solely an ANALYTICAL/PAPER STUDY?
(Non-experimental, paper and pencil, computer analysis, etc.).

YES NO

15. Respondent's Name: Andrew Zangwill Phone No.: 804-7333 Date: 11/24/86
Street: School of Physics
City: Georgia Tech State: ATL GA Zip: 30332

G-41-612

DOE/ER/45243-1

ANNUAL REPORT

**LOCAL MANY-BODY EFFECTS IN THE OPTICAL
RESPONSE OF NARROW BAND SOLIDS**

**Andrew Zangwill
David Liberman**

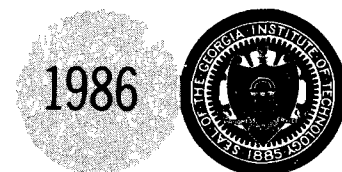
**Progress Report
March 1 1986 - February 29, 1987**

**Prepared for
The U.S. Department of Energy**

**Under
Grant No. De-FG05-86ER45243**

December 1986


GEORGIA INSTITUTE OF TECHNOLOGY
A UNIT OF THE UNIVERSITY SYSTEM OF GEORGIA
SCHOOL OF PHYSICS
ATLANTA, GEORGIA 30332



U. S. DEPARTMENT OF ENERGY

UNIVERSITY CONTRACTOR, GRANTEE, AND COOPERATIVE AGREEMENT
RECOMMENDATIONS FOR ANNOUNCEMENT AND DISTRIBUTION OF DOCUMENTS

See Instructions on Reverse Side

1. DOE Report No. DOE/ER/45243-1		3. Title Local Many-Body Effects in the Optical Response of Narrow Band Solids
2. DOE Contract No. DOE-FG05-86ER45243		
4. Type of Document ("x" one) <input checked="" type="checkbox"/> a. Scientific and technical report <input type="checkbox"/> b. Conference paper: Title of conference _____ Date of conference _____ Exact location of conference _____ Sponsoring organization _____ <input type="checkbox"/> c. Other (Specify) _____		
5. Recommended Announcement and Distribution ("x" one) <input checked="" type="checkbox"/> a. Unrestricted unlimited distribution. <input type="checkbox"/> b. Make available only within DOE and to DOE contractors and other U. S. Government agencies and their contractors. <input type="checkbox"/> c. Other (Specify) _____		
6. Reason for Recommended Restrictions _____		
7. Patent and Copyright Information: Does this information product disclose any new equipment, process, or material? <input checked="" type="checkbox"/> No <input type="checkbox"/> Yes If so, identify page nos. _____ Has an invention disclosure been submitted to DOE covering any aspect of this information product? <input checked="" type="checkbox"/> No <input type="checkbox"/> Yes If so, identify the DOE (or other) disclosure number and to whom the disclosure was submitted. Are there any patent-related objections to the release of this information product? <input checked="" type="checkbox"/> No <input type="checkbox"/> Yes If so, state these objections. Does this information product contain copyrighted material? <input checked="" type="checkbox"/> No <input type="checkbox"/> Yes If so, identify the page numbers _____ and attach the license or other authority for the government to reproduce.		
8. Submitted by Andrew Zangwill		Name and Position (Please print or type) Associate Professor
Organization School of Physics		Georgia Institute of Technology
Signature 	Phone (404) 894-7333	Date Dec 1 1986

FOR DOE OR OTHER AUTHORIZED
USE ONLY

9. Patent Clearance ("x" one)
 a. DOE patent clearance has been granted by responsible DOE patent group.
 b. Report has been sent to responsible DOE patent group for clearance.

DOE/ER/45243-1

LOCAL MANY-BODY EFFECTS IN THE OPTICAL RESPONSE
OF NARROW BAND SOLIDS

Progress Report

March 1 1986 - February 29, 1987

Andrew Zangwill and David Liberman

School of Physics
Georgia Institute of Technology
Atlanta, GA 30332

December 1986

PREPARED FOR THE U.S. DEPARTMENT OF ENERGY
UNDER GRANT NO. DE-FG05-86ER45243

This report is divided into two sections. Part A is a summary of our activities in the current report year to the present time. Five items are discussed therein. Part B outlines the problems we hope to attack in the next report year. More detail is provided here than usual since our proposal for this period is not a precise continuation of this year's efforts.

Part A: Summary of Current Activities

The principal completed work of the past year is contained in two papers appended to the end of this report. The first (1) is a review entitled "A Condensed Matter View of Giant Resonance Phenomena" prepared by A. Zangwill for a NATO Summer School conducted this past year at Les Houches, France. It will appear in a volume devoted to the School edited by J.-P. Connerade, J.-M. Esteve & R.C. Karnatak. The second (2) is entitled "5f-Bandwidth and Resonant Photoemission of Uranium Intermetallics" and represents the fruit of a collaboration with D.D. Sarma at the KFA -Julich, Federal Republic of Germany. The major conclusion from both works is that the interpretation of resonant photoemission from narrow band metals, *i.e.*, enhanced valence band emission near the threshold for near core level (20-200 eV) photoemission, is considerably more complex than originally suspected by workers in the field. This result (previously suspected by some experimenters) has led to the rapid development of high resolution x-ray spectroscopy (XPS) and bremsstrahlung isochromat spectroscopy (BIS) (essentially inverse XPS) for study of the electronic properties of mixed valent and heavy fermion intermetallic compounds. In this higher energy range, dielectric effects are unimportant and our local density approximation (LDA) based random phase approximation (RPA) to the optical properties is not useful. For this reason, we propose to redirect the focus of our dielectric calculations to other systems where the results will have significantly greater impact (see Part B below).

The uranium work noted above brings this point home forcefully. We observed that there is a factor of two discrepancy in the measured 5f-

bandwidth in many uranium intermetallic compounds as determined by two different experimental techniques: XPS and UV resonant photoemission experiments. Our calculations show that the resonance process distorts the density of states but cannot produce broadening to this degree. Instead, we consider a competing process: a heretofore unconsidered Auger decay channel not included in the dielectric response formulation. We predict that the UV data should be proportional to the self-fold of the occupied density of states. This broadens the resonant density of states by almost exactly a factor of two. The Julich group has planned further experiments to test our prediction.

The emphasis at the NATO School demonstrated that the resonant photoemission technique now is being championed by the atomic physicists. Here, of course, there are no ligand or band effects. We have performed relativistic TDLDA calculations to compare to this new data (Fig. 1) with the interesting result that there are discrepancies even at this level. The total cross section always comes out very well. But, the partitioning of the signal amongst various partial photoionization channels is not quite right. We believe this is related to the simplifications made in the TDLDA integral kernel - it should be frequency dependent rather than static as we choose it. We are presently preparing a large paper with Bernd Sonntag (University of Hamburg, FRG) which systematically compares our calculations (3) with gas phase data for all the elements of the lanthanide row.

Our calculations designed to study solid state effects have proceeded in two directions. As proposed, the simplest model is the atom-in-jellium using the TDLDA method. We quickly encountered severe convergence difficulties for the cases we tried (transition metals). To test our methods we then looked at the frequency dependent polarizability $\alpha(\omega)$ of a jellium ball (4) where the positive ionic charge of the atom is smeared out over a finite volume. This problem has been looked at by Ekardt [1] and Puska, Nieminen & Manninen [2] using our methods. Interestingly, we reproduce their results (Fig. 2) above the photoionization threshold except that, in addition, we recover the expected rise near the bulk plasmon frequency whereas they do not. Moreover, these workers do not recover a

rigorous result: the strict proportionality between $\omega \text{Im}\alpha(\omega)$ and the total cross section. We believe that both problems are related to these authors use of a phenomenological damping parameter in their calculations. We are in communication with Walter Ekardt on this matter.

To study ligand effects, we wished to look at the RPA response of a cluster of transition metal atoms treated in as simple a manner as possible - namely, a tight-binding model. In keeping with the real-space philosophy of the TDLDA, we adopted the method of Rogan & Ingelsfield [3] generalized to the case of finite cluster (5). This problem was given to H. Denis Rogers who was beginning his thesis studies with A. Zangwill at the beginning of the grant period. He was supported on grant funds for nine months. During that time no tangible results were forthcoming. Rogers has been removed from the project and it will proceed with another student or with Zangwill alone.

Perhaps the most important information gleaned from communication with other researchers is that new experimental techniques have come on line for study of narrow-band intermetallic compounds that obviate the critical need for theoretical studies in the near core level regime of the spectrum. Synchrotron study of these materials has been supplanted by laboratory-based XPS and BIS studies. We believe that this turn of events necessitates a reappraisal of our original goals and plans. In fact, further discussion with experimenters suggests the most obvious "mid-course correction" which simultaneously preserves the integrity of our theoretical approach and also moves us into a more timely and scientifically exciting area. We propose to redirect our research effort in the coming year to a study of the structural and dielectric properties of *inhomogenous* materials - namely, metallic clusters and artificial multilayer materials.

Part B: Future Work

In contrast to current research in intermetallic compounds, it appears that optical and ultraviolet absorption and photoemission spectra will be

crucial to quantifying the physics of inhomogeneous materials such as metallic clusters and artificial multilayers. The reason for this is that, in both cases, the wave functions which determine the response of the system to external perturbations depend on an externally imposed length scale. For the aforementioned examples, this length scale is the cluster size and the superlattice modulation wavelength, respectively. In short, the structure of these materials is reflected in their dielectric response in an unusually distinct manner. Moreover, our methods are well suited to such inhomogeneous systems whereas traditional (reciprocal space) methods are not. We propose a coordinated study of the structure and dielectric properties of these materials.

There are two reasons why this is a timely and propitious suggestion. First, the work we have performed to date moves seamlessly into the cluster problem. Second, there is strong, local, experimental support for structural and spectroscopic study of both metal clusters and artificial superlattices. Regarding the first, our intermetallic work always presupposed a cluster model from the beginning - a cluster embedded in jellium. Now we need merely confine the jellium to a finite region of space. Both the tight-binding RPA calculation and the atom-in-a-jellium-ball are appropriate models for study of truly finite clusters. There is considerable interest in this problem generally (see, e.g., Knight *et.al*, [4]) and Prof. James Gole of the School of Physics at Georgia Tech directs a vigorous research group in metal cluster spectroscopy.

The application of our methods to superlattice systems seems particularly apt as well. On the one hand, we see an opportunity to update and extend the classical work by Van Vechten & Phillips [5] who used optical data to predict bulk semiconductor phase diagrams. On the other hand Prof. Ahmet Erbil in our School is applying the MOCVD growth technique to prepare epitaxial semiconductor/metal films for the purpose of studying excitonic superconductivity. His work (also supported by DOE) would be greatly enhanced by knowledge of the superlattice wavevector and frequency dependent dielectric function. Except for rather unrealistic model studies, no calculations of $\epsilon(q,\omega)$ for these systems have been performed at the

level of the RPA. We believe our results would be of substantial interest even if no superconductivity is found.

For both the metal cluster and the multilayer problem it is essential to know the geometrical arrangement the atoms. This suggests that some effort should be devoted to this problem as well. Theoretical investigation of this issue fits in nicely with some previous research experience of one of us [6]. One research student (G.S. Bales) is currently involved in structural studies closely allied to these problems. We expect to engage a second student whose principal focus would be the dielectric properties of a metal/semiconductor system currently under experimental investigation by Erbil.

In conclusion, we wish to shift the emphasis of our optical response studies from intermetallic compounds to a more exciting class of inhomogeneous materials: metal clusters and superlattices. As before, the idea is to set up as realistic a model as possible which still permits solution of the RPA or TDLDA response equations. In addition, we intend to pay greater attention to purely structural issues - a prerequisite to the dielectric problem.

References

1. W. Ekardt, Phys. Rev. **B31**, 6360(1985).
2. M.J. Puska, R.M. Nieminen & M. Manninen, Phys. Rev. **B31**, 3486 (1985).
3. J. Rogan & J.E. Ingelsfield, J. Phys. **C14**, 3585 (1981).
4. W.D. Knight, K. Clemenger, W.A. De Heer & W.A. Saunders, Phys. Rev. **B31**, 2539 (1985).
5. J.A. Van Vechten, Phys. Rev. **B7**, 1479 (1973).
6. A.C. Redfield and A.M. Zangwill, Phys. Rev. **B34**, 1378.

photoemission

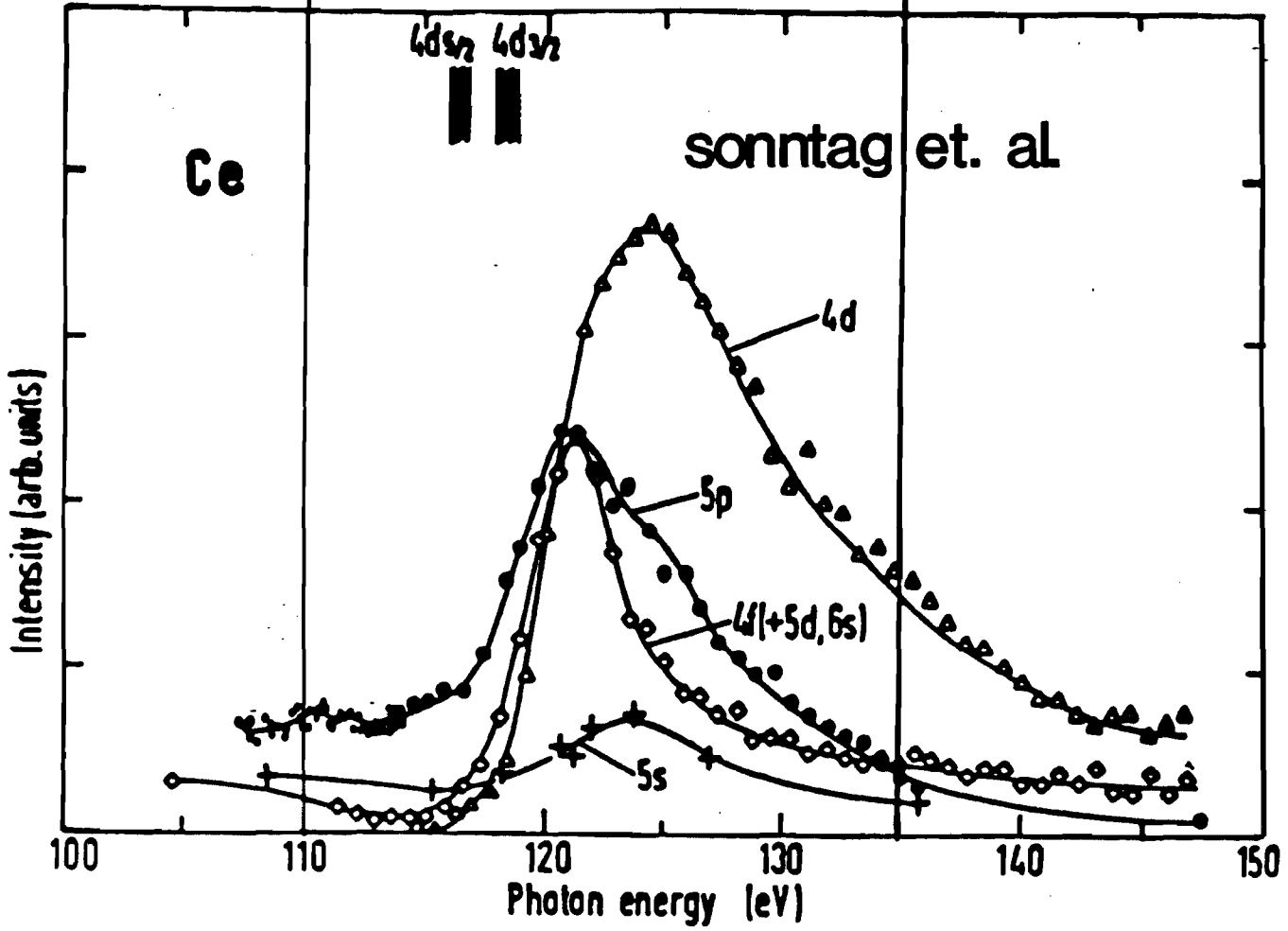
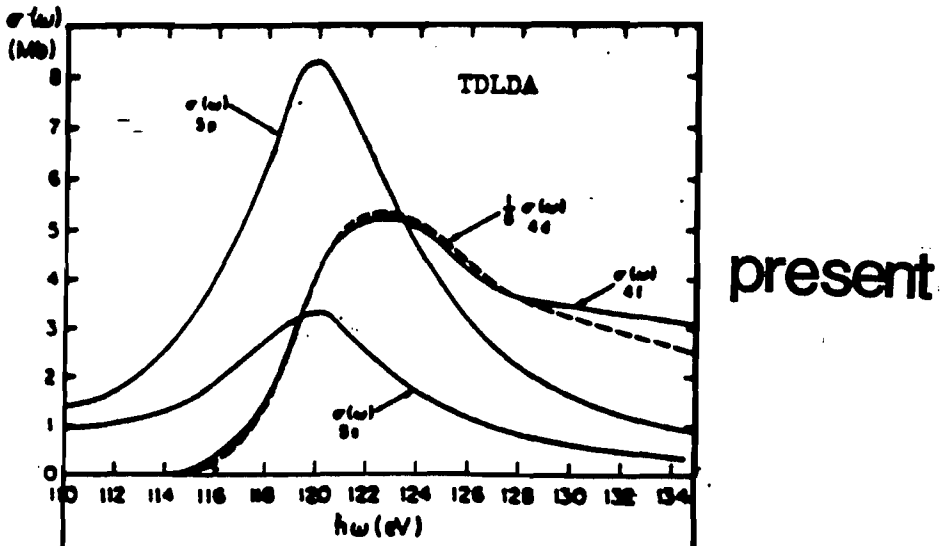


fig. 1

jellium sphere

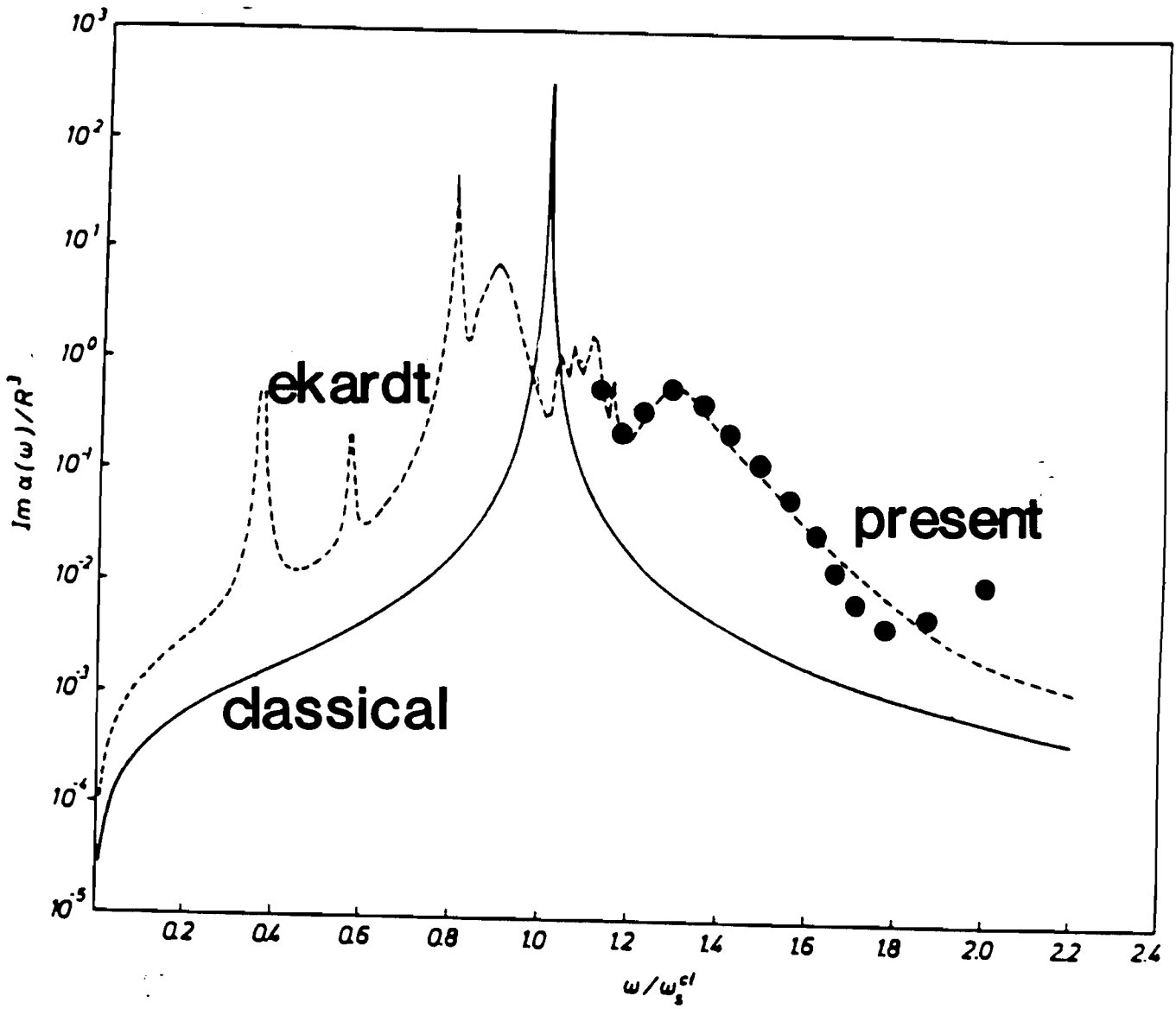


fig. 2

A CONDENSED MATTER VIEW OF GIANT RESONANCE PHENOMENA

Andrew Zangwill

School of Physics
Georgia Institute of Technology
Atlanta, Georgia 30332

INTRODUCTION

It is my intent in this article to present a view of giant resonance phenomena (an essentially atomic phenomenon) from the perspective of a condensed matter physicist with an interest in the optical properties of matter. As we shall see, this amounts to a particular prejudice about how one should think about many-body effects in a system of interacting electrons. Some of these effects are special to condensed matter systems and will be dealt with in the second half of this paper. However, it turns out that my view of the main ingredient to a giant resonance differs significantly from that normally taken by scientists trained in the traditional methods of atomic physics. Therefore, in the first section that follows, I will take advantage of the fact that my contribution to this volume was composed and delivered to the publishers somewhat after the conclusion of the School (rather than before as requested by the organizers) and try to clearly distinguish the differences of opinion presented by the lecturers from the unalterable experimental facts.

Let us take a purely pragmatic definition of a giant resonance. It is a prominent "bump" that appears in the optical absorption spectrum of an atom, molecule or solid whose leading edge is not far from a specific near core level threshold and whose integrated oscillator strength is approximately equal to the number of electrons in the atomic shell associated with that threshold. Although many different spectral features might be shoe-horned into this definition I will restrict my attention only to the most dramatic examples, i.e., those associated with intra-subshell dipole transitions from an initial state to an unfilled bound or virtual bound state characterized by the same principal quantum number. Hence, I associate "giant resonances" primarily with $np \rightarrow nd$ optical excitations in the atoms of the 3d, 4d, and 5d transition metal rows and the elements immediately preceding them and $nd \rightarrow nf$ optical excitations in the atoms of the lanthanide and actinide rows and the elements immediately preceding them. This places the excitation energies of interest in the vacuum ultraviolet part of the electromagnetic spectrum. As an illustration, Figure 1 shows the total absorption from barium metal (it has been de rigueur to discuss barium at this Summer School) just above the 4d threshold. Our task is to formulate a convenient conceptual framework within which to understand why absorption features like this one appear and why they might be interesting and/or useful.

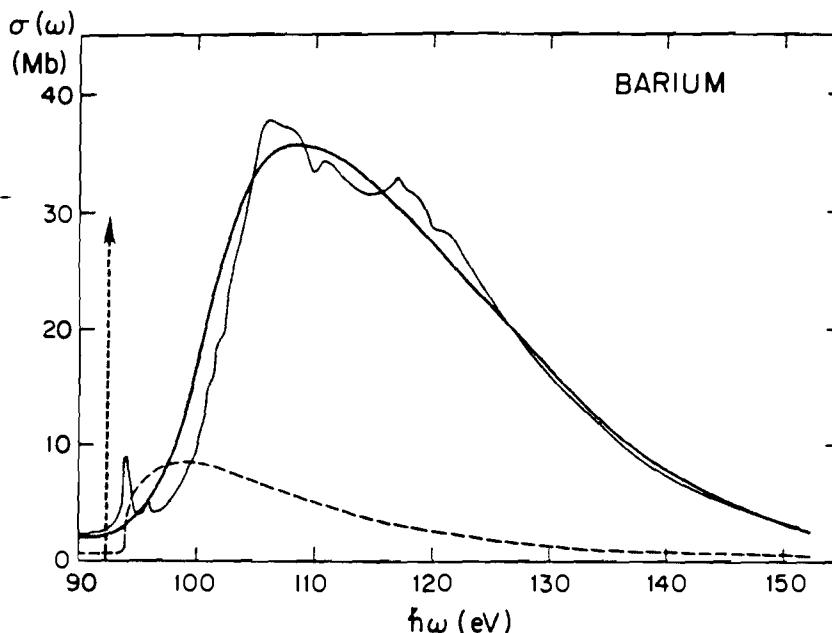


Fig. 1. Giant resonance absorption in barium metal above the 4d threshold. Data from Ref. 1; calculations discussed in the text.

ONE-BODY EFFECT OR MANY-BODY EFFECTS?

The experimental observation that giant resonances carry significant fractions of atomic shell oscillator strength immediately brings to mind the analogy with γ -ray absorption resonances in nuclei² and plasmon excitations in metals.³ Both of these phenomena commonly are regarded as "collective effects" entirely produced by many-body interactions within the nucleon or electron system, respectively. To what extent is this true in the present context? Consider the Golden Rule expression for the total photoabsorption cross section in the long wavelength limit

$$\sigma(\omega) = 4\pi^2 \alpha \hbar \omega \sum_F |\langle F | \epsilon \cdot U_{\text{ext}}(\mathbf{x}) | 0 \rangle|^2 \delta(\hbar\omega - E_F + E_0) \quad (1)$$

In this formula, $U_{\text{ext}}(\mathbf{x})$ is the dipole operator, α is the fine structure constant, and ϵ is the polarization vector of the incident radiation. At fixed excitation frequency ω the absorption occurs between the exact ground state $|0\rangle$ and one of the exact excited states $|F\rangle$. Of course, only approximate evaluation of the requisite matrix elements is possible since the exact many-electron wave functions are unknown. The simplest independent particle approximation writes these quantities as single Slater determinants constructed from one-particle orbitals that are the eigenstates of an appropriate effective potential function. The Golden Rule then takes the form

$$\sigma(\omega) = 4\pi^2 \alpha \hbar \omega \sum_{i,f} |\langle f | \epsilon \cdot U_{\text{ext}}(\mathbf{x}) | i \rangle|^2 \delta(\hbar\omega - \epsilon_f + \epsilon_i) \quad (2)$$

By definition, "many-body effects" appear when the independent particle model fails to describe the experimental data and one resorts to corrective perturbation theory of some sort. Evidently, different choices of a one-body basis set will lead to differing conclusions: one person's many-body effects might be another person's one-body effect.

This ambiguity does not arise in the nuclear and plasma resonance cases. There is broad agreement that the eigenstates of a Woods-Saxon (or related) potential and free electron plane waves, respectively, are the most natural one-particle states for these problems. The corresponding independent particle absorption cross sections fail badly and a perturbation theory sufficient to create a many-body collective resonance is required. Unfortunately, the situation is not quite so clear cut in the present case. From the point of view of traditional atomic and molecular physics, long experience suggests that Hartree-Fock orbitals ought to constitute the independent particle basis set of choice. Indeed, if one uses the most correct "term-dependent Hartree-Fock" eigenstates, many giant resonances (like the barium example⁴) are reasonably reproduced by straightforward application of Equation (2). The resonant structure simply reflects transitions to a virtual bound state in the continuum with some natural distribution of oscillator strength. One would say that one is dealing with a "shape" resonance and collective effects are insignificant. Many-body refinements ("ground-state correlations", "channel mixing", etc.) can be handled either via low-order diagrammatic perturbation theory⁵ or configuration interaction.⁶

A rather different picture emerges if one uses the most "natural" set of one-electron orbitals from the point of view of a condensed matter physicist. The Hartree-Fock approximation is notoriously poor for study of the electronic structure of extended solid state systems. For example, it yields zero density of states at the Fermi energy of a metal. By contrast, the local density approximation (LDA) to the density functional formalism of Hohenberg, Kohn and Sham⁷ has proved very effective for these problems.⁸ This approach yields a complete one-electron basis set of so-called Kohn-Sham orbitals that can be used (somewhat cavalierly) to compute optical matrix elements as in Equation (2). The results are quite reasonable for the fundamental optical spectra ($h\nu < 12$ eV) of solids traditionally studied by condensed matter physicists.⁹ However, similar independent particle LDA calculations of the photoabsorption cross section of atoms at higher excitation energy never reproduce the giant resonances of interest here. Instead, one finds (see below) that a time-dependent generalization of this theory that includes polarization-type many-body effects yields remarkably good agreement for the total cross section. In this approach the giant resonances are quite usefully viewed as strongly damped collective oscillations of entire atomic shells quite akin to the nuclear and plasmon examples. Hence, one is led to the point of view lucidly propounded many years ago by Roulet and Nozieres¹⁰ and implemented by Amusia and co-workers¹¹ and Wendin¹² through RPAE calculations using configuration average Hartree-Fock orbital basis sets.

The main point of this section is to emphasize that the assignment of "many-body effects" in the context of giant resonances in atoms, molecules and solids is very much a question of definition. There is no "correct" answer. Nevertheless, I shall argue in the next section that the interpretation of these phenomena in accordance with the dielectric response and density functional formulations common to condensed matter physics provides a particularly economical and physically appealing picture. Succeeding sections will deal with specific features that are unique to the problem of giant resonances in solid state environments.

DIELECTRIC RESPONSE

The optical properties of solids commonly are discussed in terms of the frequency dependent dielectric function $\epsilon(\omega)$ whose imaginary part is proportional to photoabsorption cross section¹³:

$$\sigma(\omega) \propto \text{Im } \epsilon(\omega) \quad (3)$$

At the elementary macroscopic level, we think of $\epsilon(\omega)$ as that function that describes the reduction (screening) of an external field by a polarizable medium. This notion remains correct at the microscopic level¹⁴ as long as we recognize the non-local spatial dependence of this phenomenon, viz.,

$$U_{\text{eff}}(\mathbf{x}|\omega) = \int \epsilon^{-1}(\mathbf{x}, \mathbf{x}'|\omega) U_{\text{ext}}(\mathbf{x}') d\mathbf{x}' \quad (4)$$

In a translationally invariant crystal we Fourier transform the spatial variables and discover that the relationship between the microscopic and macroscopic dielectric functions is non-trivial:

$$\epsilon(\omega) = \lim_{q \rightarrow 0} \frac{1}{\{\epsilon^{-1}(q+G, q+G')\}_{G=G'=0}} \quad (5)$$

For fixed frequency ω and wavelength q of the external perturbation, the dielectric function is a matrix in the reciprocal lattice vectors (G) of the crystalline lattice. Optical properties are recovered in the long wavelength limit ($q \rightarrow 0$) only after inversion of a large matrix.

We now require some expression for this dielectric matrix. In the most systematic approach, one expresses^{3,10} this quantity in terms of the density-density correlation function $\chi(\mathbf{x}, \mathbf{x}'|\omega)$,

$$\epsilon^{-1}(\mathbf{x}, \mathbf{x}'|\omega) = \delta(\mathbf{x}-\mathbf{x}') + \int d\mathbf{y} \frac{1}{|\mathbf{x}-\mathbf{y}|} \chi(\mathbf{y}, \mathbf{x}'|\omega) \quad (6)$$

The latter is simply related to a two-particle Green function for which a systematic perturbation theory is available. This type of scheme has been carried out with some success to describe the low energy optical spectra of covalent semiconductors by Hanke and collaborators¹⁵. More commonly, one adopts the result that emerges from the lowest order in perturbation theory - the so-called random phase approximation (RPA):

$$\begin{aligned} \epsilon(q+G, q+G'|\omega) = & \delta_{G, G'} + \frac{8\pi e^2}{N \Omega |q+G|^2} \sum_{k, v, c} \\ & [\langle vk | e^{-i(q+G) \cdot \vec{r}} | c \ k+q \rangle \langle c \ k+q | e^{+i(q+G') \cdot \vec{r}} | vk \rangle] \\ & \left[\frac{1}{E_c(k+q) - E_v(k) - \hbar\omega - i\delta} + \frac{1}{E_c(k+q) - E_v(k) + \hbar\omega + i\delta} \right] \end{aligned} \quad (7)$$

Here, the sums over k , v and c refer to sums over the wave vectors in the first Brillouin zone of the crystal and the one-particle states (e.g., LDA Kohn-Sham eigenfunctions) of the valence and conduction bands, respectively. The structure of this equation makes the relationship between Equations (2) and (3) more evident. Unfortunately, the sums indicated above are very difficult to perform reliably and results are available only at zero frequency. Nevertheless, even in the static limit, it is very appealing physically to actually "see" the internal effective field given by Equation (4). Figure 2 is a plot of $U_{\text{eff}}(\mathbf{x}|0)$ (actually its gradient - the electric field) for one unit cell of a zinc selenide crystal¹⁶. We see wild variations that reflect nonuniform microscopic screening of the external field by the polarizable cation and anion. The static dielectric constant of this crystal - about 5 - can be read off directly from the average value of the internal field.

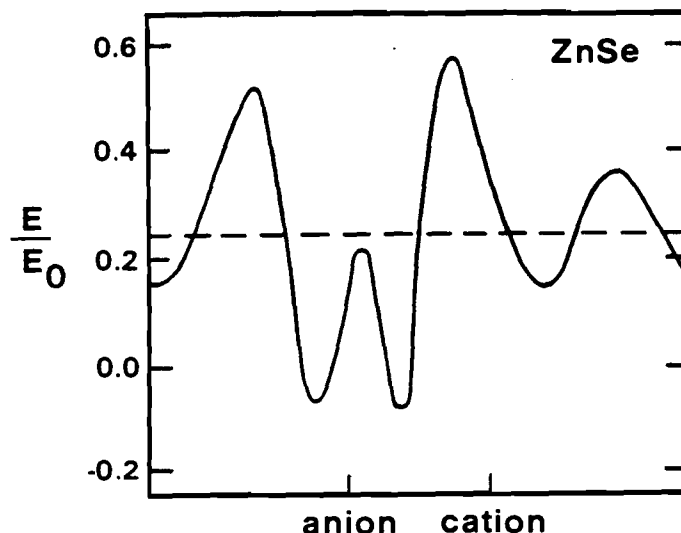


Fig. 2. Microscopic internal field $E(x)/E_{\text{ext}}$ along a cut through a ZnSe crystal. Horizontal line denotes the average microscopic field. From Ref. 16.

The RPA calculation discussed above evidently describes the polarizability of the electronic system. At zero frequency, the principal source of this polarization may be regarded as virtual transitions between occupied and unoccupied one-electron states induced by the external field¹⁷. These particle-hole pairs (relative to the ground state Slater determinant) describe a distortion of the original ground state charge density. The induced charge generates an induced dipolar potential (via Poisson's equation) and the total screened effective field is the sum of the external field and this induced field. The screening is largest in systems for which the virtual transitions have large overlap and hence large oscillator strength. With this in mind, it is quite reasonable to suppose that polarization effects will be important in photoabsorption at excitation frequencies where strongly overlapping orbitals are connected by real - rather than virtual - transitions. But, as the catalogue given in the first section indicates, this is precisely where the giant resonances occur.

TIME-DEPENDENT LOCAL DENSITY APPROXIMATION

The time-dependent local density approximation (TDLDA) was conceived as a means to include polarization-type many-body effects in a dielectric¹⁸ response formulation of photoabsorption within the context of the density functional formalism. I have reviewed this subject in some detail elsewhere¹⁹ and Wendin²⁰ has provided an account of the relationship between this method and earlier RPAE calculations. Therefore, here I shall focus on the economy and interpretative advantage offered by the method and note some recent results that point the way to further improvement.

Density functional theory⁸ provides an explicit prescription for calculation of the exact ground state charge density $n(x)$ of an N -electron system by solution of the following Hartree-like equations:

$$[-\nabla^2 + v_{\text{eff}}(x)]\psi_i(x) = \epsilon_i \psi_i(x)$$

$$v_{\text{eff}}(x) = v_{\text{ext}}(x) + e^2 \int dx' \frac{n(x')}{|x-x'|} + v_{\text{xc}}[n(x)] \quad (8)$$

$$n(x) = \sum_{i=1}^N |\psi_i(x)|^2$$

In this expression, $v_{\text{ext}}(x)$ is a fixed external potential (the nuclear Coulomb potential for the atomic case) and the functional $v_{\text{xc}}[n(x)]$ is called the exchange-correlation potential. The latter quantity contains all of the many-body quantum mechanics of the problem and is generally unknown. However, there exist a number of excellent approximations to the exact $v_{\text{xc}}[n(x)]$ beginning with the remarkable LDA⁸ and proceeding to more recent and significantly improved functionals²¹. For present purposes, I wish to emphasize that $v_{\text{xc}}[n(x)]$ is not to be confused with any approximation to the non-local exchange operator of Hartree-Fock theory such as the $X-\alpha$ scheme of Slater. Its conceptual and theoretical foundations are completely different although the frequently employed local density approximation to it turns out to be numerically similar to one choice of an $X-\alpha$ potential. In what follows, we will suppose that an adequate form of $v_{\text{xc}}[n(x)]$ is available and regard the $\psi_i(x)$ obtained from Equations (8) as basis functions for use in, say, Equation (2).

As noted earlier, the resulting independent particle LDA calculations of atomic photoabsorption fail badly in the regime of observed giant resonances. This is illustrated by the dashed curve in Figure 1 for barium. The calculated oscillator strength resides almost entirely in a delta function that corresponds to a $4d \rightarrow 4f$ bound-bound transition. By contrast, the measured resonance is significantly shifted to higher energy and broadened relative to the LDA result. Indeed, independent particle calculations of giant resonances quite generally yield strong, narrow absorption features that exhibit a characteristic transition energy ω_0 and width γ that are both smaller than observed. This fact alone already signals the importance of polarization effects as may be seen by use of a schematic driven oscillator model²².

Consider the equation motion for the change in density δn that is induced in an atom in the presence of an external field $E_0 \cos \omega t$ in the independent particle approximation:

$$\delta \ddot{n} + \gamma \delta \dot{n} + \omega_0^2 \delta n = E_0 \cos \omega t \quad (9)$$

The absorption cross section is related to the charge distortion through the complex, frequency-dependent polarizability $\alpha(\omega)$:

$$\alpha(\omega) = 4\pi \frac{\omega}{c} \text{Im } \alpha(\omega) \quad (10)$$

$$\alpha(\omega) = e \int dx z \delta n(x|\omega) \quad (11)$$

As noted earlier, optical transitions that occurs in the neighborhood of ω_0 contribute significantly to the polarizability if there is large overlap between the initial and final states, i.e., if δn is large. In that case, we are compelled to compute the induced Coulomb field,

$$E_{\text{induced}} \sim e \int \frac{\delta n(x')}{|x-x'|} dx' \sim -\kappa \delta n \quad (12)$$

written here for simplicity as if the integral kernel were a delta function. The constant κ is taken to be complex to represent the fact that the induced

density generally oscillates out of phase with the external field. Equation (12) now must be added to the right hand side of Equation (9) since the electrons cannot distinguish the external field from internal fields. Hence, the effective equation of motion is

$$\delta \ddot{n} + (\gamma + \text{Im}\kappa)\delta \dot{n} + (\omega_0^2 + \text{Re}\kappa)\delta n = E_0 \cos \omega t \quad (13)$$

which clearly demonstrates the shifting and broadening required to recover agreement with experiment.

The essence of the TDLDA is precisely that of the oscillator model sketched above - made a bit more quantitative by inclusion of the quantum-mechanical dynamical response of the atom. The most transparent statement of the defining equations is:

$$U_{\text{ind}}(x|\omega) = \int dx' \frac{\delta n(x'|\omega)}{|x-x'|} + \frac{\partial V_{xc}(x)}{\partial n(x)} \delta n(x|\omega)$$

$$\delta n(x|\omega) = \int dx' \chi_0(x, x'|\omega) [U_{\text{ext}}(x') + U_{\text{ind}}(x'|\omega)] \quad (14)$$

The first line takes account of the classical induced potential considered above and, in addition, includes an induced exchange-correlation potential. The latter can be significant ($\sim 30\%$ of the total induced field for low-density outer shells) and should not be neglected. The second line describes precisely how the electronic charge density distorts in the presence of an effective driving field $U_{\text{eff}}(x|\omega)$. This response is dictated by a density-density correlation function χ_0 appropriate to the independent particle system and is exactly calculable for an atom within the LDA. Solution of the integral equation (14) is equivalent to generating the local density analog of the random phase approximation to the exact χ from χ_0 for use in Equation (6). The cross section may be found either from the converged value of δn and Equations (10) and (11) or by replacing the external field by the effective field in the Golden Rule¹⁸, viz.,

$$\sigma(\omega) = 4\pi^2 \alpha \hbar \omega \sum_{i,f} |\langle f | \epsilon \cdot U_{\text{eff}}(x|\omega) | i \rangle|^2 \delta(\hbar\omega - \epsilon_f + \epsilon_i) \quad (15)$$

This formula is particularly valuable as an aid in the interpretation of calculations.

The heavy solid curve in Figure 1 is the result of a TDLDA calculation of the photoabsorption of barium near the 4d threshold. The agreement with the experimental "giant resonance" is quite good and is typical of what one finds with this method. In its present form, the TDLDA averages over any structure due to multi-electron excitation and/or multiplet effects. However, in my view, the principal utility of this method is that direct visual inspection of the space and frequency dependent effective driving potential $U_{\text{eff}}(x|\omega)$ (or its gradient - the internal "electric" field) leads to substantial physical insight into the excitation process. For example, the idea that the 4d shell may be thought of as a single damped driven "collective" oscillator in the giant resonance regime is borne out in the following manner. If this notion is correct, the oscillations induce a dipolar charge separation within the 4d shell (see Figure 3). Below resonance, i.e., below the peak in the absorption curve, we expect the charge to oscillate in phase with the external field. The resulting induced field then screens the external field within the 4d charge radius and antiscreens the external field at radii in excess of the 4d shell mean radius. The situation is reversed at frequencies above the resonant absorption maximum. The shell now oscillates 180° out of phase with the external field and the screening/anti-screening characteristics switch accordingly. Gratifyingly, this simple

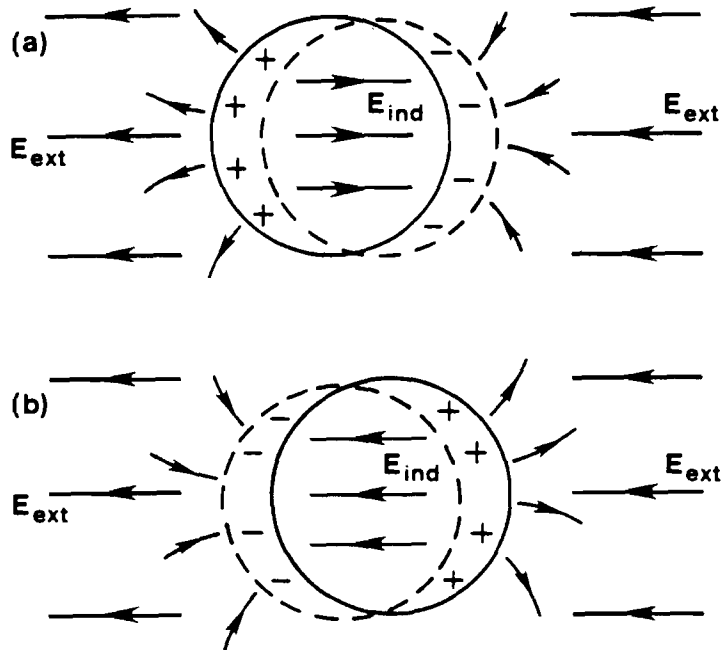


Fig. 3. Schematic model of an atom in an time-dependent electric field: (a) induced charge oscillates in phase with the field; (b) induced charge oscillates out of phase with the field.

picture is borne out precisely by the calculated effective fields¹⁹.

It is possible to cast these results in a fashion even more akin to the traditional dielectric response approach of condensed matter physics. We define an effective local screening function by the relation

$$\epsilon^{-1}(\mathbf{x}|\omega) = \frac{U_{eff}(\mathbf{x}|\omega)}{U_{ext}(\mathbf{x})} \quad (16)$$

Combining Equations (15) and (16) it is clear that the TDLDA method ascribes all of the "many-body effects" to a dielectric function that renormalizes the transition operator while retaining the original independent particle orbitals. Hence, we can retain our intuition about what orbital wave functions "look like". This contrasts with the configuration-interaction approach of atomic and molecular physics whereby one systematically improves the initial and final state wave functions. Of course, only the squared matrix element is an observable so that any partitioning of many-body effects among the initial state wave function, the transition operator, and the final state wave function is possible²³.

Now let us return to the barium example and study the behavior of the function $\epsilon^{-1}(\omega)$ ¹⁹. In particular, Figure 4 illustrates the frequency dependence of both the real and imaginary parts of this quantity at two different radial positions in the atom - an "inner" region where the 4d wave function resides and an "outer" region where the valence orbitals, e.g., 5p reside. We see immediately from Equation (15) that the partial photoionization cross section from these two orbitals are expected to be radically different. Indeed, the valence orbitals are mere spectators to the wild oscillations of the 4d shell and are "blown out" of the atom (variously termed "resonant photoemission", "direct recombination", etc.) in accordance with their spatial sampling of the effective driving field. In particular, we expect two types of resonant line shapes: one for all orbitals that occupy the same region of space as the polarizable shell and a different one for all orbitals that reside at greater radial distances¹⁸.

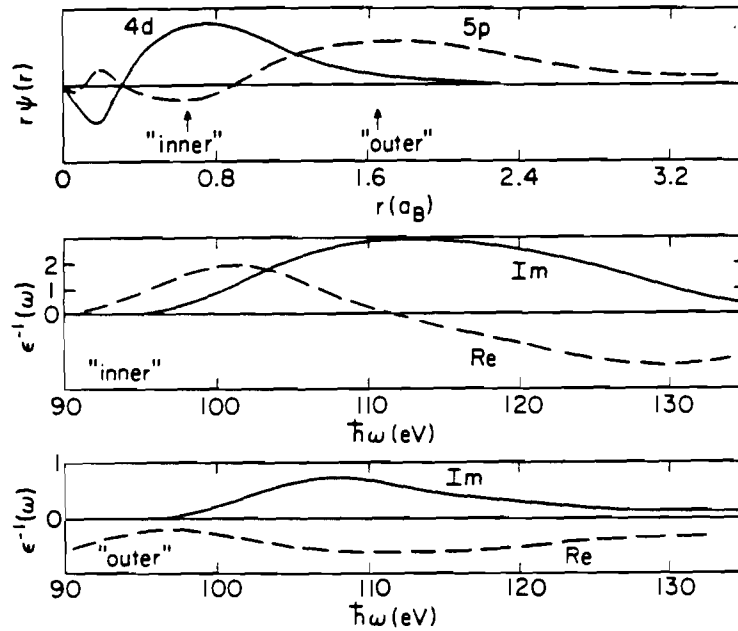


Fig. 4. Barium 4d and 5p radial wave functions and frequency dependence of the effective dielectric function at two radial distances from the nucleus. From Ref. 19.

Another advantage of the TDLDA scheme is computational economy. It is not necessary to recompute potentials anew as one enters different energy regimes. This means that many calculations can be performed rapidly in order to extract trends. For example, Figure 5 is a plot of LDA (independent particle) and TDLDA total photoabsorption cross sections over a wide energy scan for atomic ruthenium. These results were obtained by Gary Doolen of the Los Alamos National Laboratory using a relativistic version of the TDLDA²⁴. Some type of polarization effect is operative whenever these two curves differ. I have chosen this example because it illustrates an amusing case of what might be called a "double giant resonance" in the 10-100 eV range. The very sharp resonant structure around 40 eV is a giant resonance that corresponds to 4p → 4d transitions analogous to the 3p → 3d resonances in the 3d transition metal row discussed below. The interesting point is that this sharp structure is superimposed on a very broad absorption bump that occurs both in the independent particle cross section and in the TDLDA result. We would describe this feature to a dull shape resonance if it were not for the fact that the TDLDA resonance is conspicuously shifted to higher energy and broadened relative to the LDA curve by a significant amount (note the double logarithmic scale). In fact, this many-body effect arises from a polarization of the ruthenium 4d shell by "4f-like" continuum states well above threshold. If we trace this feature across the 4d transition metal row we discover that it evolves continuously into the barium giant resonance!

In closing this section it is worth remarking that the original construction of the TDLDA for photoabsorption¹⁸ was not sanctioned within formal density functional theory. The latter is a ground state theory and says nothing about excitations; one could only show that Equations (14) were valid at zero frequency²⁵. Since that time, the existence of a formal time-dependent density functional theory has been proven²⁶ and Gross and Kohn²⁷ have investigated the quality of the TDLDA in this context. Their analysis provides an a posteriori justification for the quality of the results obtained to date and suggests that future improvements in the theory, such as the inclusion of multiple excitations ("shake-up", "double-photoionization",

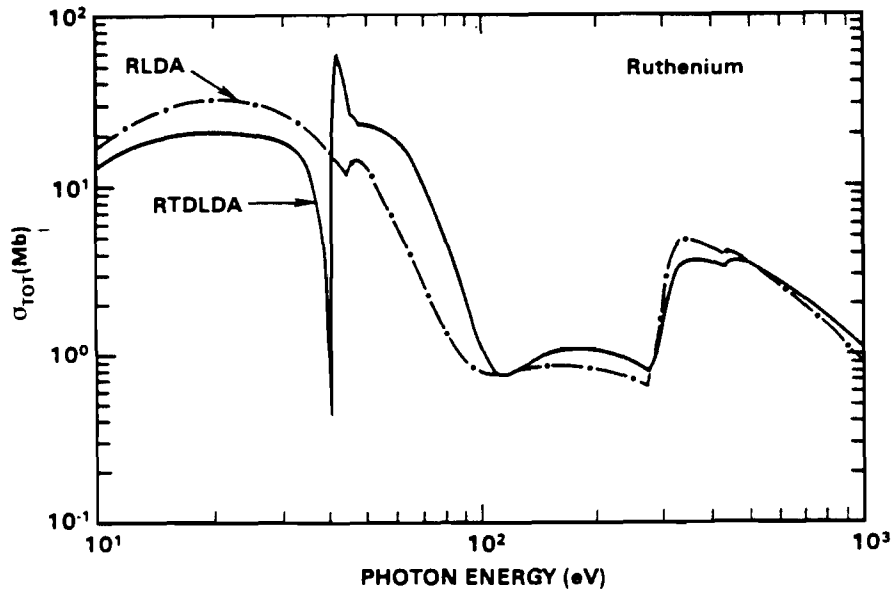


Fig. 5. Relativistic LDA and TDLDA total absorption cross sections for a ruthenium atom.

etc.) must proceed in tandem with improvements in the $v_{xc}[n(x)]$ functional itself beyond the LDA.

RESONANT PHOTOEMISSION IN SOLIDS

By far the most common application of giant resonance phenomena in solid state physics is the use of resonant photoemission to "project out" angular-momentum resolved components of the valence band density of states. At its root, this technique relies on a simple quantum mechanical effect. Suppose that two distinct one-electron excitation processes can occur at precisely the same photon energy, e.g., a bound-bound transition and a bound-free transition (Figure 6). The total absorption exhibits a characteristic line shape that reflects the interference between these two

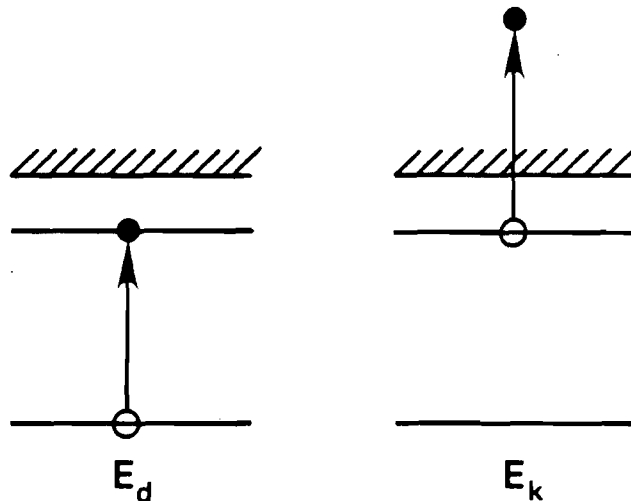


Fig. 6. Two degenerate excitation processes that interfere to produce a Fano absorption profile.

channels. This problem was first analyzed by Fano²⁸ using configuration interaction theory. Here I will sketch a derivation that uses a method more common to condensed matter physics - a model Hamiltonian.

First, let us rewrite Equation (1) in a slightly different form using the symbol T to stand for the transition operator.

$$\begin{aligned}
 \sigma(\omega) &= \sum_{-} |\langle F|T|0\rangle|^2 \delta(\hbar\omega - E_F + E_0) \\
 &= \frac{1}{\pi} \sum \langle 0|T^\dagger|F\rangle \operatorname{Im} \frac{1}{\hbar\omega - E_F + E_0 - i\eta} \langle F|T|0\rangle \\
 &= \frac{1}{\pi} \operatorname{Im} \langle 0|T^\dagger \frac{1}{\hbar\omega + E_0 - H} T|0\rangle \\
 &= \frac{1}{\pi} \operatorname{Im} \langle 0|T^\dagger GT|0\rangle
 \end{aligned} \tag{17}$$

Since T connects the ground state to the excited states we see that the photoabsorption depends only on the matrix elements of the Hamiltonian within the manifold of excited states. One way to proceed is to write down explicitly a model Hamiltonian, calculate the excited states (usually approximately) and compute the matrix elements (cf. the contribution of Gunnarsson to this volume). Alternatively, one can simply assign the matrix elements. This is the practical approach for our simple problem:

$$\begin{aligned}
 \langle d|H|d\rangle &= E_d \\
 \langle k|H|k\rangle &= E_k \\
 \langle d|H|k\rangle &= V_k
 \end{aligned} \tag{18}$$

E_d and E_k are the energies of the bound-bound and bound-free transitions (the latter is degenerate with the former for one particular value of k) and V_k is a coupling matrix element that describes the dipole-dipole interaction between the two types of particle-hole pairs or, less precisely, describes the decay of one excitation into the other. All that remains is algebra²⁹ and one finds the familiar Fano result that the pure absorption cross section to the continuum is multiplied by a modulation factor that reflects the interaction with the discrete excitation:

$$\begin{aligned}
 \sigma(\omega) &= \sum |T_{ok}|^2 \delta(\hbar\omega - E_k) \frac{(q+\epsilon)^2}{1+\epsilon^2} \\
 q &= \frac{T_{od} + \sum T_{ok} \frac{V_k}{\hbar\omega - E_k}}{\pi \sum T_{ok} V_k \delta(\hbar\omega - E_k)} \\
 \epsilon &= \frac{\hbar\omega - E_d - \sum \frac{|V_k|^2}{\hbar\omega - E_k}}{\pi \sum |V_k|^2 \delta(\hbar\omega - E_k)}
 \end{aligned} \tag{19}$$

What happens if more than one continuum channel is open, i.e., there exist one-hole final states where the hole can occur in different subshells? A (rather more complicated) multi-channel Fano-type calculation is possible³⁰ and one finds resonances of the form of Equation (19) with different

q-values for each of these partial photoionization cross sections. The resonances are particularly large and distinctive if one of the degenerate channels exhibits a large one-particle transition moment - much of this oscillator strength can be transferred to resonant photoemission in a different channel. This is precisely the situation at a giant resonance. One finds core-to-valence absorption strength transferred to valence band photoemission intensity. The reader will recognize that the TDLDA approach discussed above provides a ready means to gauge the relative partitioning of strength amongst the open partial photoionization channels: unless direct emission from the polarizable core level itself predominates, the strongest resonance will occur from the state with maximal overlap with the core level and, hence, with the effective driving field. One reaches the same conclusion by asking which of the V_k Coulomb matrix elements is largest. This idea has been used particularly extensively to accentuate the 4f and 5f partial densities of states in lanthanide³¹ and actinide³² materials near their respective 4d and 5d giant resonances*.

The explicit application of these ideas to the barium example (and more generally to the whole lanthanide row) provides another opportunity to emphasize that "many-body" effects can be partitioned in different ways to suit different purposes. Previously we imagined a one-step process whereby the polarization effects built into the TDLDA transferred spectral oscillator strength from a bound-bound transition below the 4d threshold to a broad giant resonance above threshold. An alternative and equally valid point of view first was propounded by Dehmer et al.³³. They broke the problem into two parts. First, the large overlap-driven Coulomb exchange integral between the 4d initial state and 4f final state was imagined to drive the oscillator strength up in energy through the vacuum threshold and into the f continuum. This no-longer "discrete" excitation then interferes with, i.e., decays into, the continuum and the width and line shape have the Fano form. I wish to emphasize that the physics that enters this discussion is identical to that included in the TDLDA. One can use both languages interchangeably to illuminate different aspects of the problem.

An interesting example of giant resonance photoemission used as a tool to study an unrelated condensed matter problem occurs for samarium metal. In this case, one finds³⁴ that as the photon energy is tuned above the 4d threshold two distinct parts of the electron energy distribution curve exhibit giant resonance intensity enhancements. However, the energy dependence of these features, i.e., the 4f partial cross sections, are not identical (Figure 7). This is interesting because it is known (from other considerations) that one curve is characteristic of the bulk of the sample whereas the other is characteristic of just the uppermost atomic layer at the surface of the sample. Why might these cross sections be so different? The answer may be found by comparison of the experimental curves with relativistic TDLDA 4f partial photoionization cross sections for samarium atom in two different valence configurations: $[\text{Xe}]4f^6 6s^2$ and $[\text{Xe}]4f^5 6s^2 5d$. Bulk samarium metal is known to exhibit the trivalent configuration and the $4f^5$ cross section does indeed match nicely with the major peak in the data. However, the principal peak in the surface spectrum matches well with the $4f^6$ calculation - the configuration known to exist for a free samarium atom! We conclude that the surface atoms are in a different valence state than the bulk. This result is not outlandishly surprisingly if we note that the bonding state of a surface atom is in some sense midway between that of a normal bulk atom and a free atom. Of course, this argument applies to any

* It is worth remarking that the subtraction techniques commonly used in experimental papers to extract "f" densities of states are not without problems. Resonant photoemission from other parts of the valence band and resonant Auger processes can considerably obscure the situation.

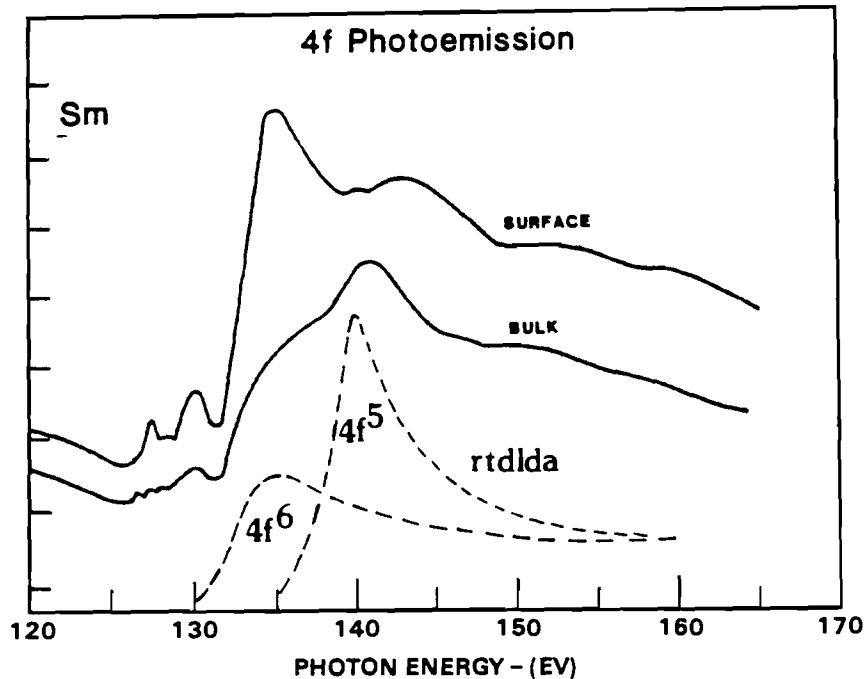


Fig. 7. 4f partial photoionization cross sections from the bulk and surface of samarium metal along with TDLDA calculations (see text). Data from Ref. 34. The experimental curves are not normalized to one another or to the theory.

solid. It turns out³⁵ that the energy balance is quite delicate and it appears that samarium has the singular distinction of being the only elemental solid whose surface atoms maintain their free atom configuration when the solid is assembled.

CASE HISTORY: 3D TRANSITION METALS

Up till now, we have taken the attitude that giant resonance phenomena in condensed matter systems is essentially an "atoms-in-solids" effect. This is certainly true for the lanthanides where both the initial and final states in the $4d \rightarrow 4f$ excitation are undoubtedly atomic-like. A major (and difficult) physics problem has been to infer the magnitude of solid state hybridization with the narrow f-states (see e.g., Ref. 31; a different approach to this problem is discussed by J. Fuggle in this volume). However, I now wish to argue that a new richness enters the problem if we study cases where explicit, solid state, one-body (finite bandwidth) and many-body (conduction electron response) effects come into play. To make this point I draw two examples from the 3d transition metal row: nickel and chromium.

Suppose many body effects did not exist. Then, for a metal, optical absorption from a core level is described by a Golden Rule expression that factorizes into the product of an atomic-like transition moment and the bulk unoccupied density of states³⁶. This simple scheme is well borne out, for example, by $L_{2,3}$ absorption into the empty 3d states of nickel³⁷. The simplest guess would be that $M_{2,3}$ absorption in the same system would reflect exactly the same 3d partial density of states. Unfortunately, it does not. Instead, the total absorption in nickel metal above the 3p

threshold is almost identical to the corresponding spectrum for nickel vapor. (Figure 8). The unoccupied 3d-density of states of the metal is completely distorted by the large polarizability of the nickel 3p shell (as reflected by a large 3p/3d exchange Coulomb integral). The oscillator strength is pushed into the continuum just as in the atom. Indeed, an atomic Fano-type calculation including multiplet effects⁴¹ reproduces the data quite well.

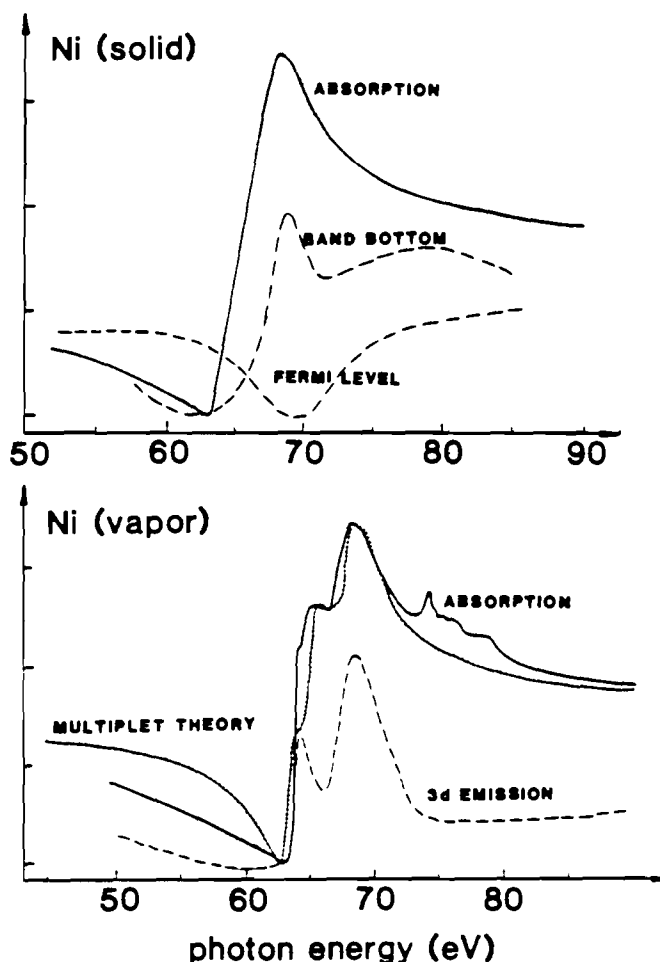


Fig. 8. Giant resonance phenomena in nickel. Top panel: total absorption (Ref. 38) and 3d partial cross sections (Ref. 39). Bottom panel: total absorption and 3d partial cross section (Ref. 40). Theory from Ref. 41.

Now focus attention on the metallic valence band photoionization cross sections. Notice that emission from occupied states near the bottom of the 3d band tracks the total absorption and is atomic-like whereas emission from 3d states near the Fermi level shows a distinct anti-resonance. I have surveyed the literature and discovered that this peculiar effect occurs in all the 3d transition metals to the right of chromium. The Fermi level emission (which corresponds to initial states near the middle and top of the band for Mn and Ni, respectively) may be explicable using a result obtained by Davis and Feldkamp³⁰. They showed that a Fano effect occurs in a purely solid state model consisting of an unfilled s-band and a single deep core level. The role of the "discrete" excitation is played by absorption from the core

level to the Fermi level. The band emission shows an anti-resonance.

Unfortunately, this model shows an anti-resonance for emission from all parts of the occupied band - including the band bottom. Hence, the question remains: why do extended 3d-states at the band bottom act like free nickel atom states? A possible solution goes back (at least) to the work of Combescot and Nozieres⁴² who were concerned with the response of a free electron solid to the sudden creation of a core hole. This is a many-body problem although the answer is easy to guess. The core hole screens itself by drawing electrons towards itself, both spatially and energetically. This tends to distort the density of states and piles up spectral weight at the bottom of the band. If the core hole potential is strong enough it "splits off" a discrete atomic-like state below the band edge. We infer from this argument that valence band wave functions at the bottom of the band are almost condensed into atomic states themselves in the presence of a core hole. Although no detailed calculations have been performed it appears that one might be in the interesting situation where the direct 3p/3d Coulomb interaction collapses extended states into localized states while the corresponding exchange interaction pushes the oscillator strength up into the giant resonance region.

The story is rather different for the transition metal elements to the left of manganese. In these materials the exchange interaction of the valence band with the 3p core hole is still large but the Coulomb interaction among the valence electrons is smaller than for the later members of the series. The latter statement means that the 3d electrons in, say, vanadium are rather less atomic like in the ground state than the 3d electrons in nickel. The best available data is for chromium (Figure 9) for which the atomic giant resonance is very much in evidence. However, neither the relevant atomic Fano calculation⁴¹ nor the simple solid state model calculation³⁰ (both broadened to account for the unoccupied chromium d-band

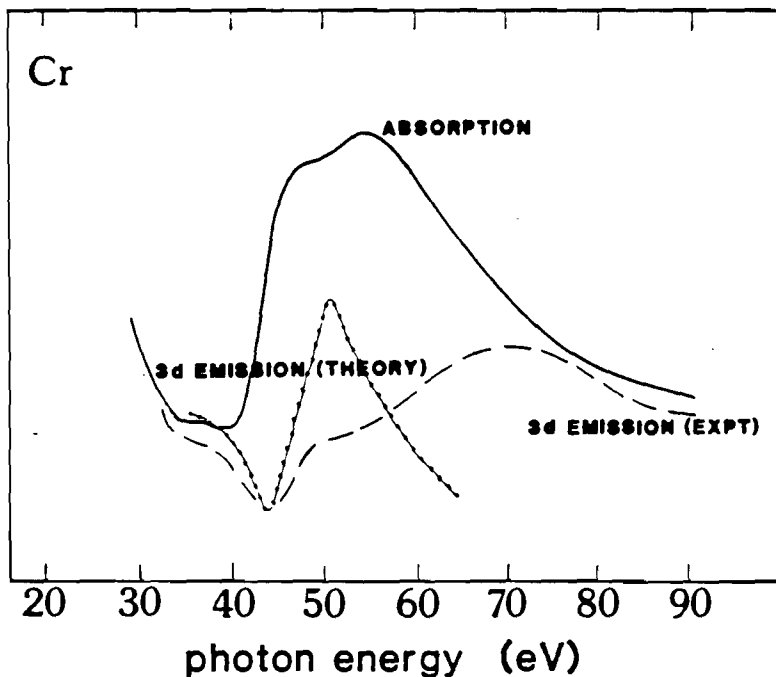


Fig. 9. Giant resonance phenomena in chromium: total absorption (Ref. 38) and 3d partial photoionization cross section (Ref. 43). Theory is described in text.

width) adequately describe the peculiar "delayed onset" of the 3d emission from this metal.

At present, I can offer only a (barely credible) suggestion that might be applicable to this situation. Oh and Doniach⁴⁴ studied the problem of resonant photoemission in the presence of core hole screening processes. However, instead of screening by a quasi-localized orbital as discussed above for nickel, they considered electron gas screening mechanisms such as plasmon and particle-hole excitation. They find that under certain circumstances oscillator strength in the main emission line indeed is shifted from the nominal peak maximum at energy ϵ to energy $\epsilon + \hbar\omega_p$ where $\hbar\omega_p$ is the plasmon energy. Unfortunately, chromium is far from a free electron metal with a well-developed collective plasma excitation. Instead, its "plasmon" is formed from weakly coupled low frequency interband transitions and an analysis along these lines is problematical. Nonetheless, my main point is that giant resonance processes persist in the early 3d transition metals (and very likely also in the nominally band-dominated 4d and 5d transition rows) but are significantly modified from a simple atomic picture. A systematic study of precisely how this dramatic effect washes away as solid state effects become increasingly important would be quite interesting - both theoretically and experimentally.

CONCLUSION

In this report I have tried to analyze the problem of giant resonance absorption and photoemission from the point of view of condensed matter physics. The basic phenomenon may be understood in a very appealing manner by the use of density functional methods in a real-space approach to the dielectric response of inhomogeneous electron systems. The resonance effect now is a standard tool in the condensed matter electron spectroscopic community and is used to probe many aspects of the electronic structure of solids that are inaccessible by other means. Here, I have focused only on metallic solids. The reader is invited to explore related work in compound semiconductors⁴⁵ and small metal particles⁴⁶ and, indeed, invent new applications himself!

I gratefully acknowledge the support of the US Department of Energy for my research on this subject under Grant DE-FG05-86ER45243.

REFERENCES

1. P. Rabe, K. Radler and H. W. Wolff in Vacuum UV Radiation Physics, edited by E. E. Koch et al. (Vieweg-Pergamon, Berlin, 1974), p. 247.
2. D. J. Rowe, Nuclear Collective Motion (Methuen, London, 1970).
3. D. Pines and P. Nozieres, The Theory of Quantum Liquids (W. A. Benjamin, New York, 1966).
4. H. P. Kelly, S. L. Carter and B. E. Norum, Phys. Rev. **A25**, 2052 (1982). See also the contribution of C. Clark to this volume.
5. H. P. Kelly, Phys. Scr. **21**, 448 (1980) and this volume.
6. C. A. Nicolaides in Advanced Theories and Computational Approaches to the Electronic Structure of Molecules, edited by C. E. Dykstra (Reidel, Dordrecht, 1984), pp. 161-184 and this volume.
7. P. Hohenberg and W. Kohn, Phys. Rev. **136**, B864 (1964); W. Kohn and L. J. Sham, Phys. Rev. **140**, A1133 (1965).
8. For a review, see Theory of Inhomogeneous Electron Gas, edited by S. Lundqvist and N. H. March (Plenum, New York, 1983).
9. C. S. Wang and B. M. Klein, Phys. Rev. **B24**, 3417 (1981) and references therein.
10. P. B. Roulet and P. Nozieres, J. Phys. (Paris) **29**, 167 (1968).

11. M. Ya. Amusia and N. A. Cherepkov, *Case Studies in Atomic Physics* 5, 47 (1975).
12. G. Wendin in *Photoionization and Other Probes of Many-Electron Interactions*, edited by F. J. Wuilleumier (Plenum, New York, 1976).
13. F. Bassani and G. Pastori Parravicini, *Electronic States and Optical Transitions in Solids* (Pergamon, Oxford, 1975).
14. A. Zangwill and Z. Levine, *Am. J. Phys.* 53, 1177 (1985).
15. W. Hanke, H. J. Mattausch and G. Strinati in *Electron Correlations in Solids, Molecules and Atoms*, edited by J. T. Devreese and F. Brosens (Plenum, New York, 1983), p. 289.
16. R. Resta and A. Baldereschi, *Phys. Rev.* B23, 6615 (1981).
17. L. I. Schiff, *Quantum Mechanics* (McGraw-Hill, New York, 1968), 3rd edition, p. 265. See also W. Brandt and S. Lundqvist, *Arkiv Physik* 28, 399 (1964).
18. A. Zangwill and P. Soven, *Phys. Rev. Lett.* 45, 204 (1980); A. Zangwill and P. Soven, *Phys. Rev.* A21, 1561 (1980).
19. A. Zangwill in *Atomic Physics* 8, edited by I. Lindgren, A. Rosen and S. Svanberg (Plenum, New York, 1983), p. 339; A. Zangwill in *EXAFS and Near Edge Structure III*, edited by K. O. Hodgson, B. Hedman and J. E. Penner-Hanh (Springer, Berlin, 1984), p. 13.
20. G. Wendin in *New Trends in Atomic Physics*, edited by G. Grynberg and R. Stora (North-Holland, Amsterdam, 1984), p. 555.
21. D. C. Langreth and M. J. Mehl, *Phys. Rev.* B28, 1809 (1983).
22. A. Zangwill and P. Soven, *J. Vac. Sci. Tech.* 17, 159 (1980).
23. Z. Crljen and G. Wendin, *Phys. Scr.* 32, 359 (1985) and to be published.
24. D. A. Liberman and A. Zangwill, *Comp. Phys. Commun.* 32, 75 (1984).
25. M. J. Stott and E. Zaremba, *Phys. Rev.* A21, 12 (1980).
26. H. Kohl and R. M. Dreizler, *Phys. Rev. Lett.* 56, 1993 (1986).
27. E. K. U. Gross and W. Kohn, *Phys. Rev. Lett.* 55, 2850 (1985).
28. U. Fano, *Phys. Rev.* 124, 1866 (1961).
29. A. Shibatai and Y. Toyozawa, *J. Phys. Soc. Jpn.* 25, 335 (1968).
30. L. C. Davis and L. A. Feldkamp, *Phys. Rev.* B23, 6239 (1981).
31. D. Wieliczka, J. H. Weaver, D. W. Lynch and C. G. Olson, *Phys. Rev.* B26, 7056 (1982).
32. A. Fujimori and J. H. Weaver, *Phys. Rev.* B31, 6411 (1985).
33. J. L. Dehmer, A. F. Starace, U. Fano, J. Sugar and J. W. Cooper, *Phys. Rev. Lett.* 26, 1521 (1971).
34. J. W. Allen, L. I. Johansson, I. Lindau and S. B. Hagstrom, *Phys. Rev.* B21, 1335 (1980).
35. B. Johansson, *Phys. Rev.* B19, 6615 (1979).
36. J. E. Muller and J. W. Wilkins, *Phys. Rev.* B29, 4331 (1984).
37. R. D. Leapman, L. A. Grunes and P. L. Fejes, *Phys. Rev.* B26, 614 (1982).
38. B. Sonntag, R. Haensel and C. Kunz, *Solid State Commun.* 7, 597 (1969).
39. J. Barth, G. Kalkoffen and C. Kunz, *Phys. Lett.* 74A, 360 (1979).
40. E. Schmidt, H. Schroder, B. Sonntag, H. Voss and H. E. Wetzell, *J. Phys.* B16, 2961 (1983).
41. L. C. Davis and L. A. Feldkamp, *Solid State Commun.* 19, 412 (1976).
42. M. Combescot and P. Nozieres, *J. Phys. (Paris)* 32, 913 (1971).
43. J. Barth, F. Gerken and C. Kunz, *Phys. Rev.* B31, 2022 (1985).
44. S. J. Oh and S. Doniach, *Phys. Rev.* B26, 1859 (1982).
45. A. Franciosi, S. Chang, R. Reifengerger, U. Debska and R. Riedel, *Phys. Rev.* B32, 6682 (1985).
46. M. J. Puska, R. M. Nieminen and M. Manninen, *Phys. Rev.* B31, 3486 (1985); W. Ekhardt, *Phys. Rev.* B31, 6360 (1985).

5f-Bandwidth and Resonant Photoemission of Uranium Intermetallics

D.D. Sarma, F.U. Hillebrecht & C. Carbone
Institut für Festkörperforschung
Kernforschungsanlage Jülich
D-5170 Jülich, FRG

and

A. Zangwill
School of Physics
Georgia Institute of Technology
Atlanta, GA 30332
USA

5f-bandwidth and Resonant Photoemission of Uranium Intermetallics

Resonant photoemission technique has been extensively used to study the valence band features of 3d transition metals¹⁻³ at the 3p-threshold energies and the rare earth systems⁴⁻⁷ at the 4d-threshold energies. Subsequently, this technique has been extended to the study of the actinide systems⁸⁻¹¹ in particular to the uranium compounds. From these studies, it has been concluded that this technique offers the possibility of unambiguous identification of the states with f-character from the states of other symmetries¹¹. The recent discovery of unusual heavy-fermion (possibly triplet) superconductivity in uranium compounds, where the f-states are believed to play a crucial role, has naturally led to the application of the resonant photoemission technique in order to determine the nature of the f-states in these compounds¹²⁻¹⁶.

In all these studies the difference between the on- and off resonant spectra has been taken as the "true" 5f spectral weight, and the width and shape of this difference spectrum have been discussed with reference to the unusual properties of these compounds. In this letter we show, using new experimental results (on UB_6 and USi_3) as well as those already existing in the literature, that the difference spectrum is not at all representative of the 5f spectral weight, but is considerably broadened by certain many-body processes that dominate the resonant excitation phenomenon. On the basis of theoretical estimates of different decay channels, we discuss the possible explanation of this behaviour in terms of resonant Auger decay channel competing with the direct recombination channel that contributes to the enhancement of the f ionization probability. Based on the systematics of the already existing data, we further show that while the difference spectra are not representative of the 5f-states in these compounds, their widths correlate with the extent of hybridization between the U 5f states and other ligand states and hence

can be used to discuss the hybridization effects in uranium compounds.

The samples of UB_4 and USi_3 were made by melting the constituents in an inductively heated levitation crucible under Ar atmosphere and were checked to be homogeneous single phase specimens by x-ray diffraction and metallography. The x-ray photoelectron spectrometer employed in the present study has been described earlier¹⁷. The synchrotron radiation photoemission spectra of UB_4 were recorded on the SX700 beamline in BESSY, Berlin and those of USi_3 were recorded in NSLS, Brookhaven. The details of the experiments are given elsewhere^{16,18}.

In Fig.1a we show the spectra of UB_4 at $h\nu = 102, 110$ and 1486.6 eV. The corresponding spectra of USi_3 are shown in Fig.1b. The 102 and 110 eV spectra of UB_4 and USi_3 are the off- and on-resonant spectra as determined by the absorption curves around 4d threshold¹⁹. Before we discuss the resonant photoemission spectra ($h\nu = 102$ and 110 eV), let us first consider the spectra recorded at an energy (1486.6 eV) above the resonant energy region. The relative atomic cross-sections²⁰ at 1486.6 eV for the different states $U5f : U6d : B2p : Si3p$ are as follows:

$$1.0 : 5.7 \times 10^{-2} : 1.9 \times 10^{-4} : 1.3 \times 10^{-2}$$

This shows that at this energy, $U5f$ states (for both the compounds) have much larger contribution to the spectra and most of the features in the experimental spectra is thus attributable to the $5f$ states. The widths of the spectra at 1486.6 eV are 1.9 and 1.3 eV for UB_4 and USi_3 respectively. Now if we turn our attention to the spectra of these two compounds recorded at $h\nu = 110$ eV, it immediately becomes clear that the spectral weight is considerably broader here compared to those recorded at $h\nu = 1486.6$ eV. At this photon

(± 10 eV)
 energy the widths of the spectra of UB_4 and USi_3 are 3.0 and 2.8 eV respectively (Fig.1).

If we subtract the off-resonant spectra from the on-resonant ones in order to extract the "pure" 5f states¹¹, the widths of the difference spectra turn out to be 2.7 and 2.5 eV for UB_4 and USi_3 respectively. These values are still much too large compared to the widths of the spectra recorded at 1486.6 eV. This makes it evident that the difference spectra are certainly not representative of the 5f states as the 5f states cannot possibly have spectral widths larger than those at 1486.6 eV representing a mixture of 5f states and other states.

Here we have shown this phenomenon of broadening of the spectral weight on resonance for two specific cases, namely UB_4 and USi_3 ; however this situation is quite general for all uranium compounds as can be seen from a compilation of spectral widths of other compounds published in the literature. We tabulate the spectral widths at different $h\nu$ values for a number of uranium compounds in Table 1. From this Table, it is clear that while the spectral widths at 1486.6 eV and 40-60 eV are comparable, these on resonance are much too broad for α -U, UBe_{13} , USi_3 , UB_4 , UGa_3 and UGe_3 . The widths at different $h\nu$ including on-resonance are comparable for $UA1_2$, UIn_3 and USn_3 . Two different systematics can be observed from Table 1. First, among the two resonant excitations ($h\nu = 98$ and 110 eV), the higher excitation (110 eV) leads to a more pronounced broadening as seen in the case of α -U and UBe_{13} . Second, if we qualitatively order the compounds in Table 1 according to the strength of hybridization between U 5f states and ligand states²¹, we find the extent of spectral broadening is larger for stronger hybridization.

Keeping in mind these observations we now turn to discuss the possible mechanism of this broadening of the spectral features on resonance excitation.

Following the resonant excitation in uranium compound, a 5d electron makes a transition into any one of the different virtual bound states (different terms of the $5d^9 5f^{n+1}$ multiplet configuration) trapped near the atom by the angular momentum barrier²². There are several decay channels that this virtual excited state can subsequently follow; three of these decay channels which are relevant to the present discussion are shown schematically in fig.2. These are: (A) direct 5d emission where the excited "5f" state tunnels out of the angular momentum barrier into the free particle ϵf continuum; (B) direct recombination or resonant 5f photoemission where a super Coster Kronig (SCK) Auger transition leads to a single hole in the 5f band; and (C) resonant Auger decay^{9,10,23-26} where the 5d hole state is filled with an SCK involving the 5f-band accompanied by a "5f" $\rightarrow E_F$ transition. It should be noted here that, very much like the decay channel B, channel C while representing an Auger like process leads to a constant binding energy feature whose energy is determined by the energy difference between the initial state ($5d^{10} 5f^n$) and the final state ($5d^{10} 5f^{n-2} E_F$). The line shape of the resonant Auger signal will be given by the self-convolution of the 5f band if the intraatomic Coulomb interaction is small. This leads to a signal at E_F which is considerably broader than the spectral weight of the 5f band; for example the self-convolution of the 5f spectrum of U metal leads to a broad peak with 3 eV full width at half maximum. Thus it is clear that if this decay channel were to become important in comparison to the direct recombination channel (B in Fig.2), the resulting spectrum near the Fermi level will be considerably broader than the pure 5f spectral width. In the following we argue that the resonant Auger decay channel can indeed steal strength from channels (A) and (B) of Fig. 2 to give rise to the experimentally observed broadening.

In order to be able to get a resonant Auger decay, the most important step of "5f" excited state $\rightarrow E_F$ transition must be realized. This requires

a substantial amount of core-hole valence electron direct Coulomb interaction (U_{cv}) to generate a quasi-localized state at E_F ; moreover the excited "5f" state must lie above the vacuum level (E_v). This can be achieved when the exchange interaction strength (U_{ex}) is larger than U_{cv} . This latter condition is almost always satisfied in metals, as the direct coulomb interaction is much better screened than the exchange interaction in metals²⁷. As pointed out earlier, we also require that the 5f Intraatomic Coulomb correlation strength (U_{vv}) be small compared^{to} the bandwidth W in order to obtain the self-convolution of the 5f band as the Auger line shape. Thus the requirement is that $U_{ex} > U_{cv} > W > U_{vv}$. Here the first of the inequalities ensures that the intermediate excited "5f" state is above E_F , the second one leads to the condensation of the band into the atomic state which is required for a pronounced resonance and also increases the probability of the excited "5f" \rightarrow 5f at E_F transition. The last inequality ensures a band-like Auger line shape. We show the estimate of these energies for various groups of metals in Table 2. From this tabulation, it is clear that the early actinides are the candidates that fulfill the requirements best. In the case of the rare earths, the Intraatomic Coulomb interaction, U_{vv} , is much larger than the bandwidth W and this leads to the splitting out of the Auger line with two holes in 4f from the single-particle excitation spectrum. The situation is very similar for Ni where the two-hole state appears 6 eV below E_F and exhibits considerable resonant enhancement at the 3p threshold. In the case of the lighter 3d transition metals, the core hole-valence electron attraction, U_{cv} , is sufficiently well screened out to lead to a low probability of excited "3d" to E_F transfer. However, even in these cases small broadening of the spectral weight close to E_F has been observed around 3p excitation threshold²⁸. In view of these facts, one should indeed anticipate a considerable contribution to the spectrum from

the resonant Auger decay channel in the light actinide systems where the conditions for such a transition is best fulfilled.

Now we turn to the question of relative strengths of the different decay channels. Estimates from relativistic time dependent local density approximation (TDLDA) calculations²⁹ show that the relative cross-sections for channels (A), σ_A , and (B), σ_B , is $\sigma_A / \sigma_B \sim 5$ for the lighter actinides. The Auger matrix element in channel (C) is similar in magnitude to that in channel (B) and the excited $5f^n \rightarrow 5f (E_F)$ transition is similar to $5f^n \rightarrow \epsilon f$ of channel (A). Thus, though the resonant Auger decay (C) describes a second order process, this channel will be comparable in strength to that of channel (B) (the direct recombination channel), even if only 20% of the channel (A), the direct $5d$ emission, is transferred to the excited $5f^n \rightarrow 5f$ at E_F transition. As discussed previously, two factors help this step in the case of uranium intermetallics. First, the sizable core hole - valence electron strength, U_{cv} , in uranium compounds enhances this transfer. Second, the hybridization of the U $5f$ with the ligand states which are more delocalized also helps. It is evident from Table I, that this second factor plays an important role in the uranium intermetallics, as the extent of broadening in these compounds clearly correlates with the extent of hybridization with ligand states. This also explains the fact that the magnetic (e.g. UIn_3) and the near-magnetic (e.g. USn_3 and UAl_2) compounds do not exhibit any pronounced broadening of the spectral features at the resonant energies.

Acknowledgements

One of us (D.D.S.) thanks W. Gudat for helpful discussion and one of us (A.Z.) acknowledges the support of the US Department of Energy under Grant No. DE-FG05-86ER45243.

References

1. C. Guillot, Y. Ballu, J. Paignel, J. Lecante, K.P. Jain, P. Thiry, R. Pinchaux, Y. Petroff and L.M. Falicov, Phys. Rev. Lett. 39, 1632 (1977)
2. M.Iwan, F.J. Himpsel and D.E. Eastman, Phys. Rev. Lett., 43, 1829 (1979)
3. J. Barth, F. Gerken and C.Kunz, Phys. Rev. B 31, 2022 (1985) and references therein.
4. W. Lenth, F. Lutz, J. Barth, G. Kalkoffen and C.Kunz, Phys. Rev. Lett., 41, 1185 (1978)
5. W. Gudat, S.F. Alvarado and M. Campagna, Solid State Comm., 28, 943 (1978)
6. W.F. Egelhoff, G.G. Tibbetts, M.H. Hecht and I. Lindau, Phys. Rev. Lett. 46, 1071 (1981)
7. L.I. Johansson, J.W. Allen, T. Gustafsson, I. Lindau and S.B.M. Hagstrom, Solid State Comm. 28, 53 (1978)
8. R. Baptist, M. Belakhovsky, M.S.S. Brooks, R. Pinchaux, Y. Bear and O. Vogt, Physica, 102B, 63 (1980)
9. M. Iwan, E.E. Koch and F.J. Himpsel, Phys. Rev. B, 24, 613 (1981)
10. M. Aono, T.C. Chiang, J.H. Weaver and D.E. Eastman, Sol. State Comm., 39, 1057 (1981)
11. B. Reihl, N. Martensson, D.E. Eastman, A.J. Arko and O. Vogt, Phys. Rev. B, 26, 1842 (1982)

12. G. Landgren, Y. Jugnet, J.F. Morar, A.J. Arko, Z. Fisk, J.L. Smith, H.R. Ott and B. Reihl, Phys. Rev. B, 29, 493 (1984)
13. R.D. Parks, M.L. den Boer, S. Raen, J.L. Smith and G.P. Williams, Phys. Rev. B, 30, 1580 (1984)
14. J.W. Allen, S.J. Oh, L.E. Cox, W.P. Ellis, M. Wire, Z. Fisk, J.L. Smith, B.B. Pate, I. Lindau and A.J. Arko, Phys. Rev. Lett. 54, 2635 (1985)
15. J. Ghijsen, R.L. Johnson, J.C. Spirlet and J.J.M. Franse, J. Electron Spectrosc. Rel. Phenom, in print.
16. D.D. Sarma, S. Krummacher, W. Gudat, C.L. Lin, L.W. Zhou, J.E. Crow and D.D. Koelling, Phys. Rev. B, submitted.
17. D.D. Sarma, F.U. Hillebrecht, W. Speier, N. Martensson and D.D. Koelling, Phys. Rev. Lett., submitted.
18. F.U.Hillebrecht et al on the NSLS, experimenal
19. D.D. Sarma et al, unpublished
20. J.J. Yeh and I Lindau, Atomic Data and Nuclear Data Tables 32, 1 (1985)
21. D.D. Koelling, hybridization
22. Dehmer et al PRL 26, 1521 (1971)
23. A Fujimori and J.H. Weaver, Phys. Rev. B, 31, 6411 (1985)
24. Eberhardt et al, PRL 41, 156 (1978)
25. A. Zangwill et al, PRB 24, 4121 (1981)

26. Girvin and Penn, J. Appl. Phys. 52, 1650 (1981)
27. Zaanen et al, PRB 32, 4905 (1985)
28. J. Barth, F. Gerken and C. Kunz, Phys. Rev. B. 31, 2022 (1985)
29. A. Zangwill, unpublished results
 - a) Y. Baer and J.K. Lang, Phys. Rev. B, 21, 2060 (1980)
 - b) M. Iwan et al, Phys. Rev. B, 24, 613 (1981) = ref 9
 - c) G. Landgren et al Phys. Rev. B, 29, 493 (1984) = ref 12
 - d) R.D. Parks et al, Phys. Rev. B, 30, 1580 (1984) = ref 13
 - e) A.J. Arko, C.J. Olson, D.M. Wlelczka, Z. Flak and J.L. Smith, Phys. Rev. Lett. 53, 2050 (1984)
 - f) D.D. Sarma et al, to be published
 - g) F.U. Hillebrecht et al, to be published
 - h) J.W. Allen et al, Phys. Rev. Lett. 54, 2635 (1985) = ref 14
 - i) D.D. Sarma et al, Phys. Rev. B, submitted = ref 16
 - j) Herbst et al, Phys. Scpt., 21, 553 (1980)
 - k) D.D. Sarma et al, Phys. Rev, Lett. submitted = ref 17
 - l) estimated from apny experimental spectra combining XPS and BIS
 - m) O. Gunnarasson et al, PR B 32, 5499 (1985); D.D. Sarma et al, Z. Phys. B, in print; D.D. Sarma, F.U. Hillebrecht and M.S.S. Brooks, J. Magn.

Mag. Mater. in print (The last one is for U-intermetallics).

- n) A. Zangwill, unpublished results = ref.29
- o) Fuggle et al, PR B 27, 4637 (1983)
- p) Treglia et al, J. Phys. C, 14, 4347 (1981) and Hodges et al, PRB 5, 3953 (1972)
- q) Fink et al, PR B 32, 4899 (1985).

Table I

Full widths at half minimum (FWHM) of the valence band spectra in uranium and its intermetallics at different photon energies⁽⁺⁾

Compound	XPS (1486.66)	On resonance	below resonance
U-Metal	1.1 ^a	1.9 (98) ^b 2.1 (108) ^b	1.1 (60) ^b
UBe ₁₃	1.6	2.1 (98) ^{c*} 2.9 (109) ^{d*}	1.8 (40) ^e
USi ₃	1.3	2.8 (110)	1.7 (40)
UGe ₃	1.9 ^f	2.2 (98) ^g	1.6 (50) ^g
UB ₄	1.5	3.0 (110)	
UAl ₂	1.3 ^g	1.1 (98) ^{h**}	
UIn ₃	1.9 ^f	1.9 (98) ^{i*}	
USn ₃		1.9 (98) ^{i*}	

(+) The photon energies are shown in brackets next to the widths. All energies are in eV. The references for the values taken from the literature are also shown.

* These widths correspond to the difference spectra between the photon energy shown in bracket and photon energy = 92 eV.

(**) Width of the background subtracted spectrum.

Table II

Estimates of different relevant energies in eV

	U_{VV}	W	U_{CV}	U_{ex}
early actinides	$\lesssim 2.5^{l,k}$	$\gtrsim 3^l$	$\sim 3.5^m$	$\gtrsim 10^n$
rare earths	$> 5^l$	$\lesssim 0.1^l$	$\sim 10^o$	$\gtrsim 10^n$
early 3d transition metals	$\lesssim 1^p$	$\gtrsim 5^p$	$\lesssim 3^q$	$\lesssim 10^n$

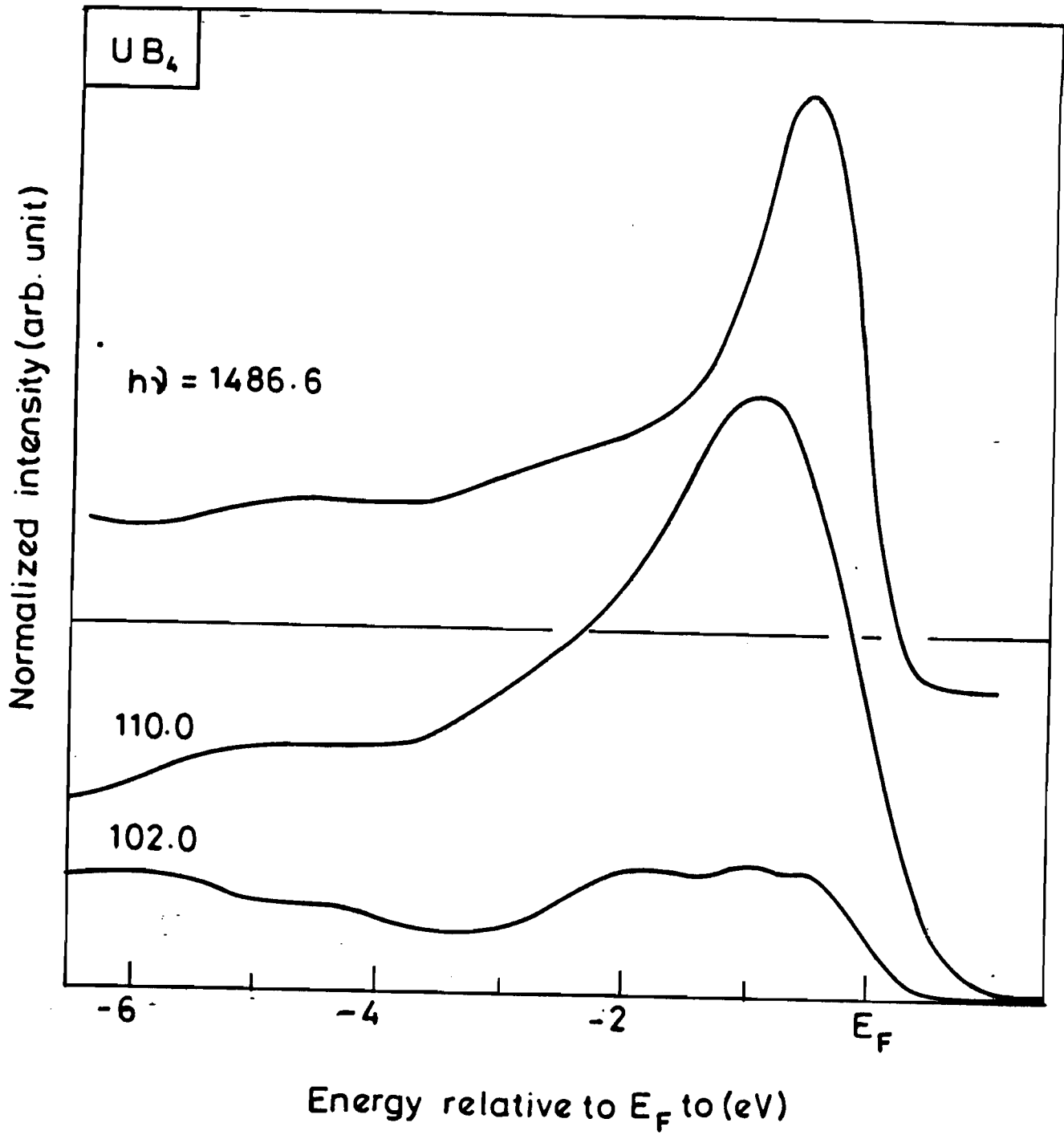


Figure 1

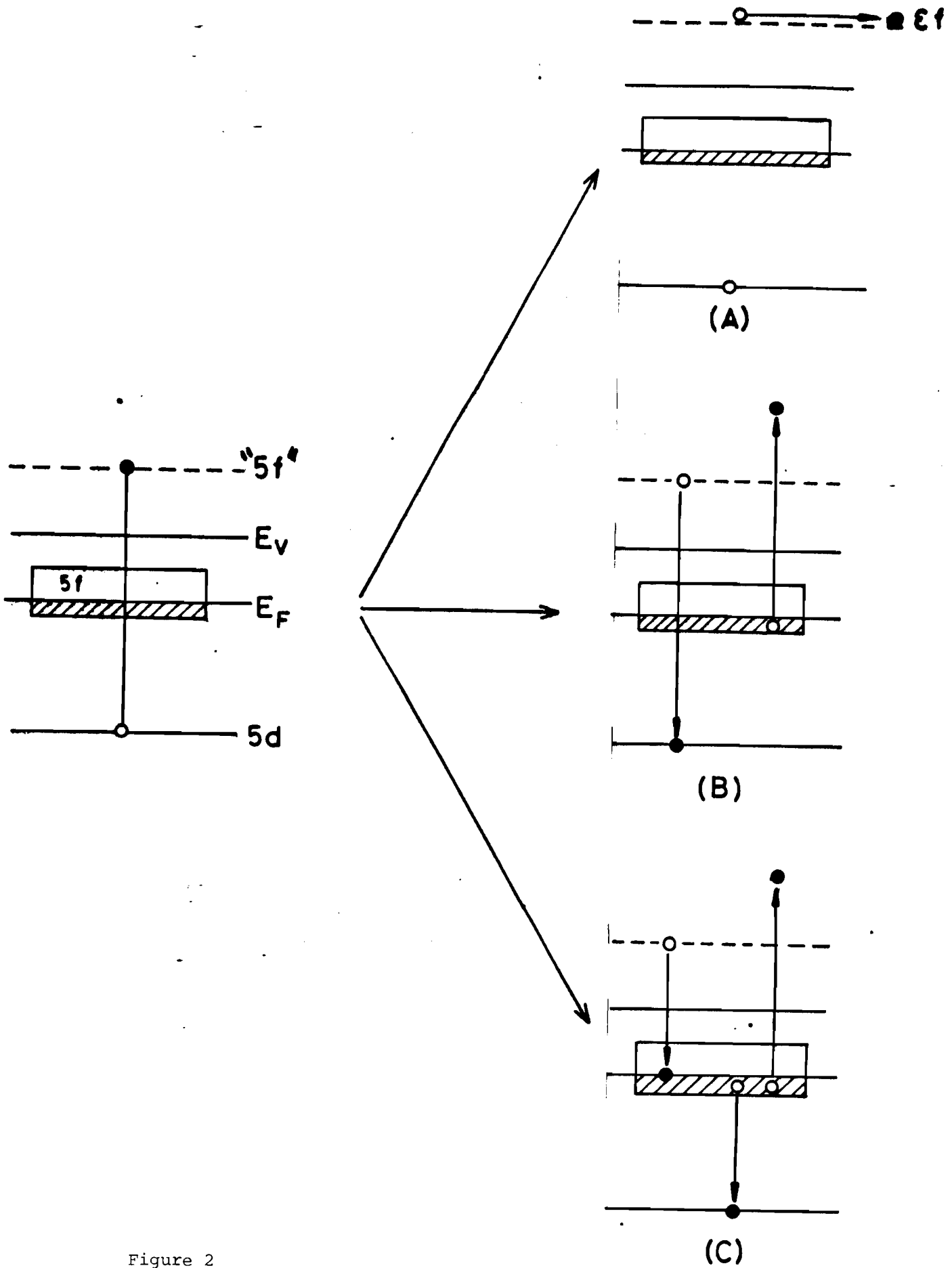


Figure 2

B-41-610

DOE F 1332.16 (10-84)
(Formerly RA-427)

OMB Approval
No. 1910-1400

U. S. DEPARTMENT OF ENERGY

UNIVERSITY CONTRACTOR, GRANTEE, AND COOPERATIVE AGREEMENT
RECOMMENDATIONS FOR ANNOUNCEMENT AND DISTRIBUTION OF DOCUMENTS

See Instructions on Reverse Side

1. DOE Report No. DOE/ER/45243	3. Title Local Many-Body Effects in the Optical Response of Narrow Band Solids
2. DOE Contract No. DE-FG05-86ER45243	

4. Type of Document ("x" one)

a. Scientific and technical report

b. Conference paper:

Title of conference _____

Date of conference _____

Exact location of conference _____

Sponsoring organization _____

c. Other (Specify) _____

5. Recommended Announcement and Distribution ("x" one)

a. Unrestricted unlimited distribution.

b. Make available only within DOE and to DOE contractors and other U. S. Government agencies and their contractors.

c. Other (Specify) _____

6. Reason for Recommended Restrictions

7. Patent and Copyright Information:

Does this information product disclose any new equipment, process, or material? No Yes If so, identify page nos. _____

Has an invention disclosure been submitted to DOE covering any aspect of this information product? No Yes

If so, identify the DOE (or other) disclosure number and to whom the disclosure was submitted.

Are there any patent-related objections to the release of this information product? No Yes If so, state these objections.

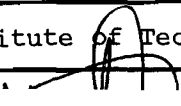
Does this information product contain copyrighted material? No Yes

If so, identify the page numbers _____ and attach the license or other authority for the government to reproduce.

8. Submitted by _____ Name and Position (Please print or type)

Andrew Zangwill/Principal Investigator

Organization
Georgia Institute of Technology

Signature 	Phone 404/894-7333	Date 5/24/88
---	-----------------------	-----------------

FOR DOE OR OTHER AUTHORIZED
USE ONLY

9. Patent Clearance ("x" one)

a. DOE patent clearance has been granted by responsible DOE patent group.

b. Report has been sent to responsible DOE patent group for clearance.

LOCAL MANY-BODY EFFECTS IN THE OPTICAL RESPONSE
OF NARROW BAND SOLIDS

Progress Report
Final Year

Andrew Zangwill and David Liberman

School of Physics
Georgia Institute of Technology
Atlanta, GA 30332

May 1988

PREPARED FOR THE U.S. DEPARTMENT OF ENERGY
UNDER GRANT NO. DE-FG05-86ER45243

This report is a summary of our activities in this the final year of our effort under the present grant. As suggested in last year's progress report, our research falls into two categories. First is the continuation of our studies of the optical response of atoms and atoms-in-a-medium with the time dependent local density approximation (TDLDA) developed by us earlier. Second is new work on the growth, structure and stability of epitaxial overlayers. This latter subject will be continued in the future under the auspices of the Department of Energy with a new grant that replaces the current one.

Four papers have appeared in the past year pertaining to our work in photoabsorption:

"5f-band width and resonant photoemission of uranium intermetallic compounds", Phys. Rev. B36, 2916 (1987).

"Open-shell and solid state effects in resonant photoemission", J. Phys. C:Solid State Phys. C20, L627 (1987).

"Optical response of an embedded atom", Phys. Rev. B36, 6705 (1987).

"Quadrupole resonances in the rare earth metals", submitted to Phys. Rev. A.

The first three of these all deal with the effect of a solid state environment on the resonant photoemission process - the stated goal of this research effort. The results for the "embedded atom" are particularly significant as they represent the first results of their kind. We were able to resolve a long-standing discrepancy between purely atomic calculations and photoabsorption data obtained in the condensed phase.

Two additional papers have appeared on the subject of epitaxial growth:

"Morphological transitions in solid epitaxial overlayers", Europhys.

Lett. 4, 729 (1987).

"Phenomenological approach to multilayer growth and stability", in Multilayers: Synthesis, Properties and Non-Electronic Applications, (Materials Research Society, Pittsburgh, 1988).

The main idea behind this work is to construct macroscopic models which contain the essential features of the problem, viz., strain and surface tension. New predictions have been made concerning the mode of thin film growth and the existence and texture of metastable crystal phases.

All six papers are appended below.

5*f*-band width and resonant photoemission of uranium intermetallic compounds

D. D. Sarma,* F. U. Hillebrecht,† and C. Carbone
*Institut für Festkörperforschung, Kernforschungsanlage Jülich,
 D-5170 Jülich, Federal Republic of Germany*

A. Zangwill

School of Physics, Georgia Institute of Technology, Atlanta, Georgia 30332

(Received 3 April 1987)

New experimental results and theoretical arguments are used in conjunction with previously published data to demonstrate that resonant photoemission (RPS) does not provide a reliable measure of the occupied 5*f* density of states in uranium intermetallic compounds. We implicate a resonant Auger process in this phenomenon and argue that RPS measurements (in conjunction with x-ray photoemission spectroscopy data) in this context are more useful as a qualitative guide to U 5*f*-ligand hybridization.

The unique thermodynamic and transport properties of so-called "heavy-fermion" systems¹ have directed widespread attention to a number of uranium-bearing intermetallic compounds: UBe₁₃, UPt₃, UAl₂, UCu₃, etc. Most theoretical analyses of these materials intimately involve the 5*f*-electron spectral density—either as input or output.² As a result, experiments designed to measure this quantity have been plentiful.³⁻⁷ All these measurements utilize electron spectroscopy.⁸ One can probe the occupied states below the Fermi level with either x-ray (XPS) or ultraviolet (UPS) photoelectron spectroscopy, both of which provide the spectra of these states weighted by their respective cross sections. However, to measure the 5*f* part of the spectral weight, most experiments to date employ resonant photoemission spectroscopy (RPS),^{8,9} whereby electron emission from valence levels is greatly enhanced as the photon energy sweeps through the threshold of a near core level (5*d* in this case). These measurements are predicated upon the belief¹⁰ that photoemission in this context preferentially ejects 5*f* electrons and hence reveals the 5*f* partial density of states. The purpose of this Rapid Communication is to point out that resonant photoemission does *not* image the occupied 5*f* density of states in numerous uranium intermetallic compounds although (in conjunction with XPS) it can be a useful tool to estimate the amount of ligand hybridization in these materials.

Our analysis of resonant photoemission in uranium intermetallic compounds is based on new experimental results (for UB₄ and USi₃), measurements already present in the literature, and theoretical estimates of the relative decay rate of the photoabsorption intermediate state to various photoemission final states. A survey of the data reveals that, for a given system, the occupied 5*f*-band width extracted from an RPS experiment systematically exceeds the value obtained from high-resolution XPS measurements. The latter often provides a good measure of the 5*f* spectral density because the cross section for direct photoemission from 5*f* states in uranium is greater (by at least an order of magnitude) than the cross section from most other valence states at x-ray photon energies.¹¹

By contrast, we argue that a resonant Auger decay mode can (almost uniquely in light actinides) broaden the RPS signal to a width almost twice that of the 5*f* density of states.

The samples of UB₄ and USi₃ were made by melting the constituents in an inductively heated levitation crucible under an Ar atmosphere and were found to be homogeneous single-phase specimens by x-ray diffraction and metallography. The XPS measurements are identical to those of an earlier report.^{12,13} The new RPS data for UB₄ and USi₃ were recorded using synchrotron radiation from the BESSY (Berlin) and National Synchrotron Light Source (Brookhaven) storage rings, respectively. Figure 1(a) shows the measured spectra of UB₄ at photon energies $h\nu = 102, 110, \text{ and } 1486.6 \text{ eV}$. The RPS spectra correspond to off and on resonance as determined from the total absorption curves around the 5*d* threshold.¹⁴ The corresponding spectra for USi₃ are shown in Fig. 1(b).

We take the full widths at half maximum of the experimental XPS spectra (1.3 eV for both UB₄ and USi₃) as indicative of the true width of the occupied portion of the 5*f* spectral density in these materials. Such measurements presumably expose all intrinsic *f*-*f* correlation effects—which may be considerable. By contrast, the RPS spectra at $h\nu = 110 \text{ eV}$ are considerably broader than the curves obtained at x-ray photon energies. In order to isolate the 5*f* component, it is conventional⁴⁻⁷ to subtract the off-resonance spectrum from the on-resonance spectrum. These are labeled "difference" in Fig. 1. The widths of the difference spectra are 2.4 eV (UB₄) and 2.1 eV (USi₃). Clearly, these values still are much larger than the width observed at $h\nu = 1486.6 \text{ eV}$. It is evident that the RPS curves cannot be representative of the 5*f* density of states; the spectra cannot exhibit a width greater than that revealed by x-ray photons which (at worst) represents a mixture of 5*f* states with other valence states.

The anomalous broadening of resonant photoemission spectra compared to XPS spectra for UB₄ and USi₃ is not confined to these particular materials. It is, in fact, a quite general phenomenon for many uranium intermetal-

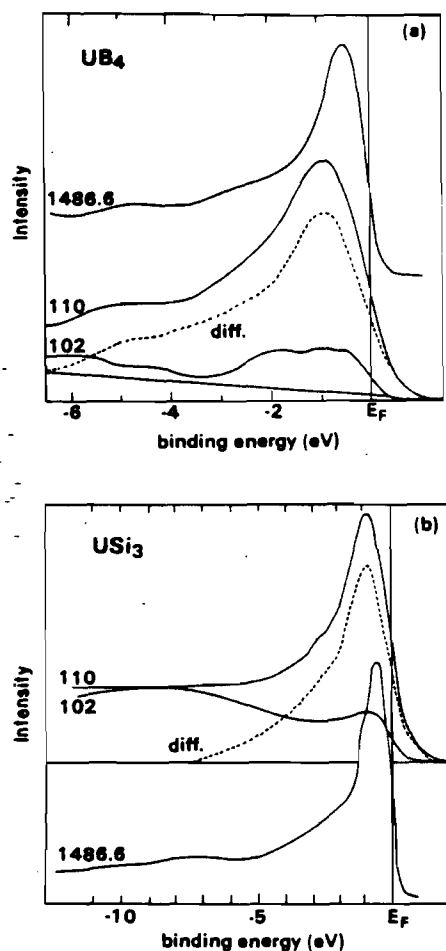


FIG. 1. Photoelectron spectra of (a) UB_4 and (b) USi_3 at photon energies $h\nu = 1486.6$ (XPS), 110.0 (on-resonance), and 102.0 eV (off-resonance). The difference spectra between the on- and off-resonance spectra are also shown (dashed curve) in each case.

lic compounds. This can be seen from a compilation of spectral widths at different photon energies taken from the recent literature (Table I). Notice that the widths at high (1486.6) and low (40–60 eV) photon energies are comparable for α -U, UBe_{13} , USi_3 , and UB_4 , while the on-resonance widths are much greater. The discrepancy disappears for UGl_3 , UAl_2 , UIn_3 , and USn_3 . The results in Table I reveal two systematics. First, if one qualitatively orders the compounds in Table I according to the extent of hybridization between U $5f$ states and ligand states,²⁰ the systems with greater hybridization exhibit greater spectral broadening. Second, greater broadening occurs for resonant excitation at the $5d_{3/2}$ threshold (110 eV) than at the $5d_{5/2}$ threshold (98 eV).

Our problem is to discover a *differential* broadening mechanism, i.e., one which operates at RPS photon energies but not at XPS photon energies. Since we cannot account for the observed widths merely by adding the resonant contribution⁹ from overlapping $6d$ states, we propose instead an explanation based on an analysis of the resonant photoemission process. We presume (as usual) that the initial excitation step is quasiatomic: a $5d$ electron makes an optical transition from the ground state

TABLE I. Full width at half maximum (eV) of the valence-band spectra of uranium and its intermetallic compounds as determined by photoelectron spectroscopy at different incident photon energies. The photon energies (eV) are indicated in parentheses.

Compound	XPS	On resonance	Below resonance
	(1486.6)		
U-metal	1.1 ^a	1.9 (99) ^b 2.1 (108) ^b	1.1 (60) ^b
UBe_{13}	1.3 ^c	2.1 (98) ^{d,e} 2.3 (109) ^{f,g}	1.5 (40) ^h
USi_3	1.3	2.3 (110)	1.5 (40) ^b
UGe_3	1.9 ^h	1.9 (98) ^h	1.5 (50) ^b
UB_4	1.3	2.5 (110)	
UAl_2	1.3 ^h	1.1 (98) ^{ij}	
UIn_3	1.9 ^h	1.6 (98) ^k	
USn_3	1.9 ^h	1.6 (98) ^k	

^aReference 15.

^bReference 16.

^cReference 3.

^dReference 4.

^eThese widths correspond to the difference spectra between the photon energy shown in the bracket and 92-eV excitation energy.

^fReference 5.

^gReference 17.

^hReference 18.

ⁱReference 6.

^jWidth of the background subtracted spectrum.

^kReference 19.

($5d^{10}5f^36d^26s$) into a virtual bound state (" $5f^*$ ") in the continuum (one of the terms of the $5d^95f^46d^26s$ multiplet) trapped near the atom by an angular momentum barrier.²¹ This intermediate state decays to one of a number of different final ionic states. The three channels most relevant to the present discussion are shown in Fig. 2. These are (a) direct $5d$ photoemission which can be viewed as a tunneling of the excited " $5f^*$ " state into the ϵf continuum, (b) resonant $5f$ photoemission wherein a super-Coster-Kronig (SCK) Auger transition fills the $5d$ hole and ejects a $5f$ electron from the valence band, and (c) resonant Auger decay^{22–25} wherein a " $5f^* \rightarrow E_F$ " transition accompanies a SCK Auger event which fills the $5d$ hole from the $5f$ band.

The key observation is that the line shape of the resonant Auger signal is given by a self-convolution of the $5f$ band if the intra-atomic Coulomb interaction U_{ee} is not too large. This produces a signal near E_F which is considerably broader than the spectral weight of the $5f$ band; for α -U metal this procedure leads to a broad peak with a full width at half maximum of 3 eV. Moreover, the " $5f^* \rightarrow E_F$ " transition guarantees that this feature appears in the observed spectrum at constant binding energy²⁶ rather than constant kinetic energy as in the case of a conventional Auger process. Consequently, the experimentally observed broadening can result if the resonant Auger decay channel steals sufficient strength from the "usual"

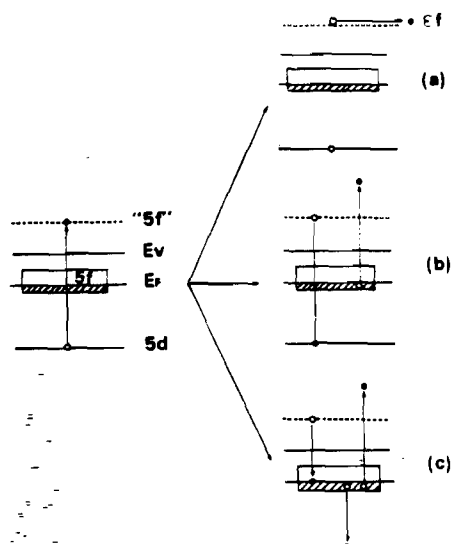


FIG. 2. Schematic representation of different decay channels of intermediate excited state ($5d^5 5f^4$) following the resonant absorption ($5d \rightarrow 5f$): (a) direct $5d$ emission, (b) autoionization leading to resonant photoemission from $5f$, and (c) resonant Auger decay.

decay modes [Figs. 2(a) and 2(b)]. In the following, we argue that this is indeed the case for uranium-bearing materials—and almost uniquely so.

The resonant Auger process envisioned above will reproduce the experimental results only for a particular ordering of the important energies in the problem. The " $5f$ " $\rightarrow E_F$ transition is an essential ingredient. For this to occur, there must exist a non-negligible $5d$ - $5f$ direct Coulomb interaction U_{cv} .²⁶ On the other hand, there must be substantial oscillator strength into the initial $5d \rightarrow 5f$ transition well above the Fermi level. This means that we require the $5d$ - $5f$ exchange interaction U_{ex} to exceed U_{cv} .²¹ In practice, this is no problem since metals always screen the direct interaction more efficiently than the exchange interaction.²⁷ However, U_{cv} also must be comparable to (or exceed) the $5f$ band width W to ensure that " $5f$ " actually has quasiatomic character and that a resonant optical transition occurs in the first place. Finally, as noted above, the intraband Coulomb interaction U_{vv} must be small enough so that a bandlike Auger line shape obtains. Putting all this together, the required sequence is $U_{ex} > U_{cv} > W > U_{vv}$.

Table II demonstrates that an Auger process can cloak the valence band in an RPS experiment only for a very restricted range of materials. For lanthanides, $U_{vv} \gg W$ and the spectrum is essentially atomiclike.⁹ In nickel metal, U_{vv} is comparable to W , but still large enough to split the resonant Auger satellite 6 eV below the valence band.³¹ The ratio U_{vv}/W is well below unity for all the other transition metals, but d -band screening generally drives $U_{cv} < W$.³³ Hence, one is left with only the early actinides and their intermetallic compounds. Of course, this does not prove that the process in Fig. 2(c) actually occurs in these systems to any significant degree. Unfortunately, the relevant rate calculations are extremely difficult to perform in the condensed state. Nonetheless, we can build a strong circumstantial case using intuitive argu-

TABLE II. Estimates of various energies (eV) relevant to the discussion of resonant Auger emission. See text.

	U_{vv}	W	U_{cv}	U_{ex}
Light actinides	2.5 ^{a,b}	3 ^c	5.5 ^d	10 ^e
Rare-earth metals	5 ^a	0.1 ^a	10 ^f	10 ^e
Light 3d transition metals	1 ^g	5 ^h	3 ^h	10 ^e

^aReference 28.

^bReference 12.

^cEstimated from many XPS and BIS spectra.

^dReference 29.

^eAtomic theoretical estimate.

^fReference 30.

^gReference 31.

^hReference 32.

ments and quantitative atomic calculations.

We have performed relativistic time-dependent local-density-approximation (RTDLDA) calculations³⁴ for the relative photoemission cross sections corresponding to processes (a) and (b) of Fig. 2 for a uranium atom near the $5d$ threshold. These results (which do not include the resonant Auger channel) reveal that $\sigma_a(\omega)/\sigma_b(\omega) \sim 5$. Moreover, the Auger matrix element in channel (b) and the excited " $5f$ " $\rightarrow 5f(E_F)$ transition amplitude is similar to the $5f \rightarrow \epsilon f$ amplitude in channel (a). Thus, even though it is a higher-order process, resonant Auger decay (c) will be comparable in strength to direct resonant photoemission (b) even if only 20% of channel (a) is transferred to the Auger channel. As indicated earlier, there are two factors which promote this transfer for the case of uranium intermetallic compounds. First, the relatively large value of U_{cv} enhances the effective $5f$ density of states at E_F .²⁶ Second, any hybridization with delocalized ligand orbitals increases the efficiency of overlap-driven transfer of the localized " $5f$ " orbital to a delocalized $5f$ band state. This last observation accounts for the correlation noted in Table I and explains the fact that the magnetic (e.g., UIn_3) and near-magnetic (e.g., USn_3 and UAl_2) compounds do not exhibit any broadening of their spectral features in RPS as compared to that in XPS excitation.

In summary, this Communication presents new experimental data to show that resonant photoemission does not image the occupied $5f$ density of states in uranium intermetallic compounds. We marshal experimental results and theoretical arguments to show that a resonant Auger process obscures the valence band in UPS measurements of these materials. This conclusion seriously questions the conventional practice of extracting $5f$ spectral weight from resonant photoemission spectroscopy of these compounds. RPS remains useful (when employed in conjunction with XPS) as a qualitative indicator of ligand hybridization.

We thank M. Campagna for his support of this work. One of us (D.D.S) thanks W. Gudat for helpful discussion and another one of us (A.Z.) acknowledges the support of the U.S. Department of Energy under Grant No. DE-FG05-86ER45243.

- ^{*}Present and permanent address: Solid State and Structural Chemistry Unit, Indian Institute of Science, Bangalore 560 012 India.
- [†]Present address: Max-Planck-Institut für Festkörperforschung, D-7000 Stuttgart 80, West Germany.
- ¹Z. Fisk, H. R. Ott, T. M. Rice, and J. L. Smith, *Nature (London)* **320**, 124 (1986).
- ²P. A. Lee, T. M. Rice, J. W. Serene, L. J. Sham, and J. W. Wilkins, *Comments Condens. Mater. Phys.* **12**, 99 (1986).
- ³E. Wuilloud, Y. Baer, H. R. Ott, Z. Fisk, and J. L. Smith, *Phys. Rev. B* **29**, 5228 (1984).
- ⁴G. Landgren, Y. Jugnet, J. F. Morar, A. J. Arko, Z. Fisk, J. L. Smith, H. R. Ott, and B. Reihl, *Phys. Rev. B* **29**, 493 (1984).
- ⁵R. D. Parks, M. L. denBoer, S. Raaen, J. L. Smith, and G. P. Williams, *Phys. Rev. B* **30**, 1580 (1984).
- ⁶J. W. Allen, S.-J. Oh, L. E. Cox, W. P. Ellis, M. S. Wire, Z. Fisk, J. L. Smith, B. B. Pate, I. Lindau, and A. J. Arko, *Phys. Rev. Lett.* **54**, 2635 (1985).
- ⁷W.-D. Schneider, B. Reihl, N. Martensson, and A. J. Arko, *Phys. Rev. B* **26**, 423 (1982).
- ⁸See, for example, Y. Baer, in *Handbook of the Physics and Chemistry of the Actinides*, edited by A. J. Freeman and G. H. Lander (North-Holland, Amsterdam, 1984), Vol. 1, pp. 271-339.
- ⁹A. Zangwill and P. Soven, *Phys. Rev. Lett.* **45**, 204 (1980).
- ¹⁰B. Reihl, N. Martensson, D. E. Eastman, A. J. Arko, and O. Vogt, *Phys. Rev. B* **26**, 1842 (1982).
- ¹¹J. J. Yeh and I. Lindau, *At. Data Nucl. Data Tables* **32**, 1 (1985).
- ¹²D. D. Sarma, F. U. Hillebrecht, W. Speier, N. Martensson, and D. D. Koelling, *Phys. Rev. Lett.* **57**, 2215 (1986).
- ¹³D. D. Sarma, S. Krummacker, A. Wallash, and J. E. Crow, *Phys. Rev. B* **34**, 3737 (1986).
- ¹⁴D. D. Sarma, S. Krummacker, F. U. Hillebrecht, and W. Gudat, in *Proceedings of the International Conference on Valence Fluctuations*, Bangalore, 1987 (unpublished).
- ¹⁵Y. Baer and J. K. Lang, *Phys. Rev. B* **21**, 2060 (1980).
- ¹⁶M. Iwan, E. E. Koch, and F. J. Himpsel, *Phys. Rev. B* **24**, 613 (1981).
- ¹⁷A. J. Arko, C. J. Olson, D. M. Wieliczka, Z. Fisk, and J. L. Smith, *Phys. Rev. Lett.* **53**, 2050 (1984).
- ¹⁸F. U. Hillebrecht and D. D. Sarma (unpublished).
- ¹⁹D. D. Sarma, S. Krummacker, W. Gudat, C. L. Lin, L. W. Zhou, J. E. Crow, and D. D. Koelling (unpublished).
- ²⁰D. D. Koelling, B. D. Dunlap, and G. W. Crabtree, *Phys. Rev. B* **31**, 4966 (1985).
- ²¹J. L. Dehmer, A. F. Starace, U. Fano, J. Sugar, and J. W. Cooper, *Phys. Rev. Lett.* **26**, 1521 (1971).
- ²²W. Eberhardt, G. Kalkoffen, and C. Kunz, *Phys. Rev. Lett.* **41**, 156 (1978).
- ²³M. Aono, T.-C. Chiang, J. H. Weaver, and D. E. Eastman, *Solid State Commun.* **39**, 1057 (1981).
- ²⁴A. Fujimori and J. H. Weaver, *Phys. Rev. B* **31**, 6411 (1985).
- ²⁵G. Wendin, *Comments At. Mol. Phys.* **17**, 115 (1986).
- ²⁶S. M. Girvin and D. R. Penn, *J. Appl. Phys.* **52**, 1650 (1981).
- ²⁷J. Zaaen, G. a. Sawatzky, J. Fink, W. Speier, and J. C. Fuggle, *Phys. Rev. B* **32**, 4905 (1985).
- ²⁸J. Herbst, *Phys. Scr.* **21**, 553 (1980).
- ²⁹O. Gunnarsson, K. Schonhammer, D. D. Sarma, F. U. Hillebrecht, and M. Campagna, *Phys. Rev. B* **32**, 5499 (1985); D. D. Sarma, F. U. Hillebrecht, U. Gunnarsson, and K. Schonhammer, *Z. Phys.* **63**, 305 (1986).
- ³⁰J. C. Fuggle, F. U. Hillebrecht, J.-M. Esteve, R. C. Karnatak, D. Gunnarsson, and K. Schonhammer, *Phys. Rev. B* **27**, 4637 (1983).
- ³¹G. Treglia, M. C. Desjonqueres, F. Ducastelle, and D. Spanjaard, *J. Phys. C* **14**, 4347 (1981).
- ³²J. Fink, Th. Muller-Heinzerling, B. Scheerer, W. Speier, F. U. Hillebrecht, J. C. Fuggle, J. Zaaen, and G. A. Sawatzky, *Phys. Rev. B* **32**, 4899 (1985).
- ³³Resonant photoemission experiments near the 3p edge actually do reveal some small broadening of the spectral weight close to E_F for the early 3d transition metals. See J. Barth, F. Gerken, and C. Kunz, *Phys. Rev. B* **31**, 2022 (1985).
- ³⁴A. Zangwill, in *EXAFS and Near Edge Structure*, edited by K. O. Hodgson, B. Hedman, and J. E. Penner-Hahn (Springer, Berlin, 1984), pp. 13-17.

LETTER TO THE EDITOR

Open-shell and solid state effects in resonant photo-emission

Andrew Zangwill

School of Physics, Georgia Institute of Technology, Atlanta, GA 30332, USA

Received 30 June 1987

Abstract. Experimental total photo-absorption and partial photo-ionisation cross sections for Eu atoms and Eu metal are compared to new relativistic time-dependent local density calculations and previous many-body perturbation theory results. This comparison makes explicit for the first time the influence of open-shell and solid state effects in giant resonant absorption and resonant photo-emission.

The use of synchrotron radiation as a tool for spectroscopic studies of atoms, molecules and solids has matured considerably in the past decade. Early investigations (see, for example, Kunz 1979) which focused on the total absorption cross section have largely been supplanted by detailed studies that analyse the relative partial cross sections of various subshell and satellite emission channels (see, for example, Bizau *et al* 1984). In particular, considerable attention has been directed towards the study of the lanthanides in the vicinity of their so-called 'giant resonance' absorption feature (Connerade *et al* 1987). These systems provide a rare example where systematic studies of both photo-absorption and photo-emission have been performed across a row of the periodic table in both the vapour phase and the condensed phase. The purpose of the present Letter is to compare some of these data (for Eu atoms and Eu metal) with new state-of-the-art calculations and thereby alert the condensed-matter spectroscopic community to some previously unappreciated features of the resonant photo-emission process.

The total absorption cross section of rare-earth metals at photon energies just above the 4d core-level threshold (Haensel *et al* 1970) is nearly identical with the corresponding quantity measured in the gas phase (Radtke 1979). It is observed that essentially all the oscillator strength associated with the 4d shell is deposited into a 'giant resonance' of relatively narrow spectral width. The origin of this behaviour was elucidated in seminal work by Dehmer *et al* (1971) who pointed out that strong 4d \rightarrow 4f dipole transitions from the $4d^{10}4f^N$ ground configuration (which would otherwise be concentrated into an intense sub-threshold line) are driven far above the 4d threshold and multiplet split by Coulomb interactions within the final-state $4d^9 4f^{N+1}$ configuration of the core-excited atom.

An alternative (and equally correct) interpretation was proposed by Amusia and Cherepkov (1975) and Wendin (1976) on the basis of random phase approximation with exchange (RPAE) calculations. Therein, one imagines a heavily damped 'collective' oscillation of the entire 4d shell in analogy with plasmon excitation in solids and giant dipole absorption in nuclei (Wendin 1984). These oscillations decay via one- (or few-)

particle excitations, that is, the aforementioned photo-ionisation channels. This particular many-body point of view was adopted as well in a study (Zangwill and Soven 1980) of photo-absorption and photo-emission from Ce atoms in the resonance region using a time-dependent local density approximation (TDLDA). The latter is closely related to the RPAE.

Based upon the substantial successes of the TDLDA (Nuroh *et al* 1982, Parpia and Johnson 1983, Zangwill 1984), it came as a surprise when measurements (Meyer *et al* 1986) of the various photo-ionisation decay channels of Ce vapour clearly disagreed with the corresponding calculations. The latter predict $\sigma_{4d}(\omega)/\sigma_{4f}(\omega) \sim 8$ with identical lineshapes whereas the experiment finds $\sigma_{4d}(\omega)/\sigma_{4f}(\omega) \sim 2$ with somewhat different lineshapes. Interestingly, this lineshape anomaly had been noted in an earlier photo-emission study of Ce metal (Gerken *et al* 1982). But, in that case, the observed cross section ratios were found to be in excellent agreement with the atomic TDLDA calculation! One immediately thinks of the well known mixed-valent character of Ce metal as a possible source of this discrepancy, and calculations along these lines have been performed (Gunnarsson and Schonhammer 1987). Our results instead point to a more general phenomenon which we illustrate here for the specific case of resonant photo-emission from Eu.

It is instructive to begin with the case of the free atom. Figure 1 displays experimental results (Becker *et al* 1986) for the 4f, 4d and 5p partial cross sections of Eu vapour compared to recent diagrammatic many-body perturbation theory (MBPT) calculations by Pan *et al* (1987). These computations take account of open-shell effects and the agreement with experiment evidently is quite good. This is not too surprising since the calculation retains diagrams that capture the essential polarisation and auto-ionisation

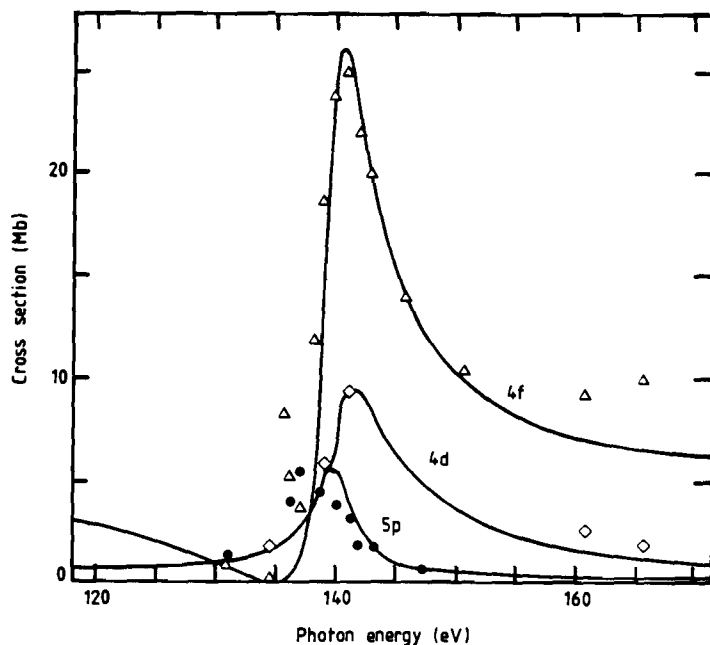


Figure 1. Partial photo-ionisation cross sections for atomic Eu. The symbols denote the experimental results of Becker *et al* (1986). The full curves are MBPT results of Pan *et al* (1987).

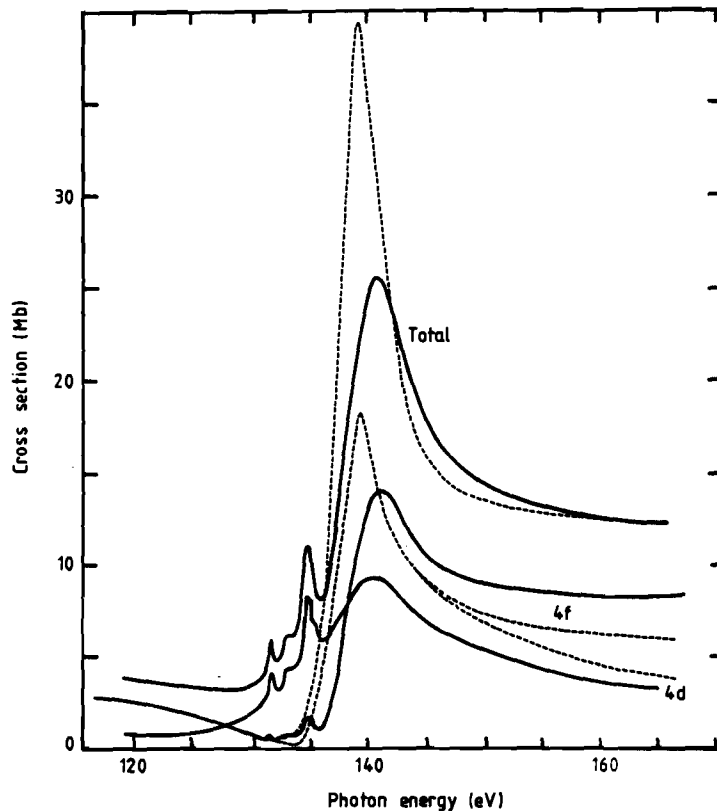


Figure 2. Full curves illustrate the total photo-absorption and 4d and 4f partial photo-ionisation cross sections for Eu metal as measured by Gerken *et al* (1982). Broken curves are the corresponding quantities obtained by the TDLDA for Eu atoms. The calculated values of $\sigma_{4d}(\omega)$ and $\sigma_{4f}(\omega)$ coincide at photon energies below 145 eV.

processes that characterise resonant photo-emission (Zangwill 1987). The RPAE and TDLDA include these effects to the same level of approximation.

In figure 2 we turn to the resonant optical properties of Eu metal in the same range of photo energy as figure 1. The curves constitute a comparison of experiment (Gerken *et al* 1982) with atomic TDLDA theory for the total photo-absorption cross section (total electron yield) and the 4d and 4f partial photo-ionisation cross sections. The computations employ a relativistic formalism developed by Liberman and Zangwill (1984). The data have been placed on an absolute scale following the considerations of Henke *et al* (1982) for the total absorption. Our confidence in this normalisation is bolstered by the excellent agreement between theory and experiment for this quantity above the resonance maximum.

We attribute the lack of good agreement for $\sigma_{\text{tot}}(\omega)$ in the range 130–140 eV to a combination of open-shell and (predominantly) solid state effects. Regarding the former (Sugar 1972), all sub-threshold structure is lost in the TDLDA because (in its present form) one explicitly performs a spherical average over the magnetic sublevels of all open shells (Zangwill and Soven 1981). On the other hand, the TDLDA total absorption agrees well with the sum of the partial cross sections as obtained from the non-relativistic MBPT

results (cf figure 1). Therefore, despite a widely held view to the contrary, the 4f shell of metallic Eu cannot be purely atomic. Hybridisation with the conduction band drives 4d-4f spectral oscillator strength out of the sharp peak to both higher and lower energy. Quantitative calculations in support of this idea have been performed for uranium metal in the neighbourhood of its 5d-5f resonance (Zangwill and Liberman 1987) where the failure of the atomic model is much more striking (Wendin and Del Grande 1985).

A more striking solid state effect becomes evident in the relative behaviour of $\sigma_{4d}(\omega)$ and $\sigma_{4f}(\omega)$. In contrast to experiment, the TDLDA predicts that these quantities are nearly identical in both lineshape and relative magnitude. Equally significant is the lack of agreement between the measurements for Eu metal and the corresponding data collected in the vapour phase (cf figure 1). The ratio $\sigma_{4f}(\omega)/\sigma_{4d}(\omega)$ differs in the two cases by a factor of two although the lineshapes agree quite well.

To understand these observations we need only recall that the MBPT results reproduce the vapour phase measurements exceedingly well. Accordingly, we conclude that open-shell angular momentum coupling effects both modify the simplest view of resonant photo-emission lineshapes (Zangwill and Soven 1980) and significantly enhance emission of 4f electrons relative to 4d electrons during resonance decay. The latter effect evidently is suppressed in the solid state due to hybridisation and/or crystal-field effects. Spherical averaging in the TDLDA eliminates both effects completely.

The foregoing scenario exhibits precisely the correct trend required to rationalise the difference between Eu and Ce. We expect the relative magnitude of TDLDA partial cross sections to conform best to solid state data in those materials where the 4f orbital is most strongly mixed with its environment (although still atomic enough to engender the resonance process itself!). The relatively better result for Ce then follows immediately from the well known increase in such mixing as one proceeds from right to left across the lanthanide row. In this connection, we note in closing the suggestion (Crljen and Wendin 1985) that certain aspects of the atomic LDA one-electron potential already mimic a metallic environment. The lineshape issue appears to be more subtle and deserves further attention.

In summary, we have used a comparison of high-resolution spectroscopic data for both atomic and metallic Eu with two sophisticated atomic physics calculations to point out explicit open-shell and solid state effects in resonant photo-emission. The latter tend to suppress the former with the paradoxical result that atomic time-dependent local density calculations of resonant photo-ionisation can be more appropriate for atoms in solids than for the free atoms themselves.

Thanks are due to Hugh Kelly (University of Virginia) for discussions and permission to reproduce his MBPT results, Gary Doolen (Los Alamos National Laboratory) for performing some of the TDLDA calculations, and the US Department of Energy for support under Grant DE-FG05-86ER45243.

References

- Amusia M Ya and Cherepkov N A 1975 *Case Studies in Atomic Physics* 5 47
Becker U, Kerkhoff H G, Lindle D W, Kobrin P H, Ferrett T A, Heimann P A, Truesdale C M and Shirley D A 1986 *Phys. Rev. A* 34 2858
Bizau J M, Gerard P, Wulleumier F J and Wendin G 1984 *Phys. Rev. Lett.* 53 2083

- Connerade J-P, Esteva J-M and Karnatak R C (ed.) 1987 *Giant Resonances in Atoms, Molecules and Solids* (New York: Plenum)
- Crijen Z and Wendin G 1985 *Phys. Scr.* **32** 359
- Dehmer J L, Starace A F, Fano U, Sugar J and Cooper J W 1971 *Phys. Rev. Lett.* **26** 1521
- Gerken F, Barth J and Kunz C 1982 *X-ray and Atomic Inner Shell Physics* ed. B Crasemann (New York: AIP) p 602
- Gunnarsson O and Schonhammer K 1987 *Giant Resonances in Atoms, Molecules and Solids* ed. J-P Connerade, J-M Esteva and R C Karnatak (New York: Plenum)
- Haensel R, Rabe P and Sonntag B 1970 *Solid State Commun.* **8** 1845
- Henke B L, Lee P, Tanaka T J, Shimabukuro R L and Fujikawa B K 1982 *At. Data and Nucl. Data Tables* **27** 1
- Kunz C 1979 *Synchrotron Radiation: Techniques and Applications* (Berlin: Springer)
- Liberman D A and Zangwill A 1984 *Comput. Phys. Commun.* **32** 75
- Meyer M, Prescher Th, von Raven E, Richter M, Schmidt E, Sonntag B and Wetzel H E 1986 *Z. Phys. D* **2** 347
- Nuroh K, Zaremba E and Stott M 1982 *Phys. Rev. Lett.* **49** 862
- Pan C, Carter S L and Kelly H P 1987 *J. Phys. B: At. Mol. Phys.* **20** L335
- Parpia F A and Johnson W R 1983 *J. Phys. B: At. Mol. Phys.* **16** L375
- Radtke E R 1979 *J. Phys. B: At. Mol. Phys.* **12** L77
- Sugar J 1972 *Phys. Rev. B* **5** 1785
- Wendin G 1976 *Photoionisation and Other Probes of Many-Electron Interactions* ed. F J Wuilleumier (New York: Plenum) p 61
- 1984 *New Trends in Atomic Physics* ed. G Grynberg and R Stora (Amsterdam: North-Holland) p 555
- Wendin G and Del Grande N 1985 *Phys. Scr.* **32** 286
- Zangwill A 1984 *EXAFS and Near Edge Structure III* ed. K O Hodgson, B Hedman and J E Penner-Hahn (Berlin: Springer) p 13
- 1987 *Giant Resonances in Atoms, Molecules and Solids* ed. J-P Connerade, J-M Esteva and R C Karnatak (New York: Plenum) p 319
- Zangwill A and Liberman D A 1987 unpublished
- Zangwill A and Soven P 1980 *Phys. Rev. Lett.* **45** 204
- 1981 *Phys. Rev. A* **21** 1561

Optical response of an embedded atom: Resonant photoemission from uranium

Andrew Zangwill

School of Physics, Georgia Institute of Technology, Atlanta, Georgia 30332

David A. Liberman

Lawrence Livermore National Laboratory, Livermore, California 94550

(Received 3 August 1987)

We have studied the effect of solid-state hybridization on the resonant photoemission process by means of relativistic time-dependent local-density calculations for a single uranium atom embedded in a spherical drop of jellium. The computed total absorption is in good agreement with experiment. We find a dramatic suppression of $5f$ photoemission relative to that of the free atom.

Resonant photoemission is a standard spectroscopic probe of the electronic structure of narrow-band materials.¹ The basic effect—a giant enhancement of valence-band photoemission cross sections as the incident photon energy sweeps through a core-level threshold—is quasiatomic and well understood.²⁻⁴ In a typical application, synchrotron radiation is used to excite lanthanide or actinide materials to energies near their respective $4d$ or $5d$ core-level thresholds. The kinetic-energy distribution of ejected photoelectrons at resonance is widely presumed to be an image of the corresponding $4f$ or $5f$ spectral density function.⁵ Alternatively, it has been suggested⁶ that the energy dependence of the valence-band cross section itself carries valuable information about hybridization and ligand field effects.

The second use of resonant photoemission cited above is of particular interest for application to uranium intermetallic compounds. This is because on the one hand there is good evidence⁷ that the $5f$ states in these materials are well delocalized and often heavily mixed with other states in the ground configuration. On the other hand, substantial orbital localization and $5d$ - $5f$ wave function overlap is required merely to ensure efficient resonant excitation. This is somewhat paradoxical at first sight and quantitative evaluation of experimental data has been impeded by the fact that very little is known about how a solid-state environment perturbs the resonant photoemission process on a particular atomic site. The purpose of the present Rapid Communication is to address this question with a simple nontrivial model: an atom embedded in a uniform electron gas. We find interesting effects which we hope will stimulate further study of this problem.

Figure 1 illustrates a comparison of high-resolution optical-absorption data for α -U metal near the spin-orbit split $5d$ threshold⁸ with a number of theoretical approaches to the problem. The solid curve is a calculation for uranium atom using a relativistic time-dependent local-density approximation (RTDLDA)⁹ which treats polarization-type many-body effects. In agreement with previous atomic results,^{4,10} the two-peak structure of the observed spectrum¹¹ is well reproduced, albeit with computed widths which are far too narrow. It has been suggested⁴ that most of this discrepancy arises from a spherical averaging procedure (inherent to the RTDLDA)

which eliminates multiplet splitting effects.

To investigate this possibility, a semirelativistic Hartree-Fock calculation¹² of the relative intensities of optical transitions between the ground configuration of U ($5d^{10}5f^3$) and the multiplets of the core-excited $5d^95f^4$ configuration was performed. The absorption is totally dominated by three transitions whose relative oscillator strengths are indicated by vertical lines in Fig. 1. The lack of additional strong lines suggests to us that one must seek a different source for broadening.¹³ We demonstrate below that hybridization of the $5f$ wave function with a free-electron environment is sufficient to reproduce the observed peak widths.

Previous workers¹⁴ have used a single atom embedded in a neutral electron gas ("jellium") as a model for calculation of optical processes in solids at x-ray energies.

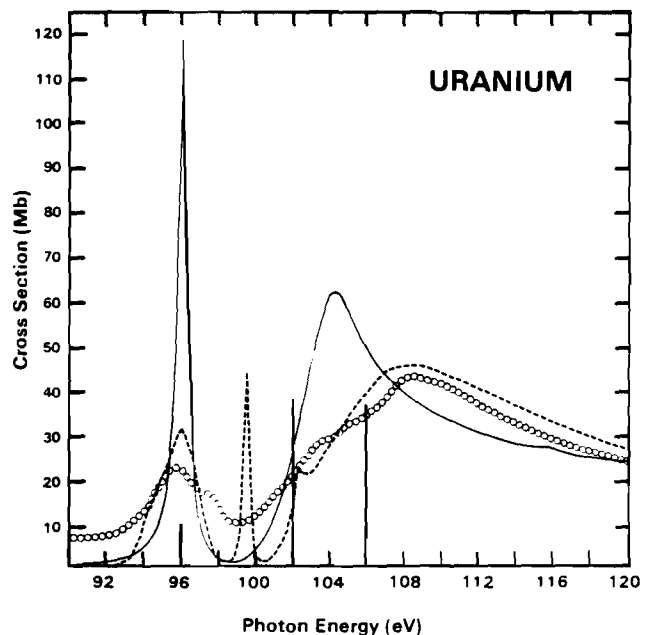


FIG. 1. Total photoabsorption for uranium in the resonance region. Data from Ref. 8 (small open circles); atomic RTDLDA calculation (solid curve); jellium drop RTDLDA calculation (dashed curve). Vertical lines represent the results of a Hartree-Fock calculation (see text). See also Ref. 11.

However, these are one-electron calculations in the sense that one merely computes Fermi's "golden rule" matrix elements of an external field operator between core level and continuum eigenstates of an effective potential for electrons. No calculation of this sort can describe the resonant photoemission process.¹ On the other hand, one could use this same effective potential in (for example) a full RTDLDA calculation. Unfortunately, the presence in the calculation of transitions between occupied continuum states and unoccupied continuum states renders this approach numerically inconvenient.¹⁵

To make progress, we consider instead the optical response of an atom embedded in a finite electron gas. More precisely, we situate the uranium atom at the center of a spherical "drop" of jellium. Empty jellium drops of this kind have been investigated with the TDLDA by others¹⁶ as models for optical absorption in very small metal particles. We will discuss in detail RTDLDA results for an enclosing drop of radius $R=8.25$ a.u. although essentially identical results were obtained for a drop with $R=9.15$ a.u. The smaller drop contains 159 electrons of which 92 reside within the U Wigner-Seitz sphere.¹⁷ Calculations are greatly simplified by the fact that all energy eigenstates are bound by the potential of the drop.

The dashed curve in Fig. 1 is the calculated photoabsorption spectrum for the uranium drop. The main effect (relative to the atom) is an increase in the width of both absorption features accompanied by a dramatic reduction in the intensity of the low-energy peak. To understand this, observe first that such giant absorption resonances generally are associated with "collective" oscillations of an entire atomic shell.^{1,18} For uranium in particular, the $5d_{3/2}$ and $5d_{5/2}$ subshells can oscillate either in phase (higher peak) or out of phase (lower peak) with one another.¹⁰ We, thus, associate increased peak widths for the embedded atom with more efficient damping than exists in the free atom.

Quantum mechanically, the subshell oscillations correspond to (virtual) transitions between occupied $5d$ states and unoccupied $5f$ states. The damping mechanism is the photoionization process itself: electrons quit occupied levels for continuum states above the vacuum level. But, the embedding process broadens the sharp atomic $5f$ energy level into an f -symmetry resonance via admixture with continuum states of the electron gas. Greater damping occurs because this resonance overlaps photoionization continuum final states far better than the original atomic $5f$ orbital.

The sharp absorption structure which appears in the calculation between the two principal peaks is a finite-size effect: an autoionization resonance associated with transitions into a bound f level just above the Fermi energy. For the larger drop, its energy position (but not that of the main peaks) shifts somewhat and another autoionization feature appears. In the limit of an infinite drop, we expect the oscillator strength associated with these resonances to broaden into a featureless continuum.

To examine the systematics of resonant photoemission, we have calculated the partial cross-section decomposition of the total absorption for both the free U atom and the U drop. A comparison of $5d$ and $5f$ photoemission in the

two cases is shown in Fig. 2. The partial cross section for emission from the remaining open channels is very small. Consequently, the ratio $\sigma_{5f}(\omega)/\sigma_{5d}(\omega)$ is a good measure of the manner by which the total initial excitation decays. By far the most striking observation is the suppression of $5f$ emission (relative to $5d$) in the drop as compared to the atom. The difference amounts to a factor of 10 for the low-energy peak around 96 eV.

This result is consistent with a recent analysis of resonant photoemission in Eu metal versus Eu atom.¹⁹ In that case, $4f$ emission dominates in the atom but is substantially suppressed in the metal. This was attributed to a com-

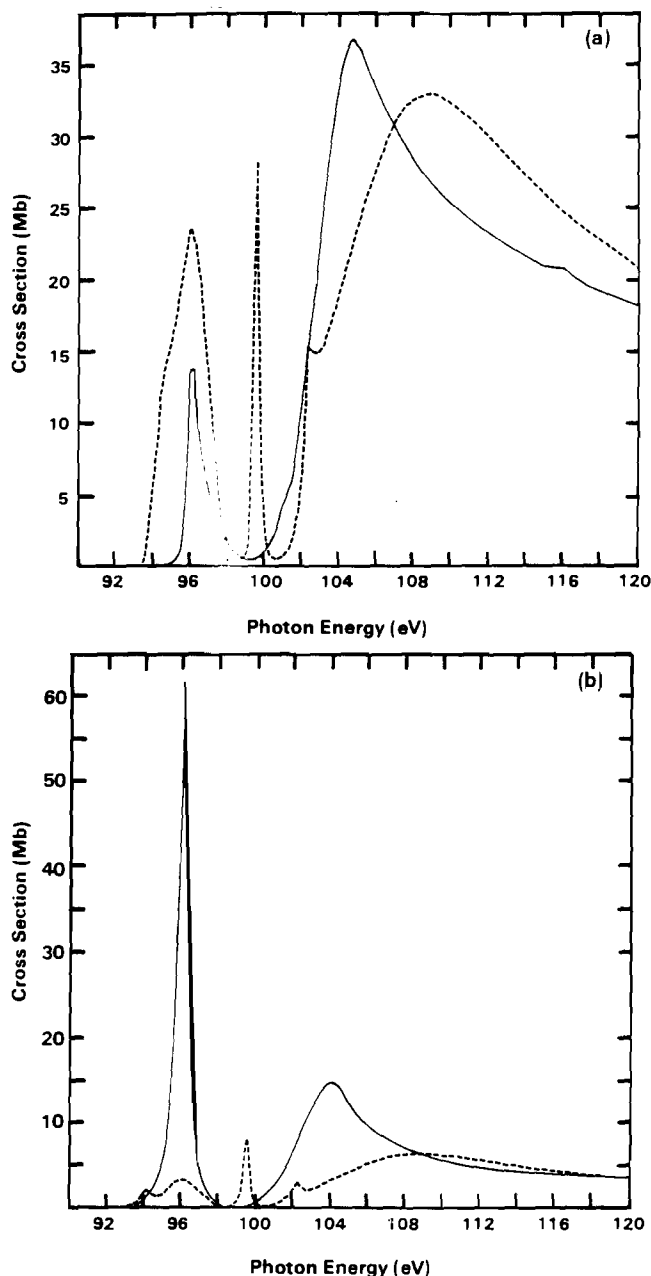


FIG. 2. Calculated partial photoionization cross sections for uranium atom (solid curve), and jellium drop (dashed curve); (a) emission from $5d$; (b) emission from $5f$. Note change of vertical scale.

bination of open-shell and hybridization effects. The present study illustrates the effect of the latter alone since all our calculations involve averaging over magnetic sub-levels.

The qualitative reason for this behavior is easy to see using the configuration (particle-hole pair) interaction picture of resonant photoemission.^{1,18} $5f$ and $5d$ photoemission, respectively, correspond to $(\epsilon g-5f)$ and $(\epsilon f-5d)$ particle-hole pair production. The relative decay probability depends upon the dipole-dipole interaction of each of these with the (virtual) $(\epsilon f-5d)$ pair created in the initial absorption step. This interaction in turn depends upon the corresponding wave-function overlaps. Hybridization of the occupied atomic $5f$ states with the continuum

reduces this overlap and hence, the $5f$ emission probability. The dynamics of the RTDLDA effective dielectric function¹⁸ (which screens the external field in Fermi's "golden rule" matrix elements) then acts to transfer oscillator strength to the $5d$ channel in order to maintain the f -sum rule. At present, we can only speculate that such an oscillator strength transfer must be more effective for "out-of-phase" subshell motion than "in-phase" subshell motion. A more detailed analysis of this point will be presented in a later publication.

We gratefully acknowledge support from the U.S. Department of Energy under Grant No. DE-FG05-86ER45243.

¹For a review of experiment, see, Y. Baer, in *Handbook of the Physics and Chemistry of the Actinides*, edited by A. J. Freeman and G. H. Lander (North-Holland, Amsterdam, 1984), Vol. 1, pp. 271-339; for a review of theory, see, A. Zangwill, in *Giant Resonances in Atoms, Molecules, and Solids*, edited by J. P. Connerade, J. M. Esteve, and R. Karnatak (Plenum, New York, 1987), pp. 319-335.

²W. Lenth, F. Lutz, J. Barth, G. Kalkoffen, and C. Kunz, *Phys. Rev. Lett.* **41**, 1185 (1978); R. Baptist, M. Belakhovsky, M. S. S. Brooks, R. Pinchaux, Y. Baer, and O. Vogt, *Physica B* **102**, 63 (1980).

³A. Zangwill and P. Soven, *Phys. Rev. Lett.* **45**, 204 (1980).

⁴G. Wendin, *Phys. Rev. Lett.* **53**, 724 (1984).

⁵For an extensive list of references and a critique of this practice, see, D. D. Sarma, F. U. Hillebrecht, C. Carbone, and A. Zangwill, *Phys. Rev. B* **36**, 2916 (1987).

⁶B. Reihl, N. Martensson, D. E. Eastman, A. J. Arko, and O. Vogt, *Phys. Rev. B* **26**, 1842 (1982); D. J. Peterman, J. H. Weaver, M. Croft, and D. T. Peterson, *ibid.* **27**, 808 (1983).

⁷J. L. Smith, A. M. Boring, and P. Weinberger, *Int. J. Quantum Chem.* **29**, 315 (1986).

⁸M. Cukier, P. Dhez, B. Gauthé, P. Jaegle, C. Wehenkel, and F. Combet-Farnoux, *J. Phys. (Paris)* **39**, L315 (1978); M. Cukier, thesis, Université de Paris-Sud, 1981 (unpublished).

⁹D. A. Liberman and A. Zangwill, *Comput. Phys. Commun.* **32**, 75 (1984); F. A. Parpia and W. R. Johnson, *Phys. Rev. A* **29**, 3173 (1984).

¹⁰G. Wendin and N. Kerr Del Grande, *Phys. Scr.* **32**, 286 (1985).

¹¹None of the theoretical methods we employ is able to predict core-level binding energies with high accuracy. For that reason, the experimental curve has been translated rigidly on

the energy axis to facilitate line-shape comparison with theory.

¹²This calculation was performed in collaboration with Robert Cowan (Los Alamos National Laboratory) using a method described in R. D. Cowan, *The Theory of Atomic Structure and Spectra* (Univ. of California Press, Berkeley, 1981). See, J. L. Dehmer, A. F. Starace, U. Fano, J. Sugar, and J. W. Cooper, *Phys. Rev. Lett.* **26**, 1521 (1971), for an interpretation of giant-resonance absorption from the point of view of such multiplet calculations.

¹³The atomic spectrum is interesting in its own right. Compare the measurements of P. K. Carroll and J. T. Costello [*J. Phys. B* **20**, L201 (1987)] with the results presented in Fig. 1.

¹⁴C.-O. Almbladh and U. von Barth, *Phys. Rev. B* **13**, 3307 (1976); G. W. Bryant and G. D. Mahan, *ibid.* **17**, 1744 (1978).

¹⁵These calculations become tractable if one is concerned only with photoabsorption or if photoemission from the valence band is negligible. See, for example, F. Grimaldi, A. Lecourt, and M. W. C. Dharma-wardana, *Phys. Rev. A* **32**, 1063, (1985).

¹⁶W. Ekardt, *Phys. Rev. B* **31**, 6360 (1985); M. J. Puska, R. M. Nieminen, and M. Manninen, *ibid.* **31**, 3486 (1985).

¹⁷The effective potential is constructed following the prescription of D. A. Liberman, *Phys. Rev. B* **20**, 4981 (1979). The definition of the Wigner-Seitz (or atomic) sphere may be found therein. An atomic radius of 3.23 a.u. is used in the present calculations.

¹⁸For further discussion of this point, see A. Zangwill, in *Atomic Physics 8*, edited by I. Lindgren, A. Rosen, and S. Svanberg (Plenum, New York, 1983), p. 339; and G. Wendin, in *New Trends in Atomic Physics*, edited by G. Grynberg and R. Stora (North-Holland, Amsterdam, 1984), p. 555.

¹⁹A. Zangwill, *J. Phys. C* **20**, L627 (1987).

Quadrupole Resonances in the Rare Earths

David Liberman
Lawrence Livermore National Laboratory
Livermore, CA 94550

and

Andrew Zangwill
School of Physics
Georgia Institute of Technology
Atlanta, GA 30332 USA

ABSTRACT

Calculations that employ a relativistic time-dependent local density approximation (RTDLDA) to atomic absorption are used to examine a recent claim to the observation of giant quadrupolar resonances in the electron scattering spectrum of Ce metal near the 4p edge. We confirm the existence of 4p→4f resonances in this energy range but suggest that a conventional autoionization interpretation is more appropriate.

PACS Numbers: 78.70Dm, 32.80.Dz

A recent experimental study [1] announced the assignment of a prominent feature in the electron energy loss spectrum (EELS) of cerium metal near the 4p threshold to a "giant" resonance in the quadrupolar 4p→4f channel. The assignment was based on a comparison of x-ray absorption data to previously obtained EELS data [2] (both reproduced in Figure 1) and relies upon the fact that photoabsorption is sensitive to dipolar transitions exclusively (at the relevant excitation energies) whereas EELS can discriminate in favor of quadrupolar and higher multipolar transitions at sufficiently large values of the momentum transfer. One-electron Hartree-Fock calculations of the 4p→4f and competing dipolar 4p→5d matrix elements were used to suggest that superior wave function overlap tips the balance in favor of the former and that it is appropriate to regard the observed feature as a quadrupole analog to the well-known "giant" dipole resonance in cerium near the 4d threshold [3].

The present Brief Report examines this claim by means of an explicit calculation of both dipole and quadrupole photoabsorption by atomic cerium in the vicinity of the 4p threshold. The computations employ a relativistic time-dependent local density approximation (RTDLDA) [4] that has been shown to yield excellent agreement with experiment for photoabsorption in both the ultraviolet [5] and x-ray [6] portions of the spectrum. Within the framework of the local density approximation to the one-electron spectrum, this method includes all the polarization type many-electron effects responsible for channel mixing, auto-ionization and dipolar "giant" resonance behavior [7].

Figure 2 shows our results for the dipole cross section $\sigma_1(\omega)$ and the quadrupole cross section $\sigma_2(\omega)$ for atomic cerium in the vicinity of the spin-orbit split 4p threshold. We immediately confirm the qualitative experimental observation that the dipole absorption exhibits only weak structure near the edges whereas sharp sub-threshold resonances appear in the quadrupole channel. Regarding the latter, bear in mind that we consider not the true

electron scattering cross section but, instead, the photoabsorption cross section in the quadrupole channel, i.e., the momentum transfer is fixed at $q=\omega/c$. Accordingly, a trivial rescaling is required to compare the relative magnitudes of our calculated cross sections to the experiments. In this manner, we readily verify the conclusion of Ref. 1 that quadrupole excitations dominate the EELS spectrum for the given experimental conditions.

We also confirm the assignment of the resonant structure in $\sigma_2(\omega)$ to strong, overlap driven transitions between the 4p core states and the highly localized 4f valence orbitals. Observe that our computed resonances are quite narrow (we have made no attempt to include possible core-hole lifetime effects) and exhibit conventional Fano [8] lineshapes. This observation leads us to our only point of contention with Matthew et. al. [1]: their suggestion that these resonances are in some sense quadrupole analogs to the 4d→4f "giant" dipole resonances that occurs in cerium and the other rare earths.

Let us point out clearly that the definition of a "giant" resonance is, to some extent, a matter of taste [7]. Nevertheless, "their appearance as strong, localized resonances" [1] is definitely not sufficient. There is no question that the one-electron external field matrix element $\langle 4f|r^2|4p\rangle$ is large in this case due to wave function overlap. On the other hand, the "giant" resonances all are characterized by a large Coulomb matrix element that couples pairs of virtual particle-hole pairs [9]. The qualitative picture of an entire shell of electrons in collective motion follows from this requirement. In the present case, we would expect the relevant (4p,4f) Slater integral to be large [10] and to push the bound-bound transition oscillator strength into a broad resonance above threshold. We find no evidence for this. Instead, the transition is clearly visible above the quadrupolar continuum as a sharp autoionization resonance of the conventional sort.

Returning to the dipole channel, we find that our computed $\sigma_1(\omega)$ is not in particularly good quantitative agreement with the x-ray absorption measurements [1]. The latter exhibit essentially no edge jump; instead, a broad feature is observed between the $4p_{1/2}$ and $4p_{3/2}$ thresholds. The authors of Ref. 1 speculated that some "interconfigurational coupling" may lead to such behavior. However, the most significant class of such coupling already is included in our RTDLDA calculations. Consequently, we must conclude that the discrepancy between theory and experiment arises from some other source.

In summary, we have performed RTDLDA calculations of the expected dipole and quadrupole response of a cerium atom for excitation energies in the vicinity of the 4p core threshold. We confirm a previous assignment [1] of a strong feature observed in EELS as a $4p \rightarrow 4f$ resonance but dispute its classification as a "giant" resonance in the sense of, say, nuclear physics. We instead regard this feature as a conventional Fano-type autoionization resonance unaffected by strong polarization-type electron-electron interactions. Our results do not preclude the possibility of a true quadrupolar "giant" resonance in some different atomic system.

This work was performed under the auspices of the U.S. Department of Energy by the Lawrence Livermore National Laboratory under contract number W-7405-ENG-48. One of us (AZ) acknowledges support by DOE Grant No. DE-FG05-86ER45243.

REFERENCES

1. J.A.D. Matthew, F.P. Netzer, C.W. Clark and J.F. Morar, Euro-phys. Lett. 4, 677 (1987).
2. G. Strasser and F.P. Netzer, J. Vac. Sci. Tech. A 2, 826 (1983).
3. A. Zangwill and P. Soven, Phys. Rev. Lett. 45, 204 (1980).
4. D.A. Liberman and A. Zangwill, Comp. Phys. Commun. 32, 75 (1984).
5. A. Zangwill, in Atomic Physics 8, edited by I. Lindgren, A. Rosen, and S. Svanberg (Plenum, New York, 1983), p. 339.
6. W. Jitschin, U. Werner, G. Materlik and G.D. Doolen, Phys. Rev. A 35, 5038 (1987).
7. A. Zangwill, in Giant Resonances in Atoms, Molecules and Solids, edited by J.P. Connerade, J.M. Esteve and R.C. Karnatak (Plenum, New York, 1987), p. 321.
8. U. Fano, Phys. Rev. 124, 1866 (1961).
9. G.E. Brown and M. Bolsterli, Phys. Rev. Lett. 3, 472 (1959).
10. This is true whether one works in a Hartree-Fock basis or in a local density functional basis. Of course, the Coulomb integral enters in different places in the two calculations.

FIGURE CAPTION

Figure 1. Electron energy loss spectrum (primary energy 1880 eV) and x-ray absorption spectrum of cerium metal from Reference 1. Note the reversal of the energy scale.

Figure 2. Calculated dipole and quadrupole photoabsorption cross sections for Ce atom in the vicinity of the spin-orbit split 4p threshold. Note the difference in vertical scales. The photon energy scale is reversed to facilitate comparison with Ref. 1.

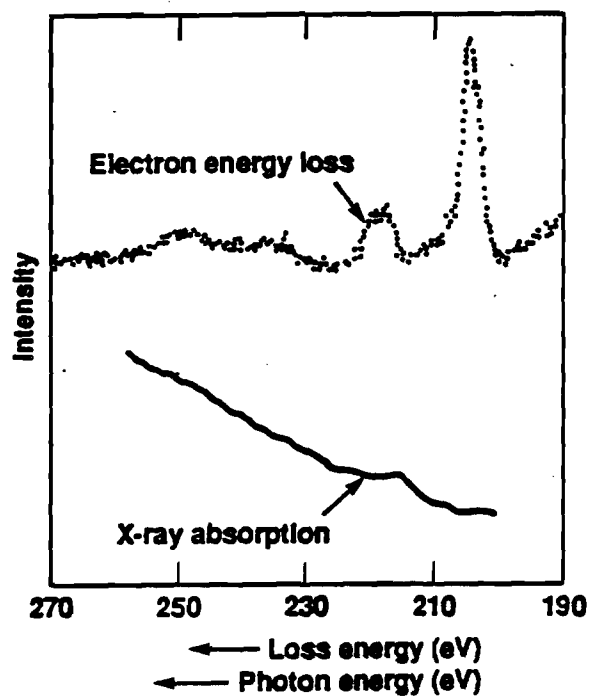
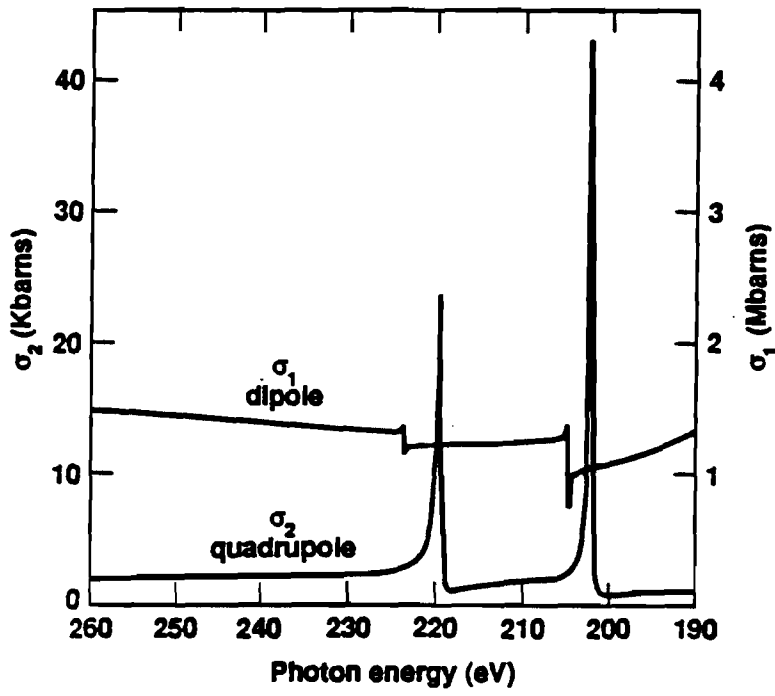


Figure 1.



D.A.L.
12/9/87

Figure 2.

Morphological Transitions in Solid Epitaxial Overlayers.

R. BRUINSMA(*) and A. ZANGWILL(**)

(*) *Physics Department and Solid State Science Centre, University of California, Los Angeles, CA 90024, USA*

(**) *School of Physics, Georgia Institute of Technology - Atlanta, GA 30332, USA*

(received 23 February 1987; accepted in final form 10 July 1987)

PACS. 68.55. - Thin film growth, structure, and epitaxy.

PACS. 61.50C - Physics of crystal growth.

PACS. 64.70K - Solid-solid transitions.

Abstract. - We present a continuum model for the growth of solid epitaxial films which takes account of both surface tension and lattice mismatch. Layer-by-layer film growth is found to be unstable for fixed particle number. We show that the conventional nucleation and growth scenario for film decay is in error above the roughening temperature. Films decay to epitaxial solid «droplets» in coexistence with a microscopically thin, strained film through a barrierless mechanism which is closely related to spinodal decomposition. The decay of the film is triggered when the layer height exceeds the critical height beyond which misfit dislocations appear at the interface.

Epitaxial overlayers exhibit three characteristic morphologies during the initial stages of growth. The first of these, the so-called Frank-van der Merwe (FM) growth, occurs in a layer-by-layer fashion. Vollmer-Weber growth (VW) corresponds to nucleation of bulk-phase clusters onto the substrate directly from the vapor phase. The third observed growth mode is a combination of these two: the Stranski-Krastanov (SK) growth mode occurs when bulk-phase clusters nucleate on the substrate only after a few monolayers have adsorbed in layer-by-layer fashion. The existence of these three modes is well documented [1] and is easy to rationalize [2]. Define a quantity $S = \gamma_s - \gamma_i - \gamma$, where γ_s , γ_i and γ denote, respectively, the specific surface free energies of the substrate-vacuum, substrate-overlayer and overlayer-vacuum interfaces. When $S < 0$, VW growth is favoured, whereas when $S > 0$, either SK or FM growth occurs.

Lattice-gas models of fluid wetting and multilayer adsorption also lead to these three scenarios [3]. Such models presume that the adsorbed film both i) is in equilibrium with its own vapor and ii) does not support any elastic strain. For solid epitaxial overlayers, misfit between the adsorbate lattice constant a) and the substrate lattice constant b) always leads to strain in the films. The first few deposited monolayers typically strain homogeneously to match the substrate lattice. Beyond a critical height h_c , misfit dislocations show up at the interface and inhomogeneous strains appear [4]. The energy cost associated with these strains can be incorporated into the lattice-gas models in a phenomenological fashion and one

finds [5] that SK growth supplants layer-by-layer growth. However, if the lattice misfit is small or if the overlayer is elastically soft, layer-by-layer growth may persist for many layers. These conclusions appear to be valid [6] for multilayer adsorption of inert gases on smooth substrates.

Unlike physisorption systems, the very low vapor pressure of metals and semiconductors typically restricts the epitaxial growth of these materials to conditions very far from thermodynamic equilibrium [7]. Except in special cases [8], the considerations of the previous paragraph do not apply to chemical vapor deposition or molecular beam epitaxy. Kinetic theories have been proposed to treat the problem of epitaxial-growth mode selection [9]. However, even though we may neglect re-evaporation for many metals and semiconductors, surface diffusion is still quite rapid at typical growth temperatures. In fact, without surface diffusion the overlayer would be amorphous. Hence, we propose that for low enough growth rates, the film morphology *can* be determined by equilibrium arguments, albeit *at fixed particle number* instead of at fixed chemical potential. In this letter we present the predictions of a fixed particle continuum model for the static and dynamic properties of epitaxial overlayers.

Statics. – Our model for wetting of solids is a generalization of the theory of fluid wetting reviewed by de Gennes [10]. For simplicity, suppose that the thickness $h(x)$ of an epitaxial overlayer depends only on one coordinate in the plane of the surface. The thermodynamic potential of the film, constrained to maintain a fixed particle number (or, equivalently, a fixed mean height) is given by

$$G = \int dx \left\{ -S + \frac{1}{2} \gamma (dh/dx)^2 + B \epsilon_{xx}^2(x) h(x) + |\epsilon_{xx}(x) - f| D (\ln(R/b_0) + 1) + \lambda h(x) \right\}. \quad (1)$$

The first term is the «spreading pressure» introduced earlier. The second term is the energy cost associated with the extra area of a curved surface compared to a flat film. Our principal approximation resides here: we restrict ourselves to temperatures above the critical temperature for roughening T_R so that it is permissible to neglect the anisotropy of the surface tension γ . The third and fourth terms in eq. (1) arise from the lattice misfit between substrate and overlayer [4]⁽¹⁾. There is an energy cost due to both a slowly varying strain $\epsilon_{xx}(x)$ in the overlayer (which does not vary in the direction normal to the film) and to an array of misfit dislocations (of Burgers vector b_0) with a repeat distance $l/a = b/|a(1 + \epsilon_{xx}) - b|$. We assume commensurability along the y -direction. The misfit $f = (b - a)/a$ is the strain required to produce registry between substrate and overlayer, while the cut-off in the logarithm $R = \min[h, la/2]$. The Lagrangian multiplier λ in the last term fixes the particle number.

We first minimize eq. (1) with respect to ϵ_{xx} . This simplifies eq. (1) to

$$G = \int dx \left\{ -S + \frac{1}{2} \gamma (dh/dx)^2 + P(h) + \lambda h \right\}, \quad (2)$$

with

$$P(h) = \begin{cases} Bf^2 h, & h < h_c, \\ -fD \ln(2f) - \frac{D^2}{4Bh} \ln^2(2f), & h \gg h_c, \end{cases} \quad (3)$$

⁽¹⁾ For a rigid substrate and an isotropic elastic overlayer with shear modulus μ and Poisson ratio ν : $B = 2\mu(1 + \nu)/(1 - \nu)$ and $D = b_0/2\pi(1 - \nu)$.

where $h_c = (D/2Bf)(\ln(h_c/b_0) + 1)$ is the critical height where misfit dislocations appear for the first time, *i.e.* where the overlayer becomes incommensurate with the substrate [11]. $P(h)$ acts as an effective repulsive interaction between substrate and overlayer. There is a discontinuity in $P''(h)$ at $h = h_c$ and, for $h > h_c$, $P(h)$ is a concave function of h , while $P(h) = \infty$ for $h < 0$. Note that for physisorption problems, $P(h)$ is the attractive (and convex) van der Waals interaction—which can be neglected for metals and semiconductors.

In equilibrium, the thermodynamic potential must be extremal with respect to variations in $h(x)$. The associated Euler-Lagrange equation is

$$\gamma \frac{d^2h}{dx^2} = \frac{dP(h)}{dh} + \lambda, \tag{4}$$

which has a first integral

$$\frac{1}{2} \gamma \left(\frac{dh}{dx} \right)^2 - P(h) - \lambda h = E. \tag{5}$$

As noted by de Gennes [10], this is formally a classical mechanics problem of a particle of mass γ , quasi-energy E and position h in a potential $V(h) = -P(h) - \lambda h$. This potential is shown in fig. 1 for various values of λ . We now classify the possible solutions:

1) $E > 0$. These solutions correspond to overlayers which begin at $h = 0$ with a «kinetic energy» E and return to $h = 0$ after a finite «time» x_{\max} . In other words, finite-size droplets on a dry substrate. The contact angle $\theta_c = \lim_{x \rightarrow \infty} dh/dx$ of an infinite droplet ($\lambda = 0$) follows from eq. (5):

$$\gamma \cos(\theta_c) = -E + \gamma - P(\infty). \tag{6}$$

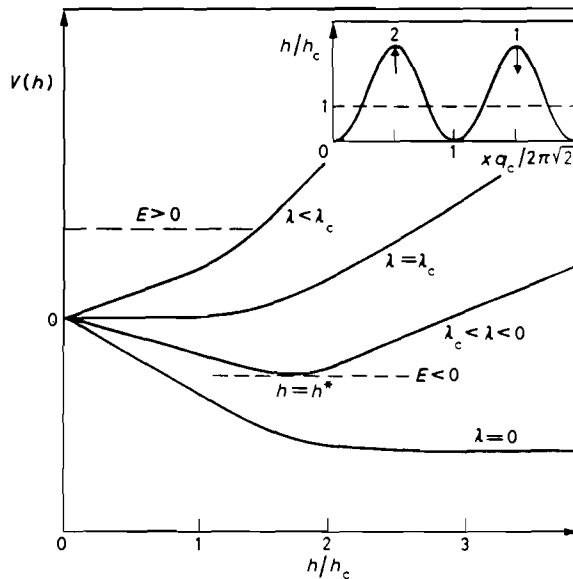


Fig. 1. – Potential energy of the mechanical problem for various values of λ . For $\lambda = \lambda_c$, the potential is flat if $h < h_c$. The quasi-energies of a droplet on a dry substrate and of the unstable Deryagin solution are indicated by dashed lines. In the inset is shown a numerical solution of eq. (4) with $E = 0$, $\lambda = -0.0045$, $f = 0.1$, $B = D = \gamma = 1$.

But we also can compute θ_c from Young's law [$\gamma \cos(\theta_c) = \gamma_s - \gamma_l - P(\infty)$] in terms of the spreading pressure with the result that $E = -S$ for positive E . Note that the contact angle vanishes at $S = P(\infty)$, not $S = 0$. We thus identify VW growth with $S < 0$ and positive quasi-energies.

2) $E = 0$, $\lambda = \lambda_c = -Bf^2$. The effective potential is flat for $h < h_c$ so, from eq. (4), a flat film with height $h < h_c$ is a solution. This must correspond to epitaxial, coherent (*i.e.* dislocation free) overlayer growth.

3) $E < 0$, $0 < \lambda < \lambda_c$. For $-P(\infty) < E < 0$ the only allowed values of λ are in the interval $[0, -Bf^2]$ and it is clear from fig. 1 that in this range the overlayer wets the substrate: h oscillates between a maximum and a minimum value (h_{\max} and h_{\min}). The wetting transition thus still takes place at $E = S = 0$. The effective potential $V(h)$ has a minimum, say at h^* . If we adjust the quasi-energy to be exactly equal to $V(h^*)$, then $h(x) = h_{\max} = h_{\min}$ and $dP(h^*)/dh = -\lambda$. This is a film of a uniform thickness in excess of h_c with a surface energy $F/A = -S + P(h^*)$ (A is the substrate area). The film height can be controlled through λ so this solution would appear to correspond to FM growth. It is the analog of the classical Deryagin solution which appears in the literature of fluid wetting (see footnote⁽¹⁾).

4) *Phase coexistence*. So far we have assumed that the film is characterised by a single value of λ and E . However, since $P(h)$ is nonanalytic at $h = 0$ and $h = h_c$, we are free to match solutions of different λ and E . The boundary conditions are that the film-height $h(x)$ and the surface energy $\gamma(dh/dx)^2$ must be continuous. By matching a bulk drop ($\lambda \rightarrow 0$, $E = 0$) with a film of vanishing (*i.e.* microscopic⁽²⁾) height ($\lambda = -Bf^2$), we obtain solutions with surface energy $F/A = -S$ and arbitrary particle number. For $S > 0$, this is obviously the lowest possible energy, since $P(h)$ is a monotonically increasing function. This is the SK morphology which in our theory must be interpreted as coexistence between a solid «bulk» phase and a solid «surface» phase. The contact angle between film and droplet is given by eq. (6) with $E = 0$.

As a function of the spreading pressure, there is thus a first-order transition at $S = 0$ from a phase with droplets on a dry surface (VW) to phase coexistence of droplets and a microscopically thin film (SK)⁽³⁾. The FM growth mode is absent in equilibrium.

Dynamics. - Of course, thick films obtained by FM growth are observed in the laboratory. This is normally explained by a nucleation argument [12]. Such arguments tacitly assume that a film is stable against small fluctuations in $h(x)$. However, a first-order phase transition need not proceed through nucleation and growth. A metastable phase becomes unstable if the degree of «supercooling» is sufficiently great.

Suppose that we have been able to grow a film to a height h . To discuss its stability, we first note that the surface diffusion current is [13]

$$J_s = -(Dv/kT) d\mu/dx, \quad (7)$$

⁽²⁾ Our continuum model of the overlayer breaks down at this point. In practice, we match bulk drop solutions to monolayer solutions. If the range of the direct overlayer-substrate adhesion potential extends beyond nearest neighbors, one also can match to very thin multilayer solutions.

⁽³⁾ Precursor wetting (see footnote⁽¹⁾), for S close to zero may smear out the phase transition. A microscopic model for the interaction between the substrate and overlayer is required to investigate this possibility.

where D is the surface diffusion constant, μ is the local chemical potential and ν is the number of surface atoms per unit area. The chemical potential near the surface is [13]

$$\mu = \left(-\gamma \frac{\partial^2 h}{\partial x^2} + \frac{\partial P}{\partial h} \right) \Omega. \quad (8)$$

In this expression, dP/dh plays the role of an effective hydrostatic pressure and Ω is the atomic volume. The continuity equation at the surface then becomes

$$\partial h / \partial t + \left(\frac{D\Omega^2\nu}{kT} \right) \frac{\partial^2}{\partial x^2} \left\{ \gamma \frac{\partial^2 h}{\partial x^2} - \frac{\partial P}{\partial h} \right\} = 0. \quad (9)$$

A capillary wave $\Delta h = h_q \sin(qx) \exp[\omega t]$ is a solution of eq. (9) if $\omega(q)$ obeys the dispersion relation

$$\omega(q) = - \left(\frac{D\xi\Omega}{kT} \right) \gamma q^2 (q^2 - q_c^2), \quad (10)$$

where $q_c = ((-d^2P(h^*)/dh^2)/\gamma)^{1/2}$. For a film with $h < h_c$, $q_c = 0$ so sufficiently thin films are indeed metastable. However, if h exceeds h_c the film is unstable against the growth of small q capillary waves. The fastest growing mode corresponds to the maximum of $\omega(q)$, *i.e.* when $q = q_c/\sqrt{2}$. The physical origin of the capillary instability is clear from fig. 1. Periodic increases and decreases in h lead to corresponding increases and decreases in the free energy through $P(h)$. But, since $P(h)$ is concave, there is a net overall reduction. The Deryagin solution of eq. (4) is now only a point of marginal stability of eq. (9).

Suppose we follow the point of marginal stability as the amplitude increases at later times. This requires oscillatory solutions of eq. (4) of larger and larger amplitude which keep the mean height (particle number) fixed. It is clear from fig. 1 that this corresponds to a steady increase in the quasi-energy E and a small increase in λ . At its maximum value, $E = 0$, the capillary wave touches the substrate and no further increase in amplitude is possible (see inset of fig. 1; note that the wave vector of this capillary wave, computed numerically, is very close to $q_c/\sqrt{2}$).

To test the stability of this solution, consider two neighbouring crests of the wave, each corresponding to a single period (*i.e.* starting and ending at $h = 0$) in the potential well with the same value of λ and $E = 0$. Now increase λ for one period to $\lambda + d\lambda_1$, decrease it for the other to $\lambda - d\lambda_2$ and match the solutions. The changes in the surface energy and the mean height of the two periods are

$$dg = \partial g / \partial \lambda (d\lambda_1 - d\lambda_2) + \frac{1}{2} \partial^2 g / \partial \lambda^2 (d\lambda_1^2 + d\lambda_2^2), \quad (11a)$$

$$dh = \partial h / \partial \lambda (d\lambda_1 - d\lambda_2) + \frac{1}{2} \partial^2 h / \partial \lambda^2 (d\lambda_1^2 + d\lambda_2^2), \quad (11b)$$

with $g(\lambda)$ and $h(\lambda)$ the free energy and average height of a single period of quasi-energy $E = 0$. By particle conservation, $dh = 0$ so after eliminating $d\lambda_2$

$$dg = \left(-\partial g / \partial \lambda \frac{\partial^2 h / \partial \lambda^2}{\partial h / \partial \lambda} + \frac{\partial^2 g}{\partial \lambda^2} \right) d\lambda_1^2. \quad (12)$$

By numerical integration of eq. (4) for $E = 0$, $f = 0.1$ and $B = D = \gamma = 1$, we found that this quantity is negative for any λ . If this result is generally valid, it is energetically favourable for a crest in the wave to grow at the expense of its neighbours. The physical reason is again the concavity of $P(h)$: the reduction in g of the smaller crest more than compensates for the

increase in g by the larger crest. This process can be repeated again and again until we are left with a few large drops (with relatively small surface area) separated by a monolayer film which wets the remainder of the surface. The late stages of this coalescence process can be treated by the Lifshitz-Slyozov theory [14].

The morphological scenario discussed above is closely related to a process of phase separation in binary alloys known as spinodal decomposition [15]. This mechanism involves no nucleation barrier and thus is expected to proceed much more rapidly than conventional nucleation and growth. On the other hand, our analysis presumes that surface diffusion is the rate limiting step for the morphological evolution, whereas changes in $h(x)$ implicitly require motion or dissolution of misfit dislocations—a process impeded by the microscopic Peierls barrier. Dislocation nucleation and motion is known to be much slower in semiconductors than in metals—sometimes completely suppressing the generation of misfit dislocations at h_c . Our theory is not applicable in those cases. Also, because the critical height is roughly the characteristic length scale of the capillary wave, we expect that our continuum theory will be valid only if h_c is large compared to a monolayer (*i.e.* small misfits).

In summary, we have studied the morphology of epitaxial films of fixed particle number in the continuum approximation. For temperatures above the roughening temperature, the lowest free energy is obtained either for nonwetting droplets of bulk solid phase ($S < 0$), or bulk drops in coexistence with a microscopically thin wetting layer of the solid surface phase ($S > 0$). We predict that, if misfit dislocations are mobile and easily nucleated, elastically strained films decay to the SK morphology ($S > 0$) via a barrierless instability if h exceeds a critical height (h_c). For $S < 0$ it is unlikely that strained films can be grown at all.

Possible candidates for experimental test of this prediction include the Ag/Si(111) [16] and Na/W(100) [17] epitaxial systems.

* * *

We acknowledge helpful conversations with A. ERBIL, M. GRABOW and A. REDFIELD and support by NSF Grant No. DMR-8603217 (RB) and DOE Grant No. DE-FGOS-86ER45243 (AZ).

REFERENCES

- [1] KERN R., LE LAY G. and METOIS J. J., in *Current Topics in Materials Science*, Vol. 3, edited by E. KALDIS (North-Holland, Amsterdam) 1979, p. 131; VENABLES J. A., SPILLER G. D. T. and HANBUCKEN M., *Rep. Prog. Phys.*, **47** (1984) 399.
- [2] BAUER E., *Z. Krist.*, **110** (1958) 372.
- [3] For a review, see WORTIS M., in *Fundamental Problems in Statistical Mechanics*, Vol. 6, edited by E. G. D. COHEN (North-Holland, Amsterdam) 1985, p. 87.
- [4] MATTHEWS J. W., in *Dislocations in Solids*, Vol. 2, edited by F. R. N. NABARRO (North-Holland, Amsterdam) 1979, p. 461.
- [5] KERN R., in *Interfacial Aspects of Phase Transformations*, edited by B. MUTAFTSCHIEV (Reidel, Dordrecht) 1982, p. 287; HUSE D. A., *Phys. Rev. B*, **29** (1984) 6985; GITTES F. T. and SCHICK M., *Phys. Rev. B*, **30** (1984) 209.
- [6] BIENFAIT M., SEGUIN J. L., SUZANNE J., LERNER E., KRIM J. and DASH J. G., *Phys. Rev. B*, **29** (1983).
- [7] CHERNOV A. A., *Modern Crystallography III* (Springer, Berlin) 1984.
- [8] LE LAY G. and IMAN Z., *Surf. Sci.*, **154** (1985) 90.
- [9] KASHCHIEV D., *J. Cryst. Growth*, **40** (1977) 29.
- [10] DE GENNES P. G., *Rev. Mod. Phys.*, **57** (1985) 841.

- [11] BRUINSMA R. and ZANGWILL A., *J. Phys. (Paris)*, **47** (1986) 2055.
- [12] GRABOW M. H. and GILMER G. H., in *Layered Structures and Epitaxy*, edited by J. M. GIBSON, G. C. OSBOURNE and R. M. TROMP (MRS, Pittsburgh) 1986, p. 13; GRABOW M. H. and GILMER G. H., *Surf. Sci.* (submitted).
- [13] HERRING C., in *The Physics of Powder Metallurgy*, edited by W. KINGSTON (McGraw-Hill, New York, N.Y.) 1951, p. 143. See also MULLINS W. W., in *Metal Surfaces* (American Society of Metals, Metals Park, OH) 1963, p. 17.
- [14] CHAKRAVERTY B. K., *J. Phys. Chem. Solids*, **28** (1967) 2401.
- [15] CAHN J. W., *J. Chem. Phys.*, **42** (1965) 93.
- [16] LE LAY G., MANNEVILLE M. and KERN R., *Surf. Sci.*, **72** (1978) 405.
- [17] MLYNCZAK A. and NIEDERMEYER R., *Thin Solid Films*, **20** (1975) 37.

PHENOMENOLOGICAL APPROACH TO MULTILAYER GROWTH AND STABILITY

ANDREW ZANGWILL

School of Physics, Georgia Inst. of Tech., Atlanta, GA, 30332

ABSTRACT

I review recent theoretical studies designed to examine the effect of strain, faceting and growth conditions on multilayer stability. A phenomenological approach is used to investigate both morphological and crystal structural phase stability.

INTRODUCTION

The fascinating and technologically useful properties of artificial multilayer structures fabricated from metals, semiconductors, and insulators have driven experimental studies of these systems for a decade or more. Accordingly, a significant body of lore has accrued that specifies under what sort of experimental conditions one should operate in order to guarantee "good", i.e., layer-by-layer growth of a heterostructure with a particular desirable crystal structure. Deviations from such well-defined "recipes" can lead to unusual and poorly understood growth structures. In this article, I focus on three archetypal issues that arise in connection with this situation: solid-on-solid wetting, morphological instability and pseudomorphy. In particular, I review recent attempts to address these phenomena by means of macroscopic and/or phenomenological models that do not require detailed material-specific information. The goal is to provide a framework to guide further experiments and more microscopic theoretical investigations.

SOLID-ON-SOLID WETTING

It is well known that thin films grown via standard vapor phase deposition techniques such as molecular beam epitaxy (MBE) or chemical vapor deposition (CVD) typically adopt one of three familiar "growth modes". So-called Frank-van der Merwe (FM) growth proceeds in a regular layer-by-layer manner. Volmer-Weber (VW) growth corresponds to nucleation of bulk-phase clusters onto the substrate directly from the vapor whereas the Stranski-Krastanov (SK) mode is said to occur when bulk phase clusters nucleate only after a few monolayers have adsorbed in layer-by-layer fashion. A clear review of the general issues recently has been supplied by Gilmer and Grabow [1] who, in addition, focus attention on the theoretical method of molecular dynamics as a means to address the thermodynamic stability of the FM growth morphology. In what follows, I discuss an alternative approach to the same issue following the phenomenological analysis of Bruinsma and Zangwill [2].

It is convenient to regard the occurrence of a particular growth mode in an epitaxial system as a problem in morphological selection. To that end, we characterize the growing overlayer by a function $h(x,y,t)$ that describes the local height of the deposited material above the substrate as a function of time. To begin, let us ignore the dynamic (growth) aspects of the problem and simply ask: what shape function $h(x,y)$ represents the thermodynamic ground state of a system of N particles epitaxially deposited onto a fixed substrate? To answer this question we

must specify the free energy of the overlayer as a functional of $h(x,y)$ and then minimize. If, for example, the solution is $h(x,y)=\text{constant}$, we should expect the FM mode under conditions of slow growth.

The dominant contributions to the free energy we require are (1) a term $S = \gamma_s - \gamma_i - \gamma$ that measures the relative surface tensions of the substrate-vacuum (γ_s), substrate-overlayer (γ_i) and overlayer vacuum (γ) interfaces; (2) a term $\gamma(\nabla h)^2$ that counts the extra energy cost if a fixed substrate area A is covered by an overlayer of surface area $> A$, i.e., if $h(x,y)$ is anything but a constant (see Figure 1); (3) a term $P(h)$ that counts the local elastic strain in the overlayer due to misfit between the substrate and overlayer lattice constants; and (4) a term that recognizes that curved surface profiles expose crystal facets whose energy depends on crystallographic orientation.

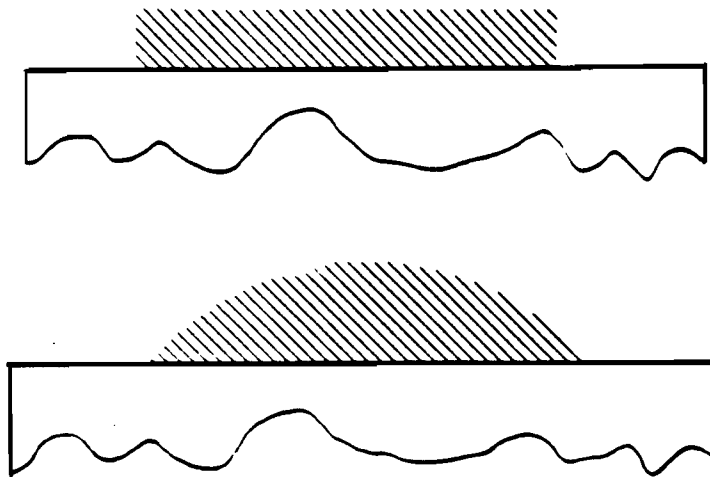


Figure 1

Specializing to a model two-dimensional system where $h=h(x)$ only, an appropriate free energy that includes all these features is:

$$F = \int dx \left[-S + \gamma (dh/dx)^2 + P(h) - y_0 \cos(2\pi h) + \lambda h \right] \quad (1)$$

The first four terms are precisely as described above. $P\{h(x)\}$ is a concave, monotonically increasing function of its argument that includes the effect of both interfacial misfit dislocations and residual elastic strain. It is described thoroughly in conventional treatments of the effect of strain during epitaxial growth [3]. Sophisticated theories of the so-called "roughening transition" (which model the destruction of crystal facets by thermal fluctuations) show that the sinusoidal term in Equation (1) is sufficient to account for the increased energy of vicinal surfaces inclined at a small angle with respect to the substrate plane [4]. The combination $\sqrt{\gamma y_0}$ is proportional to the energy of a monatomic step. Finally, the quantity λ is a Lagrange multi-

plier that guarantees that only surface profiles $h(x)$ which preserve total particle number may be considered in the variational minimization of the free energy.

The details of this minimization are non-trivial and may be found elsewhere [2,5]. On the other hand, the final results can be understood quite simply. Consider first the limit where γ_0 vanishes. This case resembles that of fluid wetting except that the overlayer can support a finite strain. In agreement with the simplest theory [6], Volmer-Weber "droplet" formation is found if $S < 0$. The system minimizes the effect of a relatively costly substrate-overlayer surface tension by minimizing the area of contact. There is no wetting.

Adhesion between substrate and overlayer is favored if $S > 0$ and we expect at least one complete monolayer to wet the substrate. However, the calculations show that further layer-by-layer growth is never favorable. That is, the Stranski-Krastanov morphology is always the ground state for non-zero misfit and $S > 0$. This surprising result arises from the concavity of $P(h)$ and the fact that the "footprint" of a three-dimensional droplet of atoms is very much smaller ($\sim 10^{-6}$) than the area covered by the same number of atoms when spread out into a monolayer. The integrated strain energy within the droplet is considerably smaller than the corresponding quantity for the layer.

This conclusion persists for moderate, non-zero values of the step energy. True FM growth is at best metastable in this regime. If one prepares such a morphology by a non-equilibrium process (as is routinely done in the laboratory!), we predict that the overlayer will transform to the SK morphology if left undisturbed indefinitely. This result agrees with that of the aforementioned microscopic calculation [1]. Nonetheless, to determine if the transformation is observable, one must specify the quantitative height of the thermal activation barrier and the mode of morphological evolution. Within the framework of Equation (1), a dynamical calculation [2,5] implicates a sinusoidal modulation of the crystal surface that is formally similar to the phenomenon of spinodal decomposition. The barrier energy is related to both the step energy and the Peierls energy for misfit dislocation motion.

Morphological evolution from FM to SK effectively is suppressed when the step energy becomes very large, or, more correctly, when the surface energy of a finite contact angle facet (see Figure 1) becomes very large. In fact, it is possible (in that limit) that the layer-by-layer morphology actually supplants SK growth as the thermodynamically stable configuration for some range of particle number. The details of the crossover have yet to be worked out.

MORPHOLOGICAL INSTABILITY DURING GROWTH

I now suppose that droplet nucleation from the vapor has been suppressed as indicated above and a multilayer is to be grown by deposition of some specified number of layers. At this point, strict adherence to an empirical growth "recipe" is important since it is well known that small variations in external control parameters (deposition rate, temperature, etc.) can have large morphological consequences. Recent theoretical studies of the CVD process illustrate this fact dramatically.

Chemical vapor deposition involves two distinct physical processes. First, the reacting gas must diffuse down through a non-

hydrodynamic "stagnant" layer to bring reactant molecules into the immediate vicinity of the growing surface. Second, some activated process (such as dissociative chemisorption) must occur that actually incorporates the material into the solid. Let us characterize the former by a diffusion constant D and the latter by a rate constant k . Quasi-static growth of the interface at velocity $v(x,y)=v(s)$ then can be modelled [7] by the following macroscopic equations:

$$\begin{aligned} \nabla^2 c(r) &= 0 \\ c(\delta) &= c_0 \\ k\{c(s)-c_{eq}(s)\}^0 &= D\nabla c \cdot n|_s \\ v(s) &\propto \nabla c \cdot n|_s \end{aligned} \quad (2)$$

That is, the concentration of diffusing reactant $c(r)$ is determined (in steady state) by Laplace's equation subject to two boundary conditions: a fixed "inlet" concentration at a distance δ above the surface and a mixed boundary condition at the growing interface that depends on the relative importance of the two transport processes noted above. The driving force for growth depends on the difference between the reactant concentration at the surface $c(s)$ and its equilibrium value $c_{eq}(s)$. The latter is determined by the surface tension γ and the local radius of curvature of the interface.

Equation (2) constitutes a moving boundary value problem. One solves the equations for a given shape of the surface and then advances each surface point according to its local growth velocity. Iteration of this two-step procedure traces out the growth profile as a function of time. The problem is highly non-linear and not amenable to simple analytic analysis. Consequently, we [8] have applied an essentially exact numerical technique to extract solutions for various values of the characteristic dimensionless parameter $v=k\delta/D$.

To focus on the question of instability, consider deposition onto a patterned substrate as might be encountered for semiconductor applications. Figure 2 illustrates the predicted morphology (after identical growth periods) for three different growth conditions. The results are striking. When incorporation into the surface is the rate limiting step ($v \ll 1$) we observe smooth layer-by-layer "template" growth; the interface follows the morphology set by the substrate. By contrast, when deposition is limited by reactant diffusion ($v \gg 1$) an instability of the Mullins-Sekerka variety [9] develops that evolves non-linearly into a pattern reminiscent of dendritic growth. Details will be presented elsewhere [8].

The reader should not suppose that the limiting cases shown below reflect unphysical values of the parameters. In fact, the top and bottom panels of Figure 2 very nearly reproduce cross-sectional micrographs obtained by van den Brekel [7] for silicon growth at $T=1010$ °C and $T=1180$ °C under otherwise identical conditions.

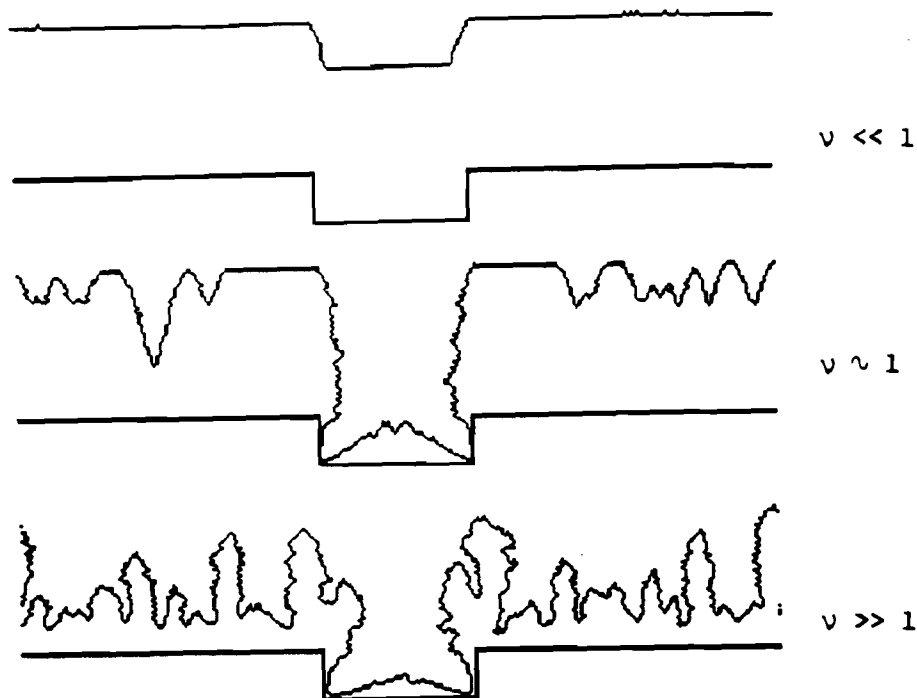


Figure 2

PSEUDOMORPHY

I now suppose that FM growth in the "template" mode has been achieved and turn to my final example of metastability relevant to multilayer growth: pseudomorphy. The general phenomenon is not new; there are many documented cases [10] of the ability of a substrate to induce an overlayer to adopt a crystal structure that differs from its bulk-stable structure. Renewed interest has been stimulated by Prinz' successful growth of surprisingly thick films of BCC cobalt on GaAs(110) [11].

The essential physics of this phenomenon has been analyzed in some detail by Bruinsma and Zangwill [12] using a phenomenological free energy model of epitaxial growth. The key idea is to extend the classic analysis of van der Merwe [13] to the case where the overlayer can respond non-linearly to a shear stress applied by the substrate. In brief, an overlayer may adopt a new crystal structure (and lattice constant) if too great a misfit energy would be incurred if epitaxy were required with the bulk-stable crystal structure and lattice constant. Evidently, an energetic trade-off is involved: energy gained at the interface must exceed energy lost by each overlayer unit cell which finds itself in an "unnatural" crystal structure. A simple surface-to-volume argument then demonstrates that a phase transition back to the bulk-stable phase must occur for sufficiently thick film growth. On the other hand, multilayers provide an attractive means to "trap" a sandwiched layer in the pseudomorphic phase.

To be more quantitative, suppose that the free energy density (free energy/unit cell) of the overlayer $f(\epsilon)$ resembles Figure 3. The independent variable represents strain along some "easy" axis. The absolute minimum corresponds to the bulk-stable crystal structure, FCC for example. But, since the FCC structure is crystallographically equivalent to a body-centered tetragonal structure, a strain of sufficiently large magnitude along the tetragonal axis converts the original FCC structure to BCC. The

existence of a metastable minimum at this value of strain (and the barrier at intermediate values of strain) can be deduced from general principles [12].

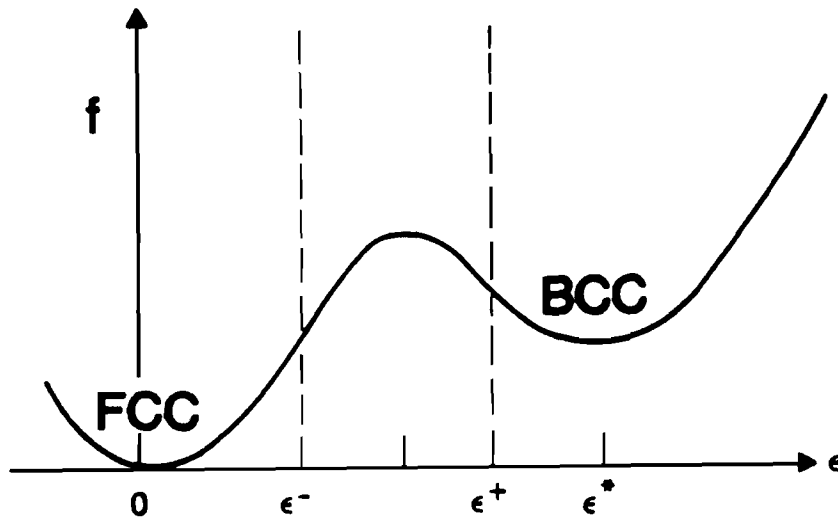


Figure 3

Now let $f=(b-a)/a$ denote the misfit between the substrate lattice constant (b) and the overlayer bulk-stable phase lattice constant (a). Then, within the Peierls model of epitaxy for (again) a model two-dimensional system, the total free energy per unit length of a film of height h can be written:

$$F = \int dx \left[hf(\partial u/\partial x) - \kappa \cos[2\pi(u - fx)/b] \right] \quad (3)$$

The strain ϵ is related to the local displacement of the overlayer $u(x)$ by $\epsilon=\partial u/\partial x$ and κ is a constant that is proportional to an interfacial shear coefficient. Equation (3) presumes a thin-film approximation wherein each layer adds an identical bulk energy per length up to the film height h . Observe also that $u(x)=fx$ if the overlayer bulk-stable phase is uniformly strained into commensurability with the substrate.

The conventional theory of epitaxy [13] concerns itself with small excursions around $\epsilon=0$ in Figure 3. If registry can be achieved at the monolayer level, some critical height h_c exists above which the strain in the film becomes excessive and must be relieved by the introduction of misfit dislocations. Here, we are concerned with the large misfit regime where the oscillatory Peierls term in Equation (3) induces an average strain $\epsilon=\epsilon^*$. In that case, epitaxy which retains the overlayer bulk-stable crystal structure is prohibitively costly in energy and does not occur. Instead, a structural transition occurs to the pseudomorphic (BCC) phase where the new lattice constant a^* is well matched to the substrate and the residual misfit f^* is small. The linear theory may then be applied to determine whether the overlayer is merely strained (coherent) or contains misfit dislocations (incoherent).

A complete (mean field) analysis of Equation (3) yields the structural phase diagram illustrated in Figure 4 for the case of strong substrate-overlayer adhesion ($\kappa \gg 1$). Near $f=0$ and $f=f^+$ we observe a coherent-incoherent transition with respect to the bulk stable and pseudomorphic phases, respectively. These transitions are continuous. More interestingly, a massive first-order transition occurs between the pseudomorphic phase and the bulk-stable phase as a function of height. This is the triumph of bulk thermodynamics over epitaxial adhesive forces alluded to earlier. However, because the transition is first order, there is a nucleation barrier to transformation. A crude estimate of the barrier height in a typical case yields [12] $E_b = 0.1$ eV/monolayer - a substantial number compared to room temperature. Thus, one may expect pseudomorphic layers to exceed equilibrium critical heights due to kinetic constraints.

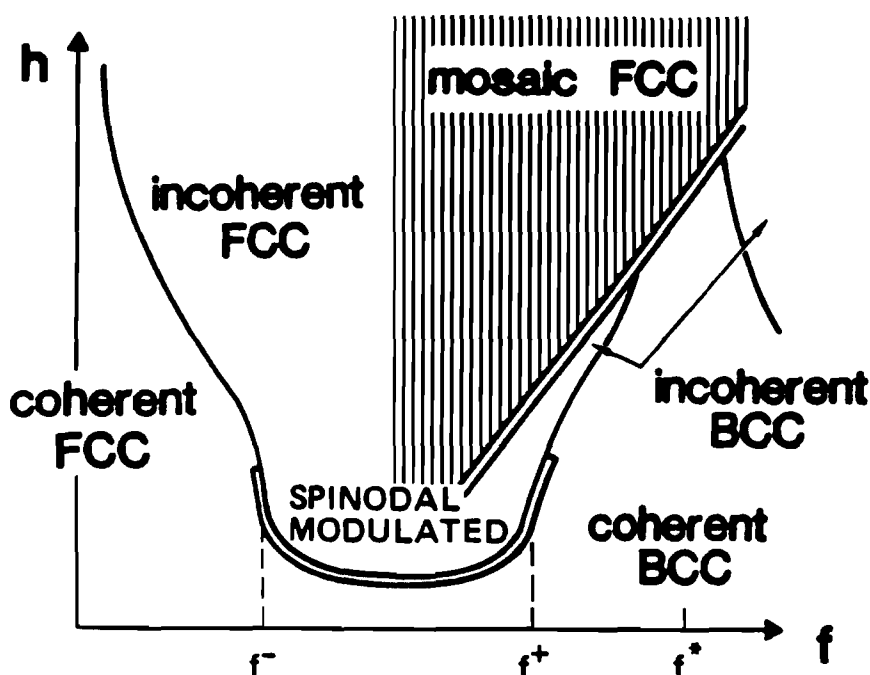


Figure 4

Two features of our phase diagram deserve special mention. First, a characteristic domain or mosaic structure appears in the overlayer once it has transformed back to its bulk-stable structure. The reason is simple: we now have forced two structures with large misfit to share a common planar boundary. Crystallographic twins (or some related defect structure) must develop in order to relieve macroscopic strain along the epitaxial interface. This prediction follows from a direct analogy to the phenomenology of martensitic phase transformations [14].

The second point of interest concerns the region of Figure 4 between the points labelled f^- and f^+ . This corresponds to a situation where the Peierls stress of the overlayer maintains an average strain in the overlayer between ϵ^- and ϵ^+ in Figure 3. There is no problem at the one or two monolayer growth level where interfacial adhesive forces dominate the total energy. However, for larger values of h , the overlayer begins to realize that it possesses negative elastic constants (due to the concav-

ity of $f(\epsilon)$! The system is mechanically unstable and must evolve towards some stable structure. Bruinsma and Zangwill [12] suggest one possibility: a spinodal type instability where some parts of the overlayer distort towards pure BCC while others distort towards pure FCC. To date, this prediction remains untested.

CONCLUSION

This report has reviewed some recent phenomenological studies of the structural and morphological stability of thin crystalline films with emphasis on those aspects germane to multilayer growth. I have focused entirely on macroscopic concepts such as surface tension, diffusion, and elastic strain in order to illustrate that much can be learned without recourse to specific microscopic models. So far, these methods have been applied more or less independently to equilibrium and near-equilibrium situations of wetting, faceting, pseudomorphy and growth. Future work aims toward combining all of these features into a single comprehensive model of direct relevance to experiment.

REFERENCES

1. G.H. Gilmer and M.H. Grabow, *J. Metals* 39, 19 (1987).
2. R. Bruinsma and A. Zangwill, *Europhys. Lett.* 4, 729 (1987).
3. R. Kern, in Interfacial Aspects of Phase Transformations, edited by B. Mutaftschiev (North-Holland, Amsterdam, 1982), p. 287.
4. J.D. Weeks, in Ordering in Strongly Fluctuating Condensed Matter Systems, edited by T. Riste (Plenum, New York, 1980), p. 293.
5. A. Zangwill and R. Bruinsma, to be published.
6. E. Bauer, *Z. Krist.* 110, 372 (1958).
7. C.H.J. van den Brekel, *Philips Res. Rpts.* 32, 118 (1977).
8. G.S. Bales and A. Zangwill, to be published.
9. R.F. Sekerka, in Crystal Growth - An Introduction, edited by P. Hartman (North-Holland, Amsterdam, 1973), p. 403.
10. R.F.C. Farrow, *J. Vac. Sci. Tech.* B1, 222 (1983).
11. G.A. Prinz, *Phys. Rev. Lett.* 54, 1051 (1985).
12. R. Bruinsma and A. Zangwill, *J. Phys. (Paris)* 47, 2055 (1986).
13. J.H. van der Merwe, *J. Appl Phys.* 34, 117 (1963).
14. Z. Nishiyama, Martensitic Transformation (Academic, New York, 1978).

U. S. DEPARTMENT OF ENERGY

UNIVERSITY CONTRACTOR, GRANTEE, AND COOPERATIVE AGREEMENT
RECOMMENDATIONS FOR ANNOUNCEMENT AND DISTRIBUTION OF DOCUMENTS

See Instructions on Reverse Side

1. DOE Report No. DOE/ER/45243--3	3. Title Local Many-Body Effect in the Optical Response of Narrow Band Solids - Final Technical Report
2. DOE Contract No. DE-FG05-86ER45243	

4. Type of Document ("x" one)

a. Scientific and technical report

b. Conference paper:
Title of conference _____
Date of conference _____
Exact location of conference _____
Sponsoring organization _____

c. Other (Specify) _____

5. Recommended Announcement and Distribution ("x" one)

a. Unrestricted unlimited distribution.

b. Make available only within DOE and to DOE contractors and other U. S. Government agencies and their contractors.

c. Other (Specify) _____

6. Reason for Recommended Restrictions

7. Patent and Copyright Information:

Does this information product disclose any new equipment, process, or material? No Yes If so, identify page nos. _____

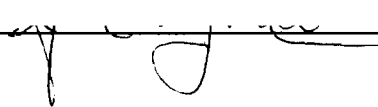
Has an invention disclosure been submitted to DOE covering any aspect of this information product? No Yes
If so, identify the DOE (or other) disclosure number and to whom the disclosure was submitted.

Are there any patent-related objections to the release of this information product? No Yes If so, state these objections.

Does this information product contain copyrighted material? No Yes
If so, identify the page numbers _____ and attach the license or other authority for the government to reproduce.

8. Submitted by
Andrew Zangwill Associate Professor of Physics

Organization
Georgia Institute of Technology

Signature / 	Phone 404-894-7333	Date December 1 1988
--	-----------------------	-------------------------

FOR DOE OR OTHER AUTHORIZED
USE ONLY

9. Patent Clearance ("x" one)

a. DOE patent clearance has been granted by responsible DOE patent group.

b. Report has been sent to responsible DOE patent group for clearance.

LOCAL MANY-BODY EFFECTS IN THE OPTICAL RESPONSE
OF NARROW BAND SOLIDS

Final Technical Report

Andrew Zangwill and David Liberman

School of Physics
Georgia Institute of Technology
Atlanta, GA 30332

December 1988

PREPARED FOR THE U.S. DEPARTMENT OF ENERGY
UNDER GRANT NO. DE-FG05-86ER45243

This report is a summary of the research activities carried out by Andrew Zangwill and David Liberman during the period from March 1 1986 to August 31 1988. This represents the total effort under Department of Energy Grant No. DE-FG05-86ER45243. As outlined in previous Progress Reports, and with the approval of our Technical Monitors, our work over this period gradually shifted from the original proposal subject, "Local Many-Body Effects in the Optical Response of Narrow Band Solids" to a new thrust area in "The Growth, Structure and Stability of Epitaxial Overlayers". In fact, the Department of Energy has recently approved a new grant, DE-FG05-88ER45369, to one of us (A.Z.) to pursue this latter subject exclusively.

In the interest of reducing the bulk of this report, we have not appended a copy of every paper published during the total granting period with acknowledged DOE support. Instead, we append only those which have been produced since the last Progress Report (May 1988). Nonetheless, we include below a list of all publications which have been produced since March 1 1986 in order to indicate the level of research activity. Those preceded by an asterix (*) include specific acknowledgement to DOE.

Research Activity (March 1 1986 - present)

- "Stacking Sequences in Close-Packed Metallic Superlattices," A. Redfield and A. Zangwill, Phys. Rev. B34, 1378 (1986).
- "Structural Transitions in Epitaxial Overlayers," R. Bruinsma and A. Zangwill, J. Phys. (Paris) 47, 2055 (1986).
- "Phase Stability and Structural Transitions in Close-Packed Metals," A. Zangwill and R. Bruinsma, Comm. Cond. Mat. Phys. 13, 1 (1987).
- * "A Condensed Matter View of Giant Resonance Phenomena," A. Zangwill, in Giant Resonances in Atoms, Molecules and Solids, edited by J.-P. Connerade, J.-M. Esteve and R. Karnatak (Plenum, New York, 1987).
- "Energetics of Icosahedral Phase Stability in Metallic Alloys," A. Redfield and A. Zangwill, Phys. Rev. Lett. 58, 2322 (1987).
- * "5f-Bandwidth and Resonant Photoemission of Uranium Inter-metallics," D.D. Sarma, F.U. Hillebrecht, C. Carbone and A. Zangwill, Phys. Rev. B36, 2916 (1987).
- * "Open Shell and Solid State Effects in Resonant Photoemission," A. Zangwill, J. Phys. C20, L627 (1987).
- * "Morphological Transitions in Solid Epitaxial Overlayers," R. Bruinsma and A. Zangwill, Europhys. Lett. 4, 729 (1987).
- * "Optical Response of an Embedded Atom," A. Zangwill and D. Liberman, Phys. Rev. B36, 6705 (1987).
- "Structural Selectivity in Aluminum-Transition Metal Alloys,"

A. Zangwill and A. Redfield, J. Phys. F18, 1 (1988).

"Stoichiometric Selectivity in MacKay Icosahedra," A. Redfield and A. Zangwill, Phil. Mag. Lett. 57, 255 (1988).

* "Phenomenological Approach to Multilayer Growth and Stability," A. Zangwill, in Multilayers: Synthesis, Properties and Non-Electronic Applications, edited by T.W. Barbee III, F. Spaepen and L. Greer (MRS, Pittsburgh, 1988).

* "Quadrupole Resonances in the Rare Earths," D. Liberman and A. Zangwill, Phys. Rev. A (in press).

* "Growth Dynamics of Chemical Vapor Deposition," G.S. Bales, A. Redfield and A. Zangwill, Phys. Rev. Lett. (submitted).

Book Published by A. Zangwill: Physics at Surfaces (Cambridge University Press, 1988).

Concerning the subject of local many-body response, the above cited paper on "Optical Response of an Embedded Atom" represents our most important result. Therein, we studied the many-body response (at the level of the random phase approximation) of an atom embedded in a large "droplet" of electrons. This study made contact both with the professed goal of our research - to investigate the effects of a solid state environment on atomic many-body effects - and recent studies of the optical response of metallic clusters. The spectral redistributions we observed in our calculations are very likely to be seen in all similar systems.

Concerning the subject of thin film growth and stability, our most recent study of the "Growth Dynamics of Chemical Vapor Deposition" is particularly significant because we have (for the first time) characterized the morphological pattern selection one obtains for growth processes where surface reaction kinetics stabilizes the effects of bulk diffusive transport. The interest in this work has been high - a poster version won "Best Poster" at the 1988 meeting of the American Vacuum Society.

The last mentioned paper is appended below along with the final (accepted to Phys. Rev. A) version of "Quadrupole Resonances in the Rare Earths". This was an interesting study where we extended our previous work (on dipole excitation) to higher multipoles and were thereby able to perform the first calculations of electron scattering cross sections including both many-body effects and quadrupolar excitations of the target. Good agreement with recent experiments (and an interpretation of their results!) was obtained.

Quadrupole Resonances in the Rare Earths

David Liberman
Lawrence Livermore National Laboratory
Livermore, CA 94550

and

Andrew Zangwill
School of Physics
Georgia Institute of Technology
Atlanta, GA 30332 USA

ABSTRACT

Calculations that employ a relativistic time-dependent local density approximation (RTDLDA) to atomic absorption are used to examine a recent claim to the observation of giant quadrupolar resonances in the electron scattering spectrum of Ce metal near the 4p edge. We confirm the existence of 4p→4f resonances in this energy regime but suggest that a conventional autoionization interpretation is more appropriate.

PACS Numbers: 78.70Dm, 32.80.Dz

A recent experimental study [1] announced the assignment of a prominent feature in the electron energy loss spectrum (EELS) of cerium metal near the 4p threshold to a "giant" resonance in the quadrupolar 4p→4f channel. The assignment was based on a comparison of x-ray absorption data to previously obtained EELS data [2] (both reproduced in Figure 1) and relies upon the fact that photoabsorption is sensitive to dipolar transitions exclusively (at the relevant excitation energies) whereas EELS can discriminate in favor of quadrupolar and higher multipolar transitions at sufficiently large values of the momentum transfer. One-electron Hartree-Fock calculations of the 4d→4f and competing dipolar 4p→5d matrix elements were used to suggest that superior wave function overlap tips the balance in favor of the former and that it is appropriate to regard the observed feature as a quadrupole analog to the well-known "giant" dipole resonance in cerium near the 4d threshold [3].

The present Brief Report examines this claim by means of an explicit calculation of both dipole and quadrupole photoabsorption by atomic cerium in the vicinity of the 4p threshold. The computations employ a relativistic time-dependent local density approximation (RTDLDA) [4] that has been shown to yield excellent agreement with experiment for photoabsorption in both the ultraviolet [5] and x-ray [6] portions of the spectrum. Within the framework of the local density approximation to the one-electron spectrum, this method includes all the polarization type many-electron effects responsible for channel mixing, auto-ionization and dipolar "giant" resonance behavior [7].

Figure 2 shows our results for the dipole cross section $\sigma_1(\omega)$ and the quadrupole cross section $\sigma_2(\omega)$ for atomic cerium in the vicinity of the spin-orbit split 4p threshold. We immediately confirm the qualitative experimental observation that the dipole absorption exhibits only weak structure near the edges whereas sharp sub-threshold resonances appear in the quadrupole channel. Regarding the latter, bear in mind that we consider not the true

electron scattering cross section but, instead, the photoabsorption cross section in the quadrupole channel, i.e., the momentum transfer is fixed at $q=\omega/c$. Accordingly, a trivial rescaling is required to compare the relative magnitudes of our calculated cross sections to the experiments. In this manner, we readily verify the conclusion of Ref. 1 that quadrupole excitations dominate the EELS spectrum for the given experimental conditions.

We also confirm the assignment of the resonant structure in $\sigma_2(\omega)$ to strong, overlap driven transitions between the 4p core states and the highly localized 4f valence orbitals. Observe that our computed resonances are quite narrow (we have made no attempt to include possible core-hole lifetime effects) and exhibit conventional Fano [8] lineshapes. This observation leads us to our only point of contention with Matthew et. al. [1]: their suggestion that these resonances are in some sense quadrupole analogs to the 4d→4f "giant" dipole resonances that occurs in cerium and the other rare earths.

Let us point out clearly that the definition of a "giant" resonance is, to some extent, a matter of taste [7]. Nevertheless, "their appearance as strong, localized resonances" [1] is definitely not sufficient. There is no question that the one-electron external field matrix element $\langle 4f|r^2|4p\rangle$ is large in this case due to wave function overlap. On the other hand, the "giant" resonances all are characterized by a large Coulomb matrix element that couples pairs of virtual particle-hole pairs [9]. The qualitative picture of an entire shell of electrons in collective motion follows from this requirement. In the present case, we would expect the relevant (4p,4f) Slater integral to be large [10] and to push the bound-bound transition oscillator strength into a broad resonance above threshold. We find no evidence for this. Instead, the transition is clearly visible above the quadrupolar continuum as a sharp autoionization resonance of the conventional sort.

Returning to the dipole channel, we find that our computed $\sigma_1(\omega)$ is not in particularly good quantitative agreement with the x-ray absorption measurements [1]. The latter exhibit essentially no edge jump; instead, a broad feature is observed between the $4p_{1/2}$ and $4p_{3/2}$ thresholds. The authors of Ref. 1 speculated that some "interconfigurational coupling" may lead to such behavior. However, the most significant class of such coupling already is included in our RTDLDA calculations. Consequently, we must conclude that the discrepancy between theory and experiment arises from some other source.

In summary, we have performed RTDLDA calculations of the expected dipole and quadrupole response of a cerium atom for excitation energies in the vicinity of the 4p core threshold. We confirm a previous assignment [1] of a strong feature observed in EELS as a $4p \rightarrow 4f$ resonance but dispute its classification as a "giant" resonance in the sense of, say, nuclear physics. We instead regard this feature as a conventional Fano-type autoionization resonance unaffected by strong polarization-type electron-electron interactions. Our results do not preclude the possibility of a true quadrupolar "giant" resonance in some different atomic system.

This work was performed under the auspices of the U.S. Department of Energy by the Lawrence Livermore National Laboratory under contract number W-7405-ENG-48. One of us (AZ) acknowledges support by DOE Grant No. DE-FG05-86ER45243.

REFERENCES

1. J.A.D. Matthew, F.P. Netzer, C.W. Clark and J.F. Morar, *Europhys. Lett.* 4, 677 (1987).
2. G. Strasser and F.P. Netzer, *J. Vac. Sci. Tech. A* 2, 826 (1983).
3. A. Zangwill and P. Soven, *Phys. Rev. Lett.* 45, 204 (1980).
4. D.A. Liberman and A. Zangwill, *Comp. Phys. Commun.* 32, 75 (1984).
5. A. Zangwill, in Atomic Physics 8, edited by I. Lindgren, A. Rosen, and S. Svanberg (Plenum, New York, 1983), p. 339.
6. W. Jitschin, U. Werner, G. Materlik and G.D. Doolen, *Phys. Rev. A* 35, 5038 (1987).
7. A. Zangwill, in Giant Resonances in Atoms, Molecules and Solids, edited by J.P. Connerade, J.M. Esteve and R.C. Karnatak (Plenum, New York, 1987), p. 321.
8. U. Fano, *Phys. Rev.* 124, 1866 (1961).
9. G.E. Brown and M. Bolsterli, *Phys. Rev. Lett.* 3, 472 (1959).
10. This is true whether one works in a Hartree-Fock basis or in a local density functional basis. Of course, the Coulomb integral enters in different places in the two calculations.

FIGURE CAPTION

Figure 1. Electron energy loss spectrum (primary energy 1880 eV) and x-ray absorption spectrum of cerium metal from Reference 1. Note the reversal of the energy scale.

Figure 2. Calculated dipole and quadrupole photoabsorption cross sections for Ce atom in the vicinity of the spin-orbit split 4p threshold. Note the difference in vertical scales. The photon energy scale is reversed to facilitate comparison with Ref. 1.

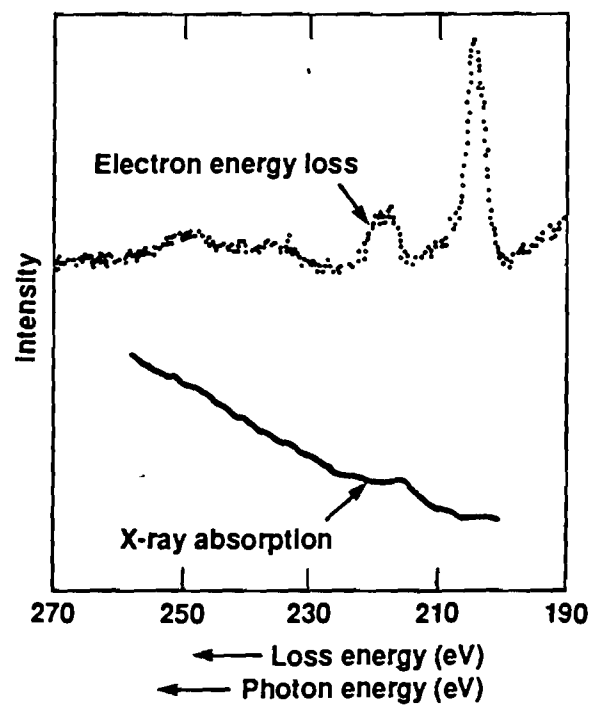
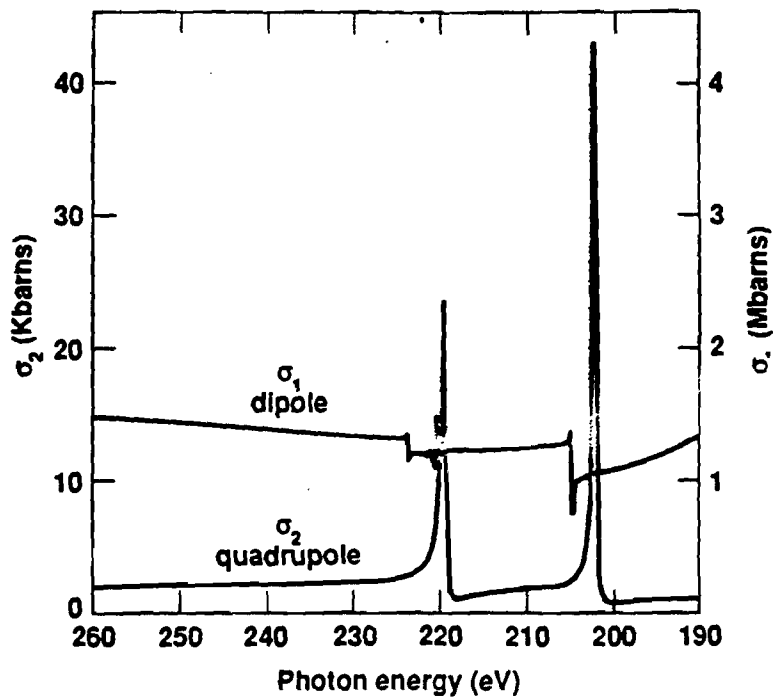


Figure 1



D.A.L.
12/9/87

Figure 2

GROWTH DYNAMICS OF CHEMICAL VAPOR DEPOSITION

G.S. Bales, A.C. Redfield^(a) and A. Zangwill
School of Physics
Georgia Institute of Technology

ABSTRACT

The morphological growth dynamics of chemical vapor deposition are studied with a model that takes account of both diffusive transport in the bulk and the kinetics of surface reactions. For the case of a fixed flux of reactant species far from the surface, we study numerically the crossover from diffusion-limited growth to surface kinetic-limited growth. In the latter case, one can qualitatively account for the morphology at early and intermediate times by use of a non-linear growth model which takes explicit account of the destabilizing influence of the bulk phase diffusion field.

PACS numbers: 05.70.Ln, 68.55.JK, 81.15.Gh

Novel crystal growth technologies which permit atomic-level compositional and thickness control are singularly responsible for our current ability to explore the properties of low dimensional microstructures. In particular, it is generally agreed [1] that molecular beam epitaxy (MBE) and metalorganic chemical vapor deposition (MOCVD) are the techniques of choice for the fabrication of research-grade heterostructures. These two dominate, in part, because crystal growers have learned to fine tune the relevant growth parameters so that extremely flat and sharp interfaces can be obtained as a routine matter. In fact, there exists a substantial experimental folklore that relates growth conditions to surface morphology. By contrast, theoretical studies of possible growth morphologies are far less numerous. While some work exists for MBE [2], little is known for CVD. The present Letter addresses this issue.

A minimal description of CVD contains three elements: (i) mass transport to the surface driven by hydrodynamic flow followed (near the surface) by vapor phase diffusion [3]; (ii) incorporation of mass into the surface by thermally activated kinetic processes [4]; and (iii) mass transport along the solid surface driven by capillary forces [5]. If only the first of these is present, one obtains the well-known fractal growth patterns of diffusion limited aggregation [6]. If both bulk phase diffusion and capillarity are present, the physics is isomorphic to that of fluid flow in a Hele-Shaw cell [7]. Only when all three elements are present does one arrive at the most general form of the solidification problem [8].

A realistic morphological model of CVD growth incorporating all the essential features was set up by van den Brekel [9] and solved by him for the case of small deviations from a flat interface. He recovered the familiar Mullins-Sekerka instability [10] and made contact with experimental studies of the deposition of polycrystalline silicon. More recently, Palmer and Gordon [11] attacked a related CVD model with a mode-coupling scheme and were able to follow morphological evolution into the weakly non-linear regime. Unfortunately, this technique fails as growth proceeds since large

non-linearities soon develop [12].

Herein, we address the growth dynamics of chemical vapor deposition by an essentially exact numerical treatment of van den Brekel's model. In this way, we are able to study morphological variation as one passes smoothly from diffusion limited growth to growth limited by the kinetics of surface reactions. As suggested earlier, the Hele-Shaw model provides a good description of the growth in the former limit. In the latter limit (defined more precisely below), we find that the surface morphology can be understood qualitatively by use of a non-linear growth model similar in spirit to one proposed by Kardar and co-workers [13].

Figure 1 defines the two-dimensional model under investigation. An external source maintains a fixed concentration c_b of reactant molecules at a distance δ above the initial surface. Diffusion (D) drives the molecules towards the surface where an interfacial reaction (e.g., dissociative chemisorption) characterized by a kinetic mass transfer coefficient k must occur before new material is incorporated into the solid. In steady state, the diffusive flux equals the incorporation flux so that the instantaneous concentration field is determined by

$$\begin{aligned} \nabla^2 c(\underline{r}) &= 0 \\ c(z=\delta) &= c_b \end{aligned} \tag{1}$$

$$k[c(\underline{s}) - c_{eq}(\underline{s})] = D \underline{n} \cdot \nabla c|_s$$

where \underline{s} is a point on the surface and \underline{n} is the local unit normal to the surface. The equilibrium concentration of reactant molecules just above the surface is given by the Gibbs-Thomson formula: $c_{eq}(\underline{s}) = c_{flat} + \Gamma \kappa(\underline{s})$ where Γ is proportional to the surface tension and $\kappa(\underline{s})$ is the local curvature [10]. Physically, this means that relaxation of the surface is presumed to occur via evaporation/condensation processes rather than surface diffusion (which dominates at reduced temperature). The model is relevant to the growth

of polycrystalline films if we neglect the anisotropy of Γ .

As for related problems [12], we work in the quasistatic limit of the growth dynamics. A Green function technique suited to the mixed boundary conditions of the problem is used to solve Equation (1) for any given morphology of the lower surface. The surface is grown (or etched) at a rate

$$v(\underline{s}) = \Omega k [c(\underline{s}) - c_{eq}(\underline{s})] \quad (2)$$

in the direction of the local normal (Ω is the atomic volume of the solid) and the process is repeated. This numerical procedure correctly reproduces the results of linear stability theory [8,9] for small sinusoidal perturbations about a flat interface. In fact, to better appreciate the non-linear results to follow, it is useful to recapitulate the predictions of this linear analysis.

Three length scales characterize the CVD problem as posed. The width of the non-hydrodynamic stagnant layer δ , a capillary length $\xi = \Gamma / (c_b - c_{flat})$, and an effective maximum distance $d = D/k$ over which portions of the surface communicate by evaporation, gas phase diffusion and re-condensation. Flat surfaces grow at a steady state velocity $V = \Omega D (c_b - c_{flat}) / (d + \delta)$. But, as shown by van den Brekel [9], the surface is unstable against small amplitude morphological perturbations with wavelengths greater than $\lambda_c = 2\pi [\xi \delta (1 + d/\delta)]^{1/2}$. Moreover, the ratio of the rate at which such a perturbation grows to the average velocity of the growth front (which varies as λ_c^{-2} for fixed Γ) declines to zero as $d \rightarrow \infty$. Hence, at the price of a very slow growth rate, one can avoid morphological instability altogether by working sufficiently far into the so-called surface kinetic-limited regime ($d/\delta \gg 1$) so that $\lambda_c > L$ (the sample size).

For practical applications, this price turns out to be too high. Hence, experimenters often work in the diffusion-limited regime [14] and growth is arrested before large instabilities occur. Clearly, the best trade-off occurs if we let d become large but insist that λ_c (and hence the growth rate) remain fixed. To do so,

let $\delta \rightarrow \infty$ and $\xi \rightarrow 0$ (i.e., $c_b \rightarrow \infty$) so that $d/\delta \ll 1$ but $\delta\xi$ remains finite. The result is a one-parameter (d/λ_c) model of CVD growth with a specified concentration gradient far from the surface.

Figure 2 illustrates the growth at $d/\lambda_c = 0$ of a surface whose initial shape is flat with small random fluctuations. As expected, the finger-like morphology which evolves is identical to that found for the Hele-Shaw problem [7]. Such patterns also are observed in the CVD growth of polycrystalline silicon [9]. For present purposes, the most notable feature of Figure 2 is the fact that one finger "noses ahead" of its neighbors [15]. As in the fluid problem, the imposed gradient guarantees relatively faster growth for this feature thereafter so that, as the smaller fingers are screened from nutrient, the asymptotic growth pattern consists of fewer, larger fingers.

Figure 3 illustrates the growth of a similarly chosen initial surface, but with $d/\lambda_c = 2.5$. Evidently, the growth proceeds in a very different manner than in the previous example [16]. To understand the difference, note that when $d=0$, the reaction kinetics are infinitely fast and the growth rate of a point on the surface is determined by the ease with which a particle can diffuse to that point. It is easy to see that growth at local minima rapidly becomes suppressed. In the opposite limit ($d \rightarrow \infty$), slow kinetics means that reactant molecules "pile up" near the surface and have time to form a layer of nearly uniform concentration. This implies that $c(\underline{g}) = \text{const.}$ over the entire surface. Since, at early times, the surface curvature is small, Equation (2) says that growth occurs at the same rate everywhere (normal to the surface). This makes plausible the first morphological effect we observe beyond the linear regime [11]: local maxima flatten out and local minima become more cusp-like. At intermediate times, the interface evolves toward a morphology that distinctly resembles a collection of parabolic fronts. Generally, larger parabolic sections grow at the expense of smaller sections.

The growth scenario to this point is highly reminiscent of the results obtained by Kardar and co-workers [13] from their analysis

of the Eden model in the continuum limit. This is not too surprising since the two effects they include (to lowest order) are precisely (i) uniform growth normal to the surface and (ii) relaxation by a condensation/evaporation mechanism. However, there is an essential difference: our CVD film does not asymptotically relax to a flat interface as does the deterministic model surface of Ref. 13 (over any given length scale L). Instead, Figure 3 shows that some parabolic segments creep ahead of their neighbors and eventually overtake them, much like the "fingers" of Figure 2.

Unlike the Eden model, the roughness observed in Figure 2 at long times is unrelated to the presence of external noise. Instead, it occurs because bulk phase diffusion guarantees that $c(\underline{s})$ is not precisely constant as long as D/k is finite. To see that this effect is sufficient to destabilize the growing surface, we replace the full growth equations by an approximate equation of motion for the local height $h(x)$ of the interface. The time evolution $\partial h/\partial t$ is chosen so that its projection along the local surface normal is equal to $v(\underline{s})$ [6,13]. A useful estimate of $c(\underline{s})$ can be obtained from the linear analysis [9] if the surface is nearly flat over long length scales and exhibits regions of (at most) small slope ∇h over short length scales. Combining this with Eqtn. (2), we obtain the following equation of motion in the comoving (V) frame of reference:

$$\frac{\partial h}{\partial t} = \alpha k \Gamma v^2 h + \frac{V}{2} (\nabla h)^2 + (V/d)h \quad (3)$$

Equation (3) is valid in the limit $d \rightarrow \infty$ (very slow kinetics) for surface profiles with morphological variations on all length scales shorter than d . It is identical to the deterministic model of Kardar et. al. save for the (crucial) addition of the final term on the right hand side.

In the linear regime, Equation (3) exhibits the same critical wavelength as the full CVD model [Equation (1)]. In the non-linear regime, it is easy to check that a particular solution is $h(x,t) = a(t)x^2 + b(t)$. In the limit that $\Gamma \rightarrow 0$ [17], we readily find

$$a(t) = a(0) \beta e^{\beta t} / [\beta + 2Va(0)(1 - e^{\beta t})] \quad (4)$$

$$b(t) = b(0) e^{\beta t},$$

with $\beta = V/d$. Observe first that no portion of the growth front relaxes to a flat surface; instead, all parabolic sections asymptotically ($t \rightarrow \infty$) approach a fixed curvature ($a \rightarrow -\beta/2V$). Second, and more importantly, the parabolic segments of the surface with greatest initial heights $b(0)$ steadily leave their smaller counterparts behind as growth proceeds.

These results are sufficient to understand our numerical observations since the qualitative features of Eqn. (3) remain valid at early and intermediate times if d is finite (but large). In particular, the parabolic segments of greatest height which emerge from the random starting surface do indeed move ahead of their neighbors. But this phenomenon increases the segments' arc lengths and (inevitably) generates regions of large slope. When this occurs, our local approximation to the diffusion field effect on $c(s)$ breaks down and the evolution of the segments towards their asymptotic curvature terminates. Rapid suppression of the concentration occurs in the narrowing grooves between parabolas and no additional growth occurs there. The result is finger-like structures as in the $d=0$ case. An analytic expression for the asymptotic form of the interface in this slow-kinetics limit is not available at present. We invite further analysis of this question.

To our knowledge, existing experimental studies of morphological evolution during CVD have been insufficiently systematic to judge the correctness of our discussion in the interesting large- d limit. Moreover, a typical lateral length scale over which morphological instabilities occur ($\sim 1 \mu\text{m}$) is competitive with a typical length scale for facet formation. Thus, any model of the CVD growth of crystalline materials must take proper account of large anisotropies in Γ . Numerical and analytic study of this problem is in progress and will be reported elsewhere.

We thank Ahmet Erbil for introducing us to the CVD problem, Eshel Ben-Jacob for bringing Ref. 7 to our attention, and Robijn Bruinsma for a critical reading of the manuscript. This work was supported in part by the Department of Energy under Grant Nos. DE-FG05-86ER45243 and DE-FG05-88ER45369.

REFERENCES

(a) Present address: Physics Department, Williams College,
Williamstown, MA 01267

1. G. Davies, Phys. Bull. 39, 22 (1988); G.B. Stringfellow, Rep. Prog. Phys. 45, 469 (1982).
2. M. Schneider, I.K. Schuller and A. Rahman, Phys. Rev. B36, 1340 (1987); A. Madhukar and S.V. Ghaisas, CRC Crit. Rev. Sol. State and Mat. Sci. 14, 1 (1988).
3. The existence of a "stagnant layer" within which gas particles diffuse to the surface is most nearly true in so-called vertical CVD reactors. See D.I. Fotiadis, A.M. Kremer, D.R. McKenna and K.F. Jensen, J. Cryst. Growth 85, 154 (1987).
4. M.E. Jones and D.W. Shaw, in Treatise on Solid State Chemistry, edited by N.B. Hannay (Plenum, New York, 1975), vol. 6, pp. 283-323.
5. W.W. Mullins, J. Appl. Phys. 28, 333 (1957).
6. P. Meakin, CRC Crit. Rev. Sol. State and Mat. Sci. 13, 143 (1987).
7. L.P. Kadanoff, J. Stat. Phys. 39, 267 (1985); S. Liang, Phys. Rev. A33, 2663 (1986).
8. P.G. Shewmon, Trans. Met. Soc. AIME 233, 737 (1965). Recent work in this area generally neglects kinetic effects entirely. See, e.g., J.S. Langer, in Chance and Matter, edited by J. Souletie, J. Vannimenus and R. Stora (North-Holland, Amsterdam, 1987), pp. 629-711.
9. C.H.J. van den Brekel, Philips Res. Rept. 32, 118 (1977); C.H.J.

- van den Brekel and A.K. Jansen, *J. Cryst. Growth* 43, 364 (1978).
10. W.W. Mullins and R.F. Sekerka, *J. Appl. Phys.* 34, 323 (1963);
J. Appl. Phys. 35, 444 (1964).
 11. B.J. Palmer and R.G. Gordon, *Thin Sol. Films* 158, 313 (1988).
 12. Y. Saito, G. Goldbeck-Wood and H. Muller-Krumbhaar, *Phys. Rev. Lett.* 58, 1541 (1987).
 13. M. Kardar, G. Parisi and Y.-C. Zhang, *Phys. Rev. Lett.* 56, 889 (1986).
 14. Operationally, the distinction between the "diffusion-limited regime" and the "kinetic-limited regime" is based on the temperature dependence of the average growth rate, Λ . In the kinetic limit, $\Lambda \propto k$, the mass transfer coefficient, which exhibits activated behavior. In the opposite, diffusive limit ($d/\delta \ll 1$), $\Lambda \propto D$, which is only weakly temperature dependent. See Reference 9 for details.
 15. D.A. Kessler and H. Levine, *Phys. Rev.* A33, 3625 (1986).
 16. Our results for $d/\lambda_c \neq 0$ are related to the so-called "dense branching morphology" and "fluid draining" effects in the Hele-Shaw problem. See the articles by E. Ben-Jacob, et.al. and S.K. Sarkar in *Superlattices and Microstructures*, vol. 3, no. 6, (1987).
 17. As in the Burgers' equation treatment of Ref. 13, the main effect of finite Γ (surface tension) is to smooth out the cusps formed where parabolic segments of the surface meet.

FIGURE CAPTIONS

- Figure 1. Schematic view of the CVD process. In steady state, the diffusion flux J_D is equal to the kinetic mass transfer flux J_{MT} .
- Figure 2. Typical surface morphology in the fast surface kinetics ($d=0$) regime. The critical wavelength λ_c is 1/10 of the figure width.
- Figure 3. Typical surface morphology in the slow surface kinetics ($d/\lambda_c=2.5$) regime. The critical wavelength λ_c is 1/32 of the figure width.

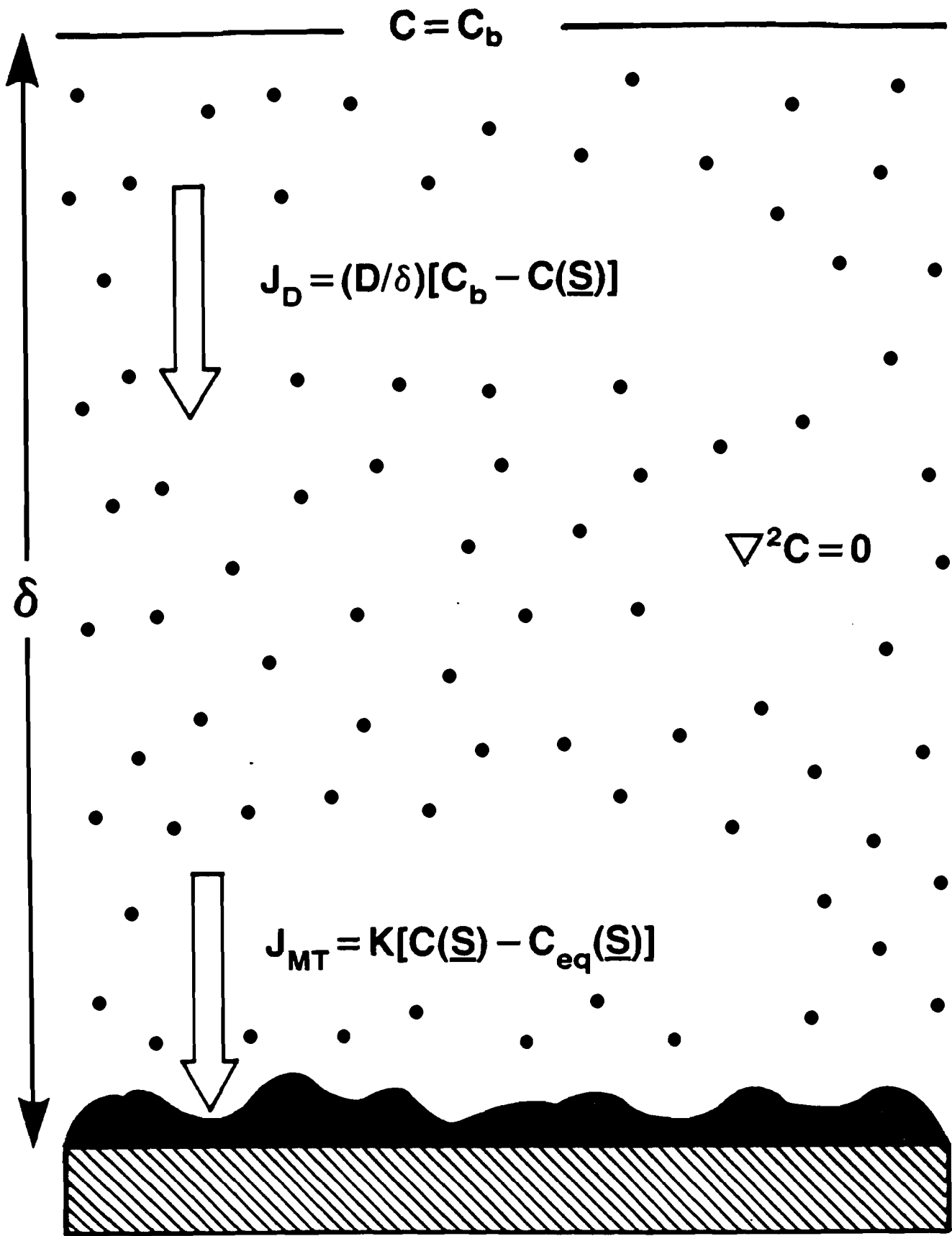
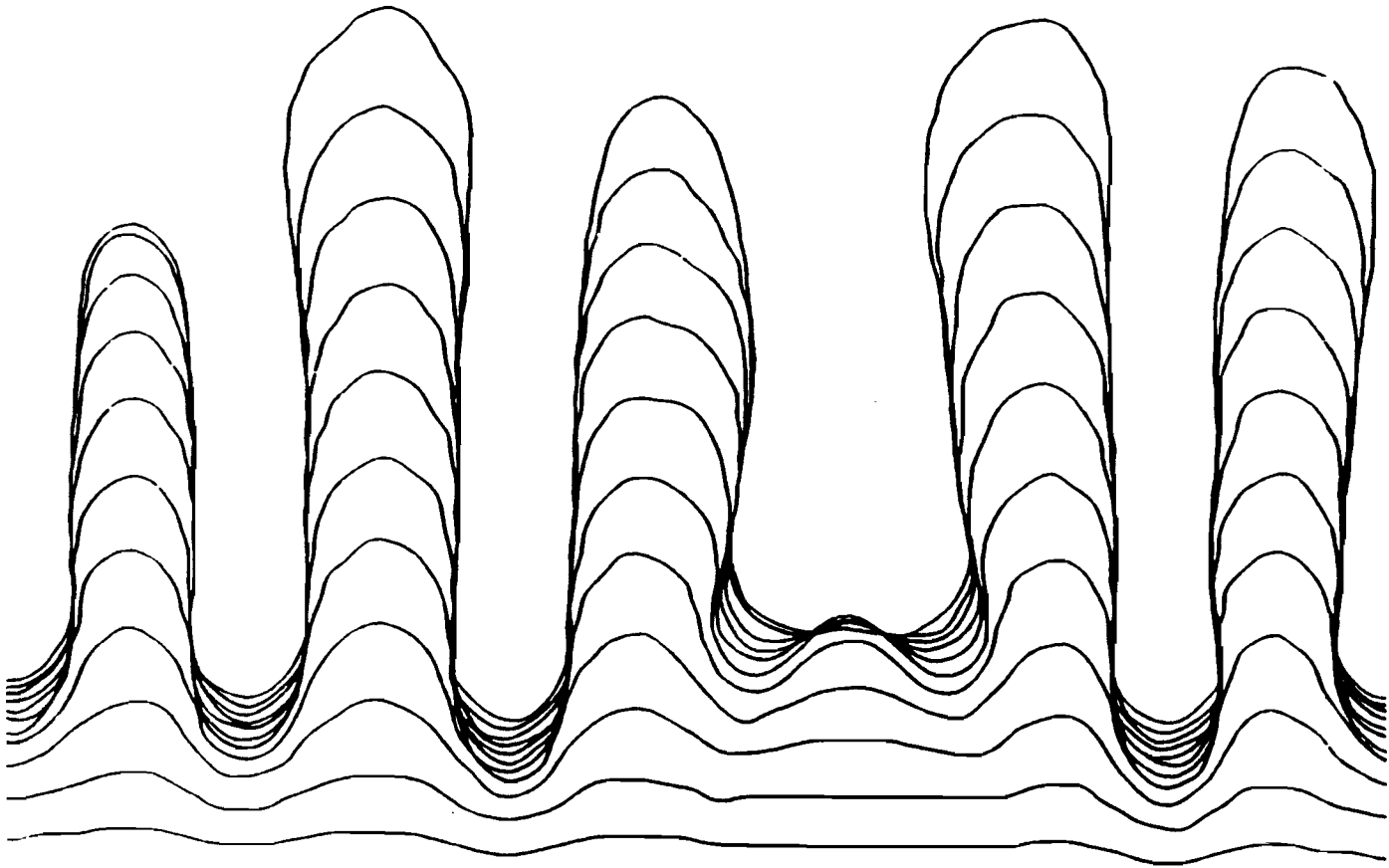


FIGURE 1

FIGURE 2



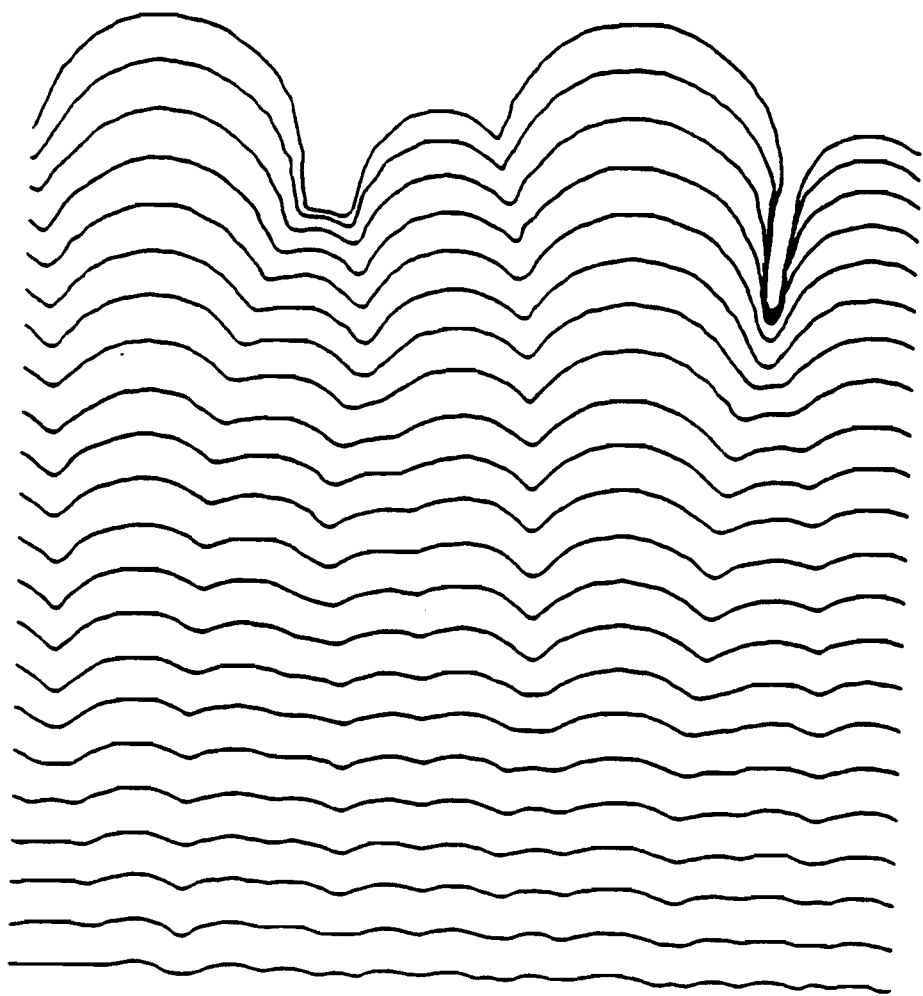


FIGURE 3